

The Pennsylvania State University
The Graduate School
Department of Energy and Mineral Engineering

INVESTIGATION OF CONICAL BIT ROTATION IN FULL SCALE CUTTING TESTS

A Dissertation in
Energy and Mineral Engineering

by

Eunhye Kim

© 2010 Eunhye Kim

Submitted in Partial Fulfillment
of the Requirements
for the Degree of

Doctor of Philosophy

December 2010

The dissertation of Eunhye Kim was reviewed and approved* by the following:

Jamal Rostami
Assistant Professor of Energy and Mineral Engineering
Dissertation Advisor
Chair of Committee

Larry Grayson
Professor of Energy and Mineral Engineering
George H., Jr., and Anne B. Deike Chair in Mining Engineering
Graduate Program Officer of Energy and Mineral Engineering

Antonio Nieto
Associate Professor of Mining Engineering
Thomas V. Falkie Faculty Fellow

Frances Costanzo
Professor of Engineering Science and Mechanics

Derek Elsworth
Professor of Energy and Geo-Environmental Engineering

Yaw D. Yeboah
Professor and Department Head of Energy and Mineral Engineering

*Signatures are on file in the Graduate School

ABSTRACT

Conical bits are very common in the excavation of soft to medium rock in many mining and construction applications and are used on machines such as roadheaders, continuous miners, drum shearers, and road milling machines. Rotation of the conical bits in its block can extend bit life through a process of even wear on the tip that allows the bit to maintain its tip shape and work more efficiently for an extended period of time. Frequently, this fact does not hold true in actual conical bit application. Grinding on one side of the bit, breaking the bit tip, and severe irregular deformations of conical bits are found when inspecting bits on the cutterhead of mechanical excavators. Strikingly, little is known about causations of bit rotation. Reliable measurement of bit rotation has not been made prior to this study. Therefore the effectiveness of bit rotation and its impact on bit life has been in doubt.

To investigate the conical bit rotation phenomenon and parameters affecting this process, a new device was designed and fabricated to measure rotation of a bit in bit holder. For a given conical pick, the main controlling parameters for bit rotation are considered to be skew angle, cut spacing, depth of penetration, and travel speed. To measure the impact of these parameters on bit rotation, full-scale cutting tests were performed at the Kennametal rock cutting lab in Latrobe, PA. This includes linear and rotary cutting tests with single and multiple bits to examine the rotation mechanism of conical bits.

Linear cutting tests involve full scale cutting of rock samples along preset lines to measure normal, drag, and side forces and bit rotation while changing the cutting geometry (including skew angle, spacing, and depth of cut). A skew plate was used to change the skew angle for testing. Two different bits, AM-470 from the mining tools and RZ-24 pick from the construction tools were selected for testing. Results of the linear cutting test showed no systematic bit rotation. Some sporadic rotation on the RZ-24 conical tool was primarily due to the

contact of the bit body with the ridges formed at higher spacing, something that should be prevented in operational conditions. As such, bit rotation did not show any trends with the primary cutting geometry parameters. A series of analytical and numerical solutions were performed to evaluate the configuration of forces at the bit tip that can cause bit rotation under various loading conditions. This analysis focused on calculation of the required lateral forces for rotation of the bit under certain axial loading of the bit which causes friction between bit shoulder and bit block. This friction prevents bit rotation. The results of the analysis supported the linear cutting test results and observations.

Subsequently, rotary cutting tests on a drum laced with a single bit were performed. And bit rotation was measured using the instrumented bits at different skew angles, cutting geometry, and cutting speeds. The results of rotary cutting test show that limited bit rotation occurs as the bit enters and exits the rock (cutting surface). Among the cutting parameters, the skew angle has a significant effect on the bit rotation. However, higher bit rotations were observed at lower skew angles from zero to six degree. The use of higher skew angles (i.e. -12° or 12°) reduced bit rotation and increased cutting forces and specific energy of cutting. Higher bit rotation also coincided with narrow spacing. Intriguingly, the direction of the bit rotation follows the face that contacts the rock surface first. Thus, positive rotation (CW) was observed with positive skew angles. Similarly, negative rotation (CCW) was measured at negative skew angle. Positive skew angle in this case was considered cutting towards the lower cutting surface (or the adjacent line that is previously cut)

Rotary cutting tests using the drum laced with multiple bits were also performed. This drum was fitted with four (4) bits at two (2) bits per line at equal circumferential spacing of 90 degrees. A higher bit rotations was observed at a lower spacing and skew angle seems to impact bit rotation. The limited data available to date are inconclusive on the final impact of the skew angle on bit rotation and optimum skew angle for maximum rotation of the bit One of the main

conclusions of the rotary cutting tests is that the bit rotation occurred at small increment at each revolution during the point of entry and exit of the bit into the cut. At this stage, several mechanisms have been proposed to improve bit rotation. The effectiveness of these solutions requires confirmation by additional full scale cutting tests.

TABLE OF CONTENTS

LIST OF FIGURES	viii
LIST OF TABLES	xiii
ACKNOWLEDGEMENT	xiv
Chapter 1 Introduction	1
1.1 Rotation of conical bit	2
1.2 Statement of purpose	5
1.3 Objectives	5
1.4 Hypotheses	6
1.5 Methodology	6
1.6 Contents of this dissertation	7
1.7 Glossary	8
Chapter 2 Literature Review	9
2.1 Introduction of literature review	9
2.2 Subgroup bits of drag type bit	11
2.3 Cutting mechanism	12
2.4 Conical bit tip type and skew angle	17
2.5 Cutting efficiency and bit wear	19
2.6 Cutting force and bit rotation	22
Chapter 3 Linear Cutting Experiment Setting	25
3.1 Instrumentation and installation	25
3.2 Conical Bit Instrumentation	27
3.3 Linear cutting test in limestone	31
3.3.1 Linear cutting test design in limestone	33
3.3.2 Preparation for experiment condition setting in limestone	35
3.4 Linear Cutting Test in Grout	36
Chapter 4 Data Analysis on Linear Cutting Tests in Limestone and Grout	39
4.1 Data Analysis Program	39
4.2 Test Results and Data Analysis in Limestone	39
4.2.1 AM 470 bit in limestone	39
4.2.2 RZ 24 bit in limestone	45
4.3 Test results and Data analysis of linear cutting test in grout	50
4.3.1. Review of Linear Cutting Test Results for AM470 bit in grout	50
4.3.2 RZ24 bit in grout	51

4.3.3 Comparison of measured rotation of the bits in limestone and grout sample RZ24 bit in grout.....	52
4.4 Summary of Conclusions for linear cutting tests	57
4.5 Simulation of Bit Rotation with Analytical and Numerical Methods	57
4.5.1 Analytical solution of conical bit rotation.....	57
4.5.2 Numerical simulation on conical bit rotation	61
4.6 Conclusion of linear cutting tests.....	67
 Chapter 5 Measurement of Bit Rotation in Rotary Cutting Test	 72
5.1 Introduction.....	72
5.2 Initial setting of rotary cutting test.....	73
5.3 Experiment procedure for rotary cutting test	73
5.4 Procedure of data analysis of rotary cutting test	76
5.5 Results of single bit rotary cutting test on AM-470 bit.....	80
5.5.1 Study on speed and RPM effect on bit rotation.....	82
5.5.2 Results and analysis of rotary cutting tests for single bit drum using AM470 bit at 2.5cm (1”) depth of cut	84
5.5.3 Results and analysis of AM470 bit single at 5 cm (2”) depth of cut.....	90
5.5.4 Discussion of the results of single bit rotary cutting tests using AM-470.....	96
5.6 Analysis of RZ24 bit single cutting test.....	99
5.7 Rotary cutting tests of the drum with multiple bit drum	105
5.7.1 Experiment setting for multiple AM470 bits	106
5.7.2 Results and analysis of rotary cutting tests with multiple bit drum using AM-470 bit at 2.5 cm (1”) depth of cut.....	111
5.7.3 Results and analysis of rotary cutting test with multiple bit drum using AM470 bit at 5cm (2”) depth of cut	113
5.7.4 Summary and conclusion on rotary cutting tests with multiple bit cutting drum using AM470 bit	118
5.8 Analytical and Numerical modeling of suggested solution using spring loading	122
5.8.1 Analytical solutions on the spring concept.....	123
5.8.2 Numerical modeling of the spring loading concept.	125
 Chapter 6 Conclusions and Recommendations.....	 127
6.1 Conclusions of bit rotation.....	127
6.2 Recommendations of bit rotation study	129
References.....	131
Appendix.....	138
Suppl. 1 Summary files of the Rotary cutting tests	138

LIST OF FIGURES

Figure 2-1 Plot Pictures of conical bit application: (a) Roadheader (b) Shearer (http://www.ulancoal.com.au) (c) Continuous miner (Joy Mining Machinery) (d) Trenching (Kennametal Catalog).....	10
Figure 2-2 Two types of picks on a cutting head, Forward attack or conical, wedge type or Radial (Roxborough and Sen, 1986).....	11
Figure 2-3 Schematic view of metal cutting and rock cutting	12
Figure 2-4 Schematic view of Evan’s tensile theory and its application	14
Figure 2-5 Pictures of carbide tip and plug: (a) three different tungsten carbide shapes/styles (Kennametal Catalogue) (b) location of plug insert on bit body.....	18
Figure 2-6 Conical bit cutting on the sample at skew angle of 12° (Schematic view of the skew angle based on line of cut and its projection of bit axis).....	19
Figure 2-7 Example of three direction of forces with schematic view of Kennametal Inc system	23
Figure 3-1 Picture of cutting test fixture in Kennametal cutting lab.....	26
Figure 3-2 Schematic view of measurement of bit rotation.....	28
Figure 3-3 Pictures of selected bits :(a) AM 470 bit and K25S block (b) RZ 24 bit and KPF301 block (c) instrumented U 756 bit and KPF 301 block; RZ 24 bit and R25s bit block.....	30
Figure 3-4 Pictures of (a) test set up with load cell mounted on the gear box using the new bracket (b) AM 470 bit ready for testing with the bit rotation sensor	31
Figure 3-5 Picture of rock surface with different cut spacing during the linear cutting tests (Kim et al., 2009)	31
Figure 3-6 Calibration of load cells which are embedded on the sample tables and behind the bit(Kim et al., 2009)	33
Figure 3-7 Test matrix of the 2.54 mm, 5.08mm, and 7.62mm (0.1”, 0.2”, and 0.3”) depth of cut with 0°, 6°, 12° skew angles in Indiana limestone.....	36
Figure 3-8 Test matrix of the 5 mm, 10 mm & 15 mm (0.2”, 0.4”& 0.6”) depth of cut with 0°, 6°, 12° skew angles.	37
Figure 4-1 Plot of forces measured by load cells on bit and rotation measured by instrument versus time: (a) AM 470 bit at 0 ° skew angle (b) the AM 470 bit at 6° skew angle (c) the AM 470 bit at 12° skew angle.....	41

Figure 4-2 Plot of forces for various skew angle, depth of cut, and spacing of AM 470 in limestone (a) normal forces (b) drag forces (c) side forces.....	42
Figure 4-3 Plot of specific energy as a function of skew angle, depth of cut, and spacing for AM 470 in limestone.....	44
Figure 4-4 Plot of normalized average bit rotation (degree/centimeter) for AM 470 bit in limestone.....	45
Figure 4-5 Plot of forces and bit rotation for RZ 24 bit: (a) no rotation with 0° skew angle (b) several full 360° rotations 6° skew angle (c) partial rotation with 0° skew angle (d) partial rotation with 0° skew angle.....	46
Figure 4-6 Plot of forces for RZ24 bit in limestone sample regarding skew angle, depth of cut, and spacing: (a) normal forces (b) drag forces (c) side forces (Kim et al., 2010)....	48
Figure 4-7 Plot of specific energy for RZ24 bit in limestone sample as a function of skew angle, depth of cut, and spacing.....	49
Figure 4-8 Plot of rotation (degrees/meter) for RZ24 bit in limestone sample regarding skew angle, depth of cut, and spacing.....	49
Figure 4-9 Box-plot of data of AM-470 bit in grout regarding skew angle, depth of cut and spacing (a) normal forces (b) drag forces (c) side forces (d) specific energy	51
Figure 4-10 Box-plot of testing RZ 24 bit in grout regarding skew angle, depth of cut and spacing. (a) normal forces (b) drag forces (c) side forces (d) specific energy	52
Figure 4-11 Box-plot of the rotation with AM 470 bit in limestone regarding skew angle, depth of cut, and spacing.....	53
Figure 4-12 Boxplot of bit rotation for RZ24 bit in limestone regarding skew angle, depth of cut, and spacing	54
Figure 4-13 Box-plot of bit rotations for AM470 bit in the grout sample regarding skew angle, depth of cut, and spacing.....	55
Figure 4-14 Box-plot of the bit rotation for RZ 24 bit in the grout sample regarding skew angle, depth of cut, and spacing.....	56
Figure 4-15 Schematic view of the coordination transformation.....	59
Figure 4-16 Schematic view of ANSYS program: constraints of displacement and load and a pair of forces assigned for AM 470 bit geometry.....	62
Figure 4-17 The location of the point of effect of paired forces on AM 470 bit in simulation: This same setting was used for analytical calculation to verify the simulation results.	63

Figure 4-18 Results of displacements after force calculation which initiated bit rotation with ANSYS. (a) rotated-x direction displacement (b) rotated-y direction displacement (c) no rotation in z direction displacement.....65

Figure 4-19 Assumed force location on the RZ 24 bit when bit rubbed against ridge in (a) & (b).....66

Figure 5-1 Pictures of calibration on: (a) normal force (b) drag force (c) the proximeter setting.....74

Figure 5-2 Picture of rotary cutting tests using a single bit on the cutting drum.....75

Figure 5-3 Examples of the recorded data and step by step process of the identification of each revolution. (a) typical input data (b) process of superimposing data with MATLAB.....78

Figure 5-4 Data analysis process. (a) Snap shot of superimposed data (b) output of MATLAB process into Excel file including normal, drag, side forces, and bit rotation79

Figure 5-5 RSM of the RPM and speed relationship: (a) contour plot (b) surface plot.....82

Figure 5-6 Comparison of the bit rotation data with old circuit (Dec _23_09) and new circuit (June _10_10): (a) at 2.5cm (1”) (sample number = 47) (b) at 5 cm (2”) depth of cut (sample number =52).....84

Figure 5-7 Multivariable plot of bit rotation of AM470 bit at 2.5cm (1”) depth of cut regarding skew angle, travel speed, and spacing sorted by: (a) spacing (b) travel speed85

Figure 5-8 Multivariate plot of force trend at 2.5cm (1”) depth of cut regarding spacing, travel speed and skew angle in rotary cutting test: (a) normal forces (b) drag forces (c) side forces.....87

Figure 5-9 Plots of bit rotation and forces of AM470 single bit at 2.5 cm (1”) depth of cut regarding the skew angles, and spacing (outermost first): (a) bit rotations (b) normal forces (c) drag forces (d) side forces (c) specific energy88

Figure 5-10 RSM plots of bit rotations of AM470 bit at 2.5 cm (1”) depth of cut regarding: **a**, skew angles and spacing at 3 m/min (10ft/min) travel speed: (a1) contour plot (a2) surface plot; **b**, skew angles and travel speed at 2.5cm (1”) spacing: (b1) contour plot (b2) surface plot90

Figure 5-11 Multivariable plots of bit rotation for single drum testing of AM470 bit at 5cm (2”) depth of cut as a function of skew angle, travel speed, and spacing sorted by: (a) spacing (b) travel speed92

Figure 5-12 Multivariate plots of forces of single AM470 bit with 5 cm (2") depth of cut as a function of spacing, travel speed and skew angle: (a) normal forces (b) drag forces (c) side forces	93
Figure 5-13 Plots of bit rotation, forces, and SE of single AM470 bit cutting at 5cm (2") depth of cut: (a) bit rotation (b) normal force (c) drag forces (d) side force (e) specific energy	95
Figure 5-14 RSM plots of bit rotation of single bit drum using AM470 bit at 5cm (2") depth of cut: as a function of : a, skew angle and spacing at 4.6 m/min (15 ft/min) travel speed: (a1) contour plot (a2) surface plot; b, skew angle and travel speed at 2.5 cm (1") spacing: (b1) contour plot (b2) surface plot.....	96
Figure 5-15 Effect of depth of cut in full scale rotary cutting test using AM470 single bit for 2.5 cm and 5 cm (1" and 2") depth of cut.	97
Figure 5-16 Picture of AM740 after test : a , after data set of 2.5cm (1") depth of cut was completed: (a1) top view (a2) side view; b , after data set of 5cm (2") depth of cut was completed (b1) top view (b2) side view	98
Figure 5-17 The accumulation of dirt between bit shank and the retainer rings in the RZ24 bit.	99
Figure 5-18 Multivariable plots of bit rotation of RZ24bit at 2.5cm (2") depth of cut as a function of skew angle, travel speed, and spacing for testing sorted by: (a) travel speed (b) spacing.....	101
Figure 5-19 Multivariate plots of forces of single RZ24 bit with 2.5 cm (2") depth of cut as a function of spacing, travel speed and skew angle in rotary cutting test: (a) normal forces (b) drag forces (c) side forces.....	102
Figure 5-20 The box-plot of bit rotation, forces and SE of single RZ24 bit at 2.5 cm (1") depth of cut as a function of skew angle spacing: (a) bit rotations (b) normal forces (c) drag forces (d) side forces (e) specific energy	104
Figure 5-21 RSM plots of bit rotations of single RZ24 bit at 2.5 cm (1") depth of cut regarding : a, skew angle & spacing at 1.52 m/min (5 ft/min) travel speed: (a1) contour plot (a2) surface plot; b, skew angle & travel speed at 2.5 cm (1") spacing: (b1) contour plot of (b2) surface plot.....	105
Figure 5-22 Pictures of multiple bit cutting drum lacing for rotary cutting test: (a) side view (b) front view.....	107
Figure 5-23 Multivariable plots of bit rotation of multiple bit drum using AM470 bit at 2.5cm (1") depth of cut as a function of skew angle, travel speed, and spacing sorted by: (a) travel speed (b) spacing in each box.....	109

Figure 5-24 Multivariate plots of forces of multiple bit drum using AM470 bit at 2.5cm as a function of skew angle, spacing, and travel speed: (a) normal forces (b) drag forces (c) side forces	110
Figure 5-25 Box plot of data of multiple AM-470 bits at 2.5 cm (1") depth of cut: (a) bit rotations (b) normal forces. (c) drag forces (d) side force (e) specific energy	112
Figure 5-26 RSM analysis for bit rotation of multiple bit drum using AM470 bit at 2.5 cm (1") depth of cut against: a , skew angle and spacing at 2.3 m/min (7.5 ft/min) travel speed: (a1) contour plot (a2) surface plot ; b , skew angle and travel speed at 7.6cm (3") spacing: (b1)contour plot (b2) surface plot.....	113
Figure 5-27 Multivariable plots of bit rotation of multiple bit drum using AM470 bit at 5cm (2") depth of cut as a function of skew angle, travel speed, and spacing regarding to: (a) travel speed (b) spacing.....	114
Figure 5-28 Multivariate plots of cutting forces of multiple bit drum using AM470 bit at 5cm regarding skew angle spacing and, travel speed: (a) normal forces (b) drag forces (c) side forces	115
Figure 5-29 Box plots of rotary cutting tests with multiple bit cutting drum using AM-470 bit at 5 cm (2") depth of cut: (a) bit rotations (b) normal forces (c) drag forces (d) side forces (e) specific energy.....	117
Figure 5-30 RSM plots for bit rotation of multiple bit drum using AM470 bit at 5 cm (2") depth of cut against: a, skew angle and spacing at 1.5 m/min (5ft/min) (a1) contour plot (a2) surface plot; b, skew angle and travel speed at 10.18 cm (4") spacing (b1) contour plot (b2) surface plot.....	118
Figure 5-31 The comparison of bit rotations of the multi AM470 bit at 2.5 and 5 cm (1" & 2") depth of cut	119
Figure 5-32 Box-plot of the results of MANOVA analysis for rotary cutting test with single and multi bit drum configuration with different skew angles: (left-side) 2.5 cm (1") depth of cut (right-side) 5 cm (2") depth of cut.....	120
Figure 5-33 Three scenarios for calculating rotation forces (a) spring (b) point spring (c) no device.	123
Figure 5-34 analytical calculation of forces for rotation :left (large scale),right(zoomed in case): (a) regular spring, (b) point spring, (c) no spring	124

LIST OF TABLES

Table 3-1 Physical properties of Indiana Limestone [Kim et al, 2009]	32
Table 3-2 Test matrix for linear cutting tests with the AM470 and RZ24 at various skew angles. Each set (as shown in each row) was repeated at least twice.....	34
Table 3-3 The test matrix for full scale linear cutting tests in 10 MPa (1500 psi) grout using AM470 and RZ24 bits. Each set was repeated at least two times.	38
Table 4-1 Results of estimating forces needed for bit rotation based on analytical solution of resistance force	69
Table 4-2 Calculation of resistance force with the RZ24 bit with experiment settings	70
Table 4-3 Calculation of resistance force with the RZ24 bit with assumption that force was applied at the middle section of the belly of the bit	71
Table 5-1 Test matrix for rotary cutting on engineering grout	75
Table 5-2 Matrix of the test on effect of speed and RPM on bit rotation	75
Table 5-3 Test matrix of cutting at 2.5 and 5 cm (1" & 2") depth of cut: number of tests were performed at particular setting.	108
Table Suppl.A Summary table for the AM470 single bit in 2.5 cm (1") depth of cut.	138
Table Suppl.B RZ24 bit single bit at 2.5 cm (1") depth of cut	139
Table Suppl.C Summary table for the AM470 single bit in 5cm (2") depth of cut.	140
Table Suppl.D Summary table for the multiple rotary cutting tests config. AM470 bits at 2.5 and 5 cm (1" & 2") DCs.....	141

ACKNOWLEDGEMENTS

I would like to express my sincere gratitude and appreciation to my advisor, Dr. Jamal Rostami, for providing me with ungrudging support and guidance. I would also like to thank my doctoral committee members Dr. Francesco Costanzo, Dr. Derek Elsworth, Dr. Larry Grayson, and Dr. Antonio Nieto. Also, I would like to extend my thanks to my friends and colleagues at the Pennsylvania State University for their support.

I deeply appreciate the support of Kennametal Inc. for sponsoring this project. Special thanks to Mr. Chad Swope, Seth Colvin, Eric Gentis, George Coulston and Adam Kelly for providing continuous support throughout the research.

Personally, I would like to thank my family, Dong-Ju Kim, Gi-Sun Kwon, Ji-hye Kim, On-you Kim, and my relatives and friends, YB Park, JK, and HS for their emotional support and prayers. I thank the Lord with all my heart for His guidance.

Chapter 1

Introduction

Various excavation machines have been used for mining and construction of underground structures since the 1950s. Mechanical excavation provides an advantage for many projects in rock excavation (Deliac, 1992; Deliac, 1994). Historically, this technology has been used in many industries including tunneling, underground/surface mining, and oil drilling (Tannant and Wang, 2002). In rock excavation, two types of bits are used and they employ different principles: drag type picks/bits and roller type cutters such as disk cutters (indenters). The drag pick bit breaks the rock by applying force in the direction parallel to the rock surface/cutting (Gehring, 1989; Speight, 1997). Disc cutter or roller type cutters break the rock with an indentation process caused primarily by loading through the normal force in the direction vertical to the cutting surface (Rostami and Ozdemir, 1993; Rostami et al., 1994; Rostami et al., 1995; Rostami, 1997; Rostami et al., 1998; Gertsch, 2000; Rostami, 2008). Usually, drag type tools require less energy to excavate a given volume of rock than roller cutters and are more efficient in rock excavation. However, they have much shorter life in hard abrasive rocks to the extent that their application is infeasible.

Conical bits are one of the dominant cutting tools used in soft rock application, both in mining and civil construction. Various mining machinery use conical bits. This includes longwall drum shearers, continuous miners, and some surface mining equipment. Similarly, there are civil construction machineries that use conical bits including roadheaders, road milling machines, trenchers, a variety of microtunneling machines, and specialized drilling/reaming bits used for directional drilling.

Top priorities of machine operators and designers are optimization and efficiency of the excavation process. This refers to the selection of the proper machine and cutting tools for the application, appropriate lacing of the tools on the cutterhead, shape of the cutterhead, optimum cutting geometry (i.e. spacing of the cutters on the head, penetration), and the cutterhead profile. It also includes assuring the efficiency of the cutters during the operation by changing the cutters on regular basis and using a tool geometry that can maintain cutting efficiency over an extended period of time. A good number of publications in the literature have focused on determining the parameters that affect machine performance as well as classification of the excavation systems (Takacs et al., 2003; Thuro 2003; T. Martín et al., 2005; Whittles et al., 2006; Zaman et al., 2006; Yu and Khair, 2007; Tulu et al., 2008; Tuncdemir et al., 2008). There are many parameters that influence cutting efficiency or the efficiency of the cutting tools. For example, bit angles (rake angle, attack angle, clearance angle), drum lacing, shape and size of bit tip, bit body, and bit materials are among the most crucial parameters that control cutting efficiency. More discussions on the tool selection and optimization and related literature will be offered in chapter 2 of this dissertation. However, one of the important parameters pertinent to the efficiency of conical tools is the ability of the bits to rotate and thus maintain their cutting profile through a process of even wear. Consequently, the rotation of the conical bits is a very important issue in the application of these bits on various excavation machineries and lack of this rotation can cause premature failure of the bits and inefficient cutting.

1.1 Rotation of conical bit

This research focuses on the conical bit rotation mechanisms. Conical bits are called “self-sharpening” bits, where in fact they are “uniform wear” bits (Roxborough, 1973). Theoretically, the advantage of the conical tool is that while it cuts the rock, different sides of the

bit are exposed to the rock, creating a uniform wear pattern, and thus maintaining the conical profile at the tip.

Conical or plum-bob tools were introduced and gained popularity in the 1960s and were widely used in various applications for mining and construction. The first generation of conical tools was a pencil shaped bit. Several iterations of the model using double-sided radial bits had been introduced and used, but they had limited success (Evans, 1961). The idea behind the double-sided radial bit was to use the same bit body twice, which means that this bit life is longer than regular one sided bit since after the one side of the tip was utilized and worn out, then the bit was flipped to the opposite side and that side unused sharp tip can be used. This was rather easy due to the square shape of the bit shank and bit block on the radial tools. However, if the bit shank could be turned in a full/free rotation thus allowing the tip to experience uniform wear on all sides, it could maintain a sharp tip profile. This would naturally lead to a cone shaped tip and supporting body, hence the concept of conical bits was born and put to use.

Turning or rotation of the conical bit is very crucial for more uniform wear and extended life. In practice bit rotation process can be interrupted by certain causes and under certain circumstances. This includes the packing/jamming of the cut material in the annular space between the bit shank and the bit block. If the bit is not locked in place by fines and rock fragments, another possible problem could be the normal loading on the bit. Normal loading can prevent bit rotation due to the frictional forces between the bit shoulder and the bit block. Once the rotation of the bit stops (for any reason), then a uniform wear pattern cannot develop around the tip, and this can lead to steel washout, premature tip failure, tip loss, and overall bit wearing at high rates. Any such situation decreases the efficiency of the conical bits drastically and causes a significant increase in energy consumption during the cutting process. This will directly reduce the production rate of a given machine using the bits.

Another issue of dull or irregularly worn bits is that these bits generate more dust, heat, and/or sparks in harder rock during the cutting process. Elevated temperature at the bit tip can cause bit tip failure and damage to the machine. Any of these conditions could create safety issues and lead to higher risks. Thus there have been many attempts to study these effects and mitigate these symptoms.

There are two approaches to induce bit rotation. One of the successful approaches to maintain sharpness of the bit tip is the introduction of the bit sleeve, which provides an additional rotational contact surface between the bit and the bit block. Another approach for inducing bit rotation is the use of skew angle, which is bit angle from the line of cut. The use of sleeves arguably tends to distribute the highly concentrated stresses of the bit and the block over a larger secondary surface. The use of skew angle is usually related to the installation of the bit block which is welded into the cutting drum. The idea behind this approach is that the frictional forces between the bit tip and the cut surface, which can be subject to change of skew angle, create a torque (or tensional moment around the bit axis) and rotate the bit. Currently, there is no scientific study to support the claim that skew angle in any configuration can assist conical bits to rotate while cutting rock.

Another theory on bit rotation is that it may occur when the bit is out of the cut and is travelling/rattling through the air to get back to its cutting position. This belief is supported by observing the one sided wear pattern of conical bits when they are utilized on the cutterhead of full face machines such as microtunneling and drill bits/reamers. In these applications, the bit is constantly in contact with rock under loading.

Verification of the existence of the bit rotation is the first step to understand the parameters which affect this phenomenon through full scale cutting experiment. The advantage of full-scale cutting in the laboratory is that it can be closely monitored in regard to the cutting parameters and cutting conditions. Another advantage of the full scale cutting relative to

miniature testing is the ability to avoid the scaling problems involved with miniature cutting tests. Full scale test results can be used in explaining the bit rotation mechanism through actual observation. It can also allow for the development of verifiable means of inducing or maintaining bit rotation at various cutting conditions.

1.2 Statement of purpose

This dissertation focuses on the conical bit rotation. Conical bits are one of the most common types of bits used in rock cutting machines across the mining and civil construction industries. Its bit rotation is the primary mechanism of uniform wear of conical bits, and in turn will lead to extend bit life and improved cutting efficiency when and where these bits are applied. Therefore, increasing bit rotation will improve machine production rate and, through extended bit life, efficiency of machine utilization and lead to overall high machine productivity. This high productivity of these machines will directly contribute to lower mining cost, or in civil application, lower overall excavation costs. This study looks into the issue of increasing bit rotation to enhance bit life and cutting efficiency. The issue is of interest to the bit manufacturers and likewise to the end users due to its possible gains through overall machine productivity and lower operational costs.

1.3 Objectives

The primary objective of the study is to examine the mechanism of conical bit rotation through laboratory experiments and modeling to understand the impact of various cutting parameters on bit rotation. This can be accomplished by performing full-scale linear cutting and

rotary cutting tests with an instrumented bit under various cutting conditions. The objectives of this dissertation can be summarized as follows:

1. Development of instruments and systems to monitor and measure bit rotation while the bit is cutting
2. Investigation of bit rotation by performing laboratory experiments including full scale linear cutting and rotary cutting tests.
3. Suggestion of new methods or devices to induce or enhance bit rotation based on findings of the experimental program and modeling.

1.4 Hypotheses

This dissertation is based on the following hypotheses. 1) Rotation of a conical bit occurs by torque, which is generated by eccentric forces acting on the bit tip. 2) For bit rotation, the above noted torque should be sufficient to overcome frictional forces between the bit block and the bit shoulder that prevent the bit from rotating. 3) Using the skew angle has an impact and can induce or enhance the bit rotation. 4) Different spacing, penetration depth, and travel speed also influence bit rotation but their impact needs to be verified. 5) The vibration of the cutter head while it rotates and the contact of bit and the rock surface affect bit rotation.

1.5 Methodology

Full scale rock cutting experiments are designed to test rotation of conical bits in the rock cutting lab at Kennametal Inc, Latrobe, PA, USA. This system has enough capacity and is reliable for conducting full scale tests (Gertsch et al., 2008; Rostami et al., 2009). In addition to this system, auxiliary devices were designed and fabricated to measure the bit rotation and employ the

skew angle on cutting. An instrumented bit which includes a simple circuit was designed for measuring bit rotation. A skew plate was also designed to change skew angle on the bit for various testing configurations.

Full-scale linear cutting and rotary cutting tests were performed to simulate various cutting conditions in mine or construction sites. Linear cutting enhances the understanding of essential cutting parameters without any inference from other bits and cutter head motion. A rotary cutting experiment can demonstrate various field conditions which miners can encounter, since the rotary cutting experiment condition is analogous to mining equipment (roadheader and shearing machine). Linear cutting and rotary cutting tests were performed with different skew angles to assess the impact of skew angle on the bit rotation under various cutting conditions. Chapters 3 through 5 elaborate on the details and results of linear and rotary cutting experiments.

1.6 Contents of this dissertation

This dissertation investigates conical bit rotation as one of the aspects of improved bit and cutting efficiency. The study is based on performing linear cutting and rotary cutting tests and the analysis of the collected data. Chapter 2 addresses the literature review relevant to conical bits and some of the characteristics of conical bits. It focuses on cutting mechanism and other important issues of utilization of the conical bits. Chapter 3 explains the full scale linear cutting experiment including a review of instrumented device design for measuring bit rotation. It covers details of the experimental design for full scale linear cutting tests in limestone and in grout. In chapter 4, results of full scale linear cutting tests in limestone and in grout are described and numerical and analytical simulations are used to support the observation of the bit rotation during linear cutting tests. In chapter 5, the procedure and results of the rotary cutting tests with single and multiple bit settings are presented. This chapter includes the discussions of further testing and

recommended potential solutions. Chapter 6 is a summary of conclusions and recommendations presented by this study.

1.7 Glossary

Bit rotation: defined as the rotation of bit along its axis in tool holder in this dissertation

Cutting speed (travel speed): x- direction moving speed of drum, or cutter head (m/s or ft/min)

Specific Energy (SE): The energy consumed per unit volume of excavated rock (Kw-m³/hr or J/m³)

Skew Angle (offset angle): Angle between line of cut and bit axis projected on cutting surface

Attack Angle: The angle between the rock surface and the axis of the bit (degree)

Rake Angle: angle from the perpendicular line to face of the bit tip (degree)

Chapter 2

Literature Review

Conical tools are common cutting tools on many types of mining and construction excavation machinery for soft to medium rock types. One of the important characteristic of conical bit performance is its rotation along its axis (bit rotation). This rotation allows the bit to maintain its profile and increases bit life as well as cutting efficiency. This fact translates into reduced down time for bit change, higher productivity, and ultimately lower production costs.

Despite the fact that bit rotation is an important feature on conical tools, there is no study of this topic as a standalone subject. No attempt was made to understand the mechanism of bit rotation, when and where rotation occurs, and what controlling parameters can improve or hinder bit rotation. This chapter reexamines the issue of bit rotation in literature review, focuses on subjects related to conical bits, and provides current status of studies on mechanical rock excavation using drag type tools.

2.1 Introduction of literature review

A drag bit is a cutting tool that is generally mounted on the excavation machinery to break soft to medium strength rocks. Bits are usually classified by their types, shapes, components, and levels of cutting force they can apply to the rock surface. In general soft to medium strength rocks have a compressive strength of up to 100 MPa (15,000 psi). Many of the rock types in various mining and construction activities fall in this category including coal, evaporates, soft to medium sandstone and limestone, many types of clay and mudstones, and most shale variations. Point attack tools, which are the subject of this study, are typically used in

medium strength rocks and tolerate relatively abrasive rocks such as sandstone. Thus conical bit tools are typically employed for road headers, continuous miners, drum shearers, road milling machines, trenchers, surface miners, and borer miners (Figure 2-1). There are quite a few studies have been performed for these applications (Evans and Pomeroy, 1966; Lundberg, 1974; Hurt and Evans, 1981; Kumano and Goldsmith, 1982; Brooker, 1983; Hurt and MacAndrew, 1985; Cavender, 1999; Khair, 2001; Khair, 2006; Bilgin et al., 2006; Balci and Bilgin, 2007).

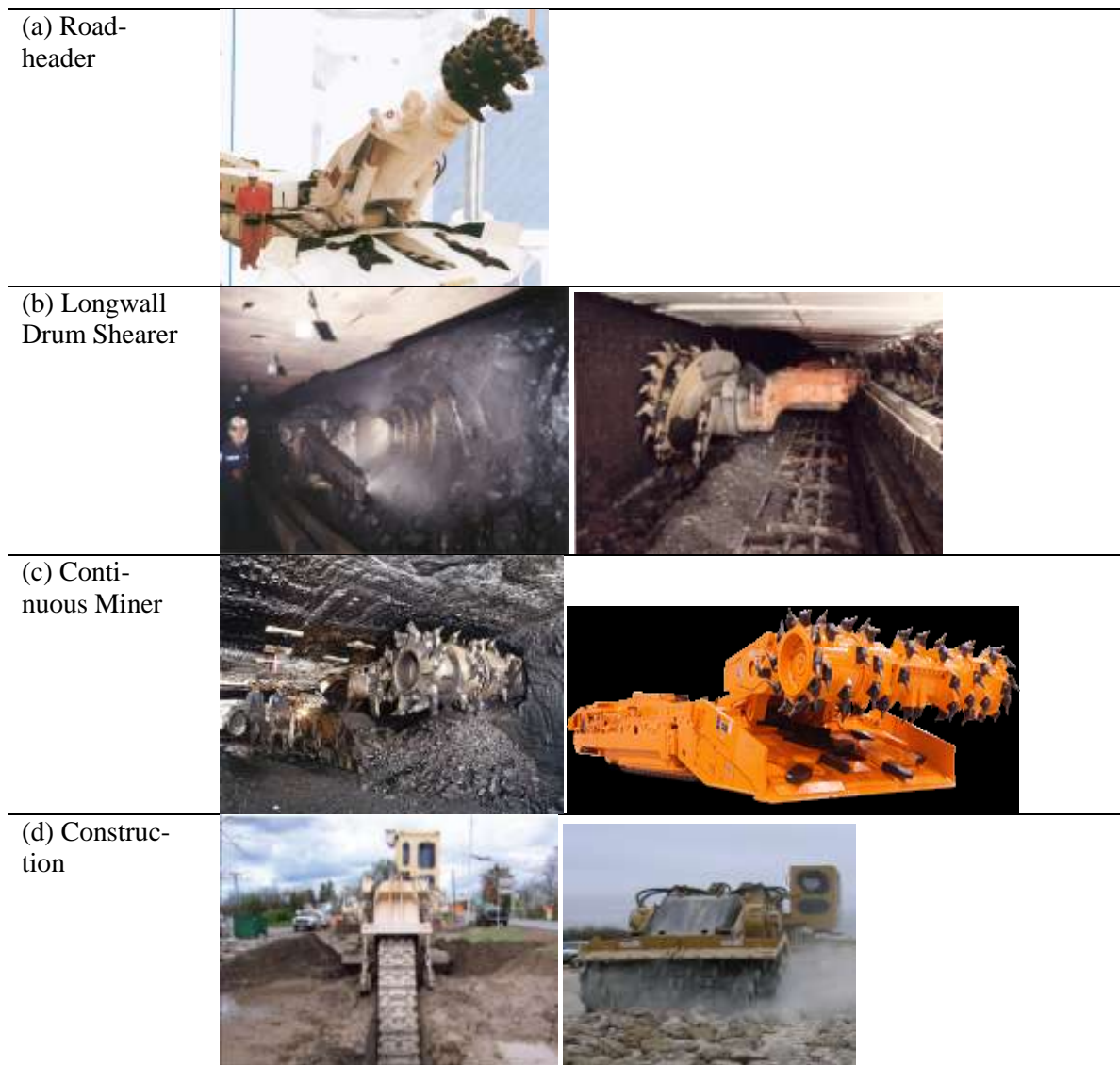


Figure 2-1 Plot Pictures of conical bit application: (a) Roadheader (b) Shearer (<http://www.ulancoal.com.au>) (c) Continuous miner (Joy Mining Machinery) (d) Trenching (Kennametal Catalog)

2.2 Subgroup bits of drag type bit

Drag tools are mainly composed of two tool types (Figure 2-2); radial tools including chisel shape bit, or wedge shape bit, and point attack tools, plum-bob, or conical bit (Roxborough, 1973) . Point attack tools are categorized into three shape types: conical tools, spherical tools, and ballistic tools (Anderson and Rostami, 1997). Sometimes, depending on tool materials, drag tools can be classified into subcategories of diamond enhanced bits (or polycrystalline diamond bit) (Zacny and Cooper, 2004) and carbide insert bits.

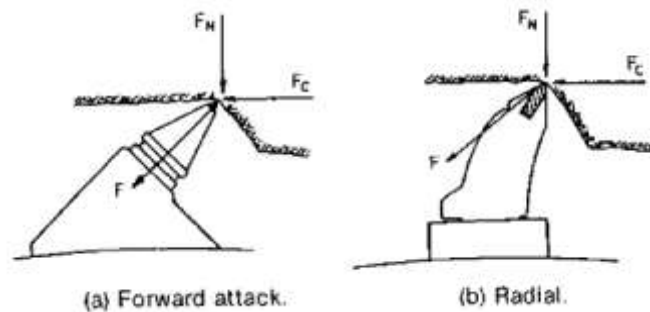


Figure 2-2 Two types of picks on a cutting head, Forward attack or conical, wedge type or Radial (Roxborough and Sen, 1986)

Each bit type has arguably different life time and wear characteristics. Wedge tools (radial tools) tend to have less cutting force, a longer life time and experience less frictional sparking, less wear, and less dust compared to point attack picks (Yilmaz et al., 2007). But their main shortcoming is rapid loss of efficiency as their tips get worn. This short bit life has been observed in many field and lab experiments. On the other hand, other researchers have suggested that point attack picks have less specific energy, and longer life with a uniform wear (Roxborough and Sen, 1986; Goktan and Gunes, 2005). Roxborough and Pedroncelli (1982) proposed that conical bits were more efficient compared to chisel shape bits at higher depth of cut based on three year scientific observation in a South African mine. They believed that in highly abrasive rock conditions, a point attack bit life was longer and more efficient than a chisel-shape

bit. This is in agreement with field and lab observations, especially the idea that conical bits experienced the uniform wear or ‘self-sharpening’ effects while they cut.

2.3 Cutting mechanism

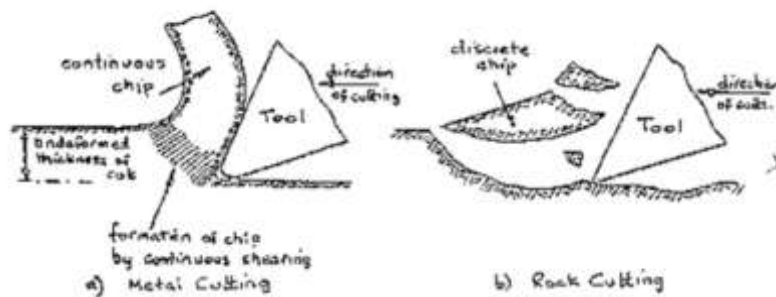


Figure 2-3 Schematic view of metal cutting and rock cutting

A good understanding of the fundamentals of rock fragmentation is necessary for proper selection and application of rock cutting tools. Many researchers have introduced various mechanisms of rock fragmentation using theoretical or experimental methods, and combinations of the two. Sometimes, rock cutting is compared with metal cutting, although metal cutting and rock cutting have some differences on cutting materials and chip production. Metal cutting produces a continuous chip due to the ductility of metal and employs Merchant’s theory to understand or estimate the forces on the bit, while rock cutting produces discrete chips due to the brittleness of rock (Figure 2-3). There is no absolute theory to estimate the cutting forces acting on a drag type cutter from the cutting geometry.

There are several mechanisms for rock failure during cutting in the literature. Some suggest tensile failure for rock fragmentation, while others shear failure to be the dominant mode of failure in rock fragmentation, and failure can also be attributed to mixed mode stress. Evans (Evans and Linzer, 1976) suggested that tensile stress cause rock fragmentation (Figure 2-4). This

theory has been accepted by several researchers. The research group at Istanbul Technical University headed by Bilgin (Balci and Bilgin, 2007) had performed many full scale rock cutting experiments and developed semi-empirical equations based on Evan's theory. Nishimatsu proposed shear stress induced rock fragmentation and employed the "Mohr's circle" to explain crack propagation (Nishimatsu, 1972). This concept was borrowed from metal cutting mechanism (Whittaker and Szwilski, 1973). As a combination of these two model, some researchers (Roxborough and Pedroncelli, 1982; Verhoef and Ockeloen, 1996) proposed that there is a transition point where the rock failure mechanism was changing from tensile stress to shear stress. This transition can be observed by changing bit tool angles or changing the cutting material property during cutting. In the first part, Roxborough indicated this phenomenon was shown at a rake angle between 15 degree and 20 degree. He also made an observation on the material properties transition from brittle to ductile or vice versa.

It is well known that in ductile materials, shearing is the dominant rock failure mechanism and in brittle mode, tensile stress is dominant rock failure mechanism. Ductility and brittleness of the rock are well known properties, which have not been well characterized, especially with qualitative and measureable characterization. These two properties are exclusive and lead to different results of the cutting process in terms of chips, fines, and the optimum pattern of cutting (Deketh, 1995). To quantify these properties, there are several approaches that have been introduced by various parties: the ratio UCS/BTS, Hoek-Brown m-value, or triaxial compression test which was believed to be the most reliable method (Verhoef and Ockeloen, 1996). Sometimes the material changes its properties in regard to stresses; stress condition also should be taken into consideration. By taking accounting estimated rock properties and stress, brittle and ductile (BD) transition stress zones can be predicted. This transient zone can be estimated by plotting volumetric stress which is the sum of the maximum and minimum principle stresses with deviatoric stress, the difference between the maximum and minimum principle

stresses. A sample with a large BD required ductile cutting mode, while a sample with a small BD zone needed brittle cutting mode. While this approach has been considered by many, it has not reached a universal acceptance as of yet.

Apart from these analytical and experimental works, computer technology also has been utilized for better understanding of the cutting process. Numerical simulation of the cutting process has been extensively studied (Jing and Hudson, 2002). Visualizing crack propagation processes in numerical modeling can enhance understanding of details of chip formation and allow for quantitative evaluation of the cutting process where conditions are not easily controlled in laboratory trials.

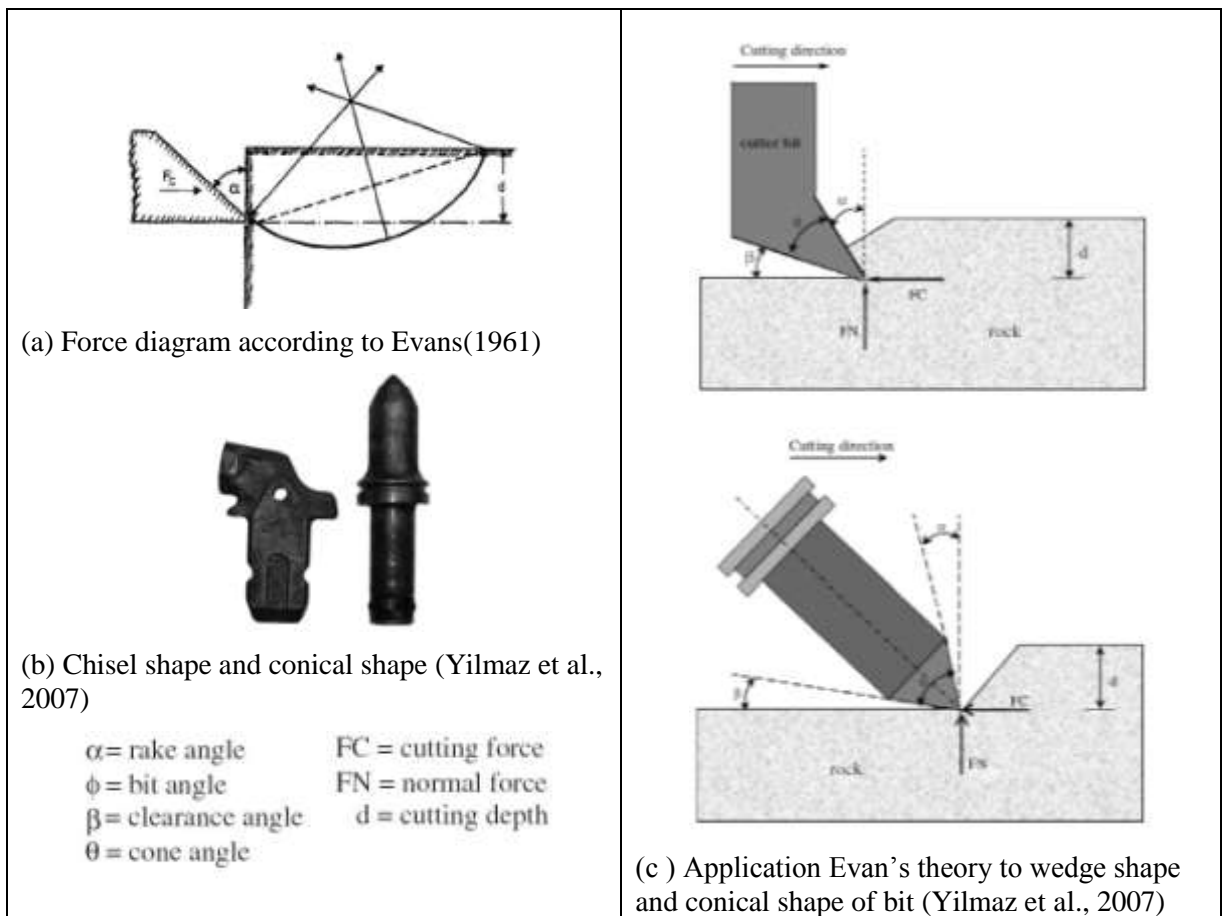


Figure 2-4 Schematic view of Evan's tensile theory and its application

In the beginning of computer simulation, a program called the self meshing FEA analysis was developed (Ingraffea and Saouma, 1985) to simulate crack propagation ahead of a radial tool and to observe crack growth. Due to the computer technology development, currently two major types of programs are widely used in rock fragmentation simulation. One is continuum models such as finite element model (FEM) and the other is discontinuous model such as discrete element model (DEM). FEM treats material as continuous model (Marrey et al., 2006; Zaman et al., 2006) and many commercial programs have employed this principle (i.e. ANSYS, ABAQUS, FLAC, NASTRAN, LS-DYNA, etc) and reveal very good results on static motion or transient dynamic motion of the materials have been obtained by these models. Rock cutting or impact (Saouma and Kleinosky, 1984; Shenghua, 2004; Chiang and Elías, 2008) or bit wear process (Pödra and Andersson, 1999) were simulated with FEM (Tannant and Wang, 2002). Some works have been done on soil and rock consisting of discontinuous grains and discontinuity spacing that would be appropriate to use models based on discrete models (i.e. PFC2D/3D, UDEC2D/3D, etc) which allow analysis of dynamic behavior with the discontinuous materials (Cundall and Strack, 1979; Cundall and Hart, 1993; Hart, 1993). Numerous studies were performed based on discrete model from simple Uniaxial test (Matsuda and Iwase, 2002; Whittles et al., 2006; Tulu et al., 2008; Zhang and Ord, 2008) to complicate rock cutting or excavation simulation with/without dynamic loading (Hentz et al., 2004; Stavropoulou, 2006; Whittles et al., 2006; Jun et al., 2007; Ledgerwood 3, 2007; Schormair and Thuro, 2007; Shmulevich et al., 2007; Yu and Khair, 2007; Onate et al., 2008; Refahi et al., 2008; Rico Ramos et al., 2008; Thuro and Schormair, 2008). The same approach was also used in modeling of excavation of granular media (Holt et al., 2005; Coetzee and Els, 2009a, 2009b) and crushed materials (Refahi et al., 2008).

However, the important factor in using numerical analysis is that good simulation requires supporting evidence or observation/measurements from experimental results or field tests. In simulation, one can carefully determine rock modeling parameters and constitutive

models, and then calibrate the model and have a good agreement with analytical solutions. After reconciliation of experimental results and numerical solution, one can proceed to the next phase for universal usage of simulation for application engineers and researchers.

The physically exerted forces are not the only controlling parameter on rock failure processes. Cutting geometry or conditions are also important factors on the chipping process. Rånman (Rånman, 1985) mentioned that spacing and depth of cut had to be considered as direct parameters affecting chip size and cutting forces (drag and vertical forces). This observation has been confirmed by almost all other researchers where an increase in cutting forces has been closely correlated with increased spacing and depth of cut (penetration). Enhancing the rock fragmentation can be done by considering spacing between cuts which can produce better spalling of the rock barrier between cut without additional energy consumption. Some researchers proposed that (Mishnaevsky Jr, 1994; Bilgin et al., 2006) crack can propagate 5 -6 times wider than depth of cut in brittle material. This can lead to optimum spacing/depth of cut and cutting efficiency. This concept is described in more detail later.

This cutting geometry was also studied in terms of production of dust and noise during cutting using dust collector and Acoustic Emission (Shen et al., 1997). Recently, Khair (Khair, 2001) suggested that optimum spacing and depth of cut (S/D) ratio could lead to efficient energy consumption and less dust, and less specific noise: optimum S/D 1-2 for soft rock, 2-3 for hard rock when using drag type tools. Also he suggested that less force in same condition led to better cutting efficiency (Achanti and Khair, 1998; Khair, 2006).

Various rock properties are needed for predicting machine performance, size and specifications of machines, cutting power, cutterhead design, cutting geometry. Bit type, its wear condition, and modes of cutting with the machine (sumping/shearing) are also important parameters for estimating cutting capabilities and production rates in various ground conditions. Tiryaki (Tiryaki, 2006), Goktan and Yilmaz (Goktan and Yilmaz, 2005), Brook (Brook, 2002),

and Bilgin (Bilgin et al., 2002) along with other researchers have explored the impact of various rock mechanic properties and indices such as fracture toughness, Brazilian Tensile test, and Schmidt Hammer Rebound value to estimate performance and production rates of various types of machine, specifically roadheaders. Also drillability plays an important role in assessing the cutting performance (Goktan and Yilmaz, 2005; Bilgin et al., 2006; Tiryaki, 2006; Tiryaki and Dikmen, 2006).

2.4 Conical bit tip type and skew angle

There are several different bit tip geometries that can be considered for use on a machine depending on applications and geological conditions. Conical type bits use a carbide tip that provides the maximum toughness. This tungsten carbides has been widely studied in its material properties (Lin et al., 1992; Appl et al., 1993; Geoffroy and Minh, 1997; Nobuyuki Mori, 2003 ; Appleby-Thomas et al., 2009; Groover, 2010). High physical bond between the steel bit body and the carbide tip is provided by brazing the carbide into or on the steel body. Bit tips can be categorized into the three classes: Plug, cap, and narrow bottom types. Plug type inserts are usually used in hard and jointed rock. This tip type bits can provide a higher strength tip and can endure high impact and excessive shear forces. Cap type tips provide maximum abrasion resistance, and are subsequently recommended for cutting of soft and/or abrasive materials. The main function of this cap design is to deflect the flow of abrasive minerals away from the bit body by using the extended flanges of the carbide tip mounted on top of the bit body. Narrow Bottom (NB) type tips are used for the intermediate condition between that of the plug and cap type (Figure 2-5).

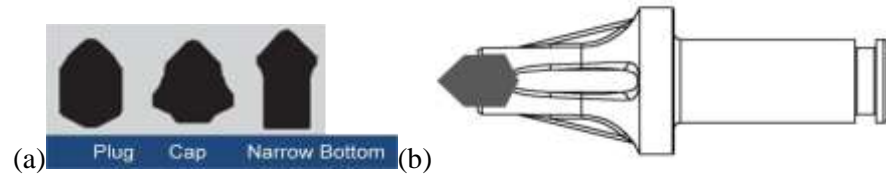


Figure 2-5 Pictures of carbide tip and plug: (a) three different tungsten carbide shapes/styles (Kennametal Catalogue) (b) location of plug insert on bit body

Bit tip geometry is not only an issue for machine designers. The configuration of the bit also requires the intensive attention of machine designer before bits are welded to the drum, since bit body shape also plays a role as a medium to hold the tip and react to the cutting forces. In hard rock applications, the bit body is bigger and wider. A slimmer version is used for softer rock or light loading applications. The slimmer bit bodies make deeper penetration into the rock, and are used where the anticipated bit penetration is more than the carbide tip of the bit. This condition occurs in very soft rocks such as coal, gypsum, trona, and similar rock types. A full discussion of the bit types and bit selection for various applications has been offered by Anderson and Rostami (1997).

One component of machine configuration is a skew angle. This is a widely used concept in the cutting industries dealing with wood, metal, rock, to name a few. In rock cutting, the skew angle is defined as the angle between the line of cut and the projection of the bit axis on rock surface (Figure 2-6). Skew angle has been used for designing the cutting drum with the duty of inducing bit rotation during cutting on the rock surface. The typical skew angle used in the design is from 3° - 5° on the face cutters to 10° - 15° on the gage cutters.

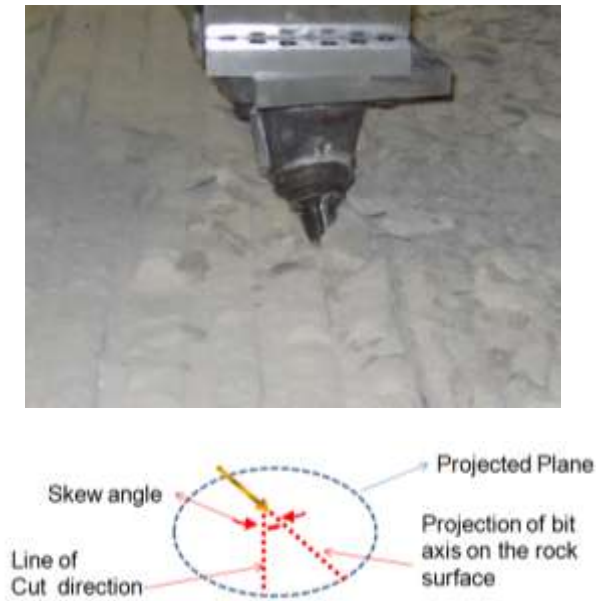


Figure 2-6 Conical bit cutting on the sample at skew angle of 12° (Schematic view of the skew angle based on line of cut and its projection of bit axis)

2.5 Cutting efficiency and bit wear

Cutting geometry (spacing and depth of cut) has a major impact on cutting efficiency. To quantify the efficiency, the concept of specific energy (SE) is employed which usually is defined as the amount of energy consumed for cutting unit volume of rock in hp-hr/cyd, hp-hr/ton, and kw-hr/m³ (Teale, 1965). Lower specific energy (SE) means higher cutting efficiency. From its introduction, there have been many attempts to find proper rock parameters that can be used to determine SE (Tiryaki and Dikmen, 2006). This concept also widely used in drag tool optimization.

Roxborough and Phillips (Roxborough and Phillips, 1975) investigated the relationship between SE and ratio of spacing to penetration (S/P) as well as cutting force, and suggested that there exists an optimum S/P ratio (Barker, 1964). For drag type tools, the optimum range of S/P

ratios falls within 2-4 for average rocks (Barker, 1964; Roxborough and Sen, 1986) and up to 6 for brittle rocks. This is to say that if a penetration of 10 mm can be achieved with a given bit in a rock type, optimum spacing between the cuts (or between the bits) can be 20-40 mm. This allows for cutterhead design optimization to achieve the lowest specific energy and highest productivity.

Recently, Bilgin (Bilgin et al., 2006) reexamined the optimum S/P ratio in their full scale cutting tests, while conducting many experiments to find good indicators for evaluating the cutting performance of excavators. They suggest that SE can be used as a good indicator than can differentiate between various rock cutting tools working in different rock types (Tiryaki, 2008). The theoretical quantity SE only holds true when the condition of the bit is consistent all the time. However, the bits used on excavation machinery undergo natural wear in a simple abrasion wear process. Also, the bit tip can break during the cutting process of the harder material due to excessive or impact loading, thermal stresses, or fatigue. Worn bits are identified during the routine inspection of the cutting drum and replaced with new bits. Unusually high bit wear or frequent breaking of bit blocks in systems generally indicate that something is wrong with a design pattern, fabrication process, the selected bit types, or altogether.

Therefore, bit wear is a key problem influencing excavation machine downtime and its performance, production rates, and costs. This wear sometimes causes critical damage to excavation machine without notice (Khair et al., 1995). As one component of machine wear, bit wear, is controlled by a few parameters: rock properties (especially rock abrasivity), bit and bit tip (carbide) quality, cutter head design and lacing, and mechanical settings and general specification of the excavation machine. The machine settings refers to the bit geometry and its position, lacing of the cutting track, the cutting speed and the cutting method (impact and shear) (Hekimoglu, 1998).

Among various rock properties, rock strength, mineral composition (quartz content), hardness, and rock texture are most relevant to bit wear (Roxborough and Sen, 1986). There are

many attempts to investigate the force on excavation machines considering abrasivity of the target materials (West, 1989; Ersoy and Waller, 1995; Nobuyuki Mori, 2003; Takacs et al., 2003; Ozturk et al., 2004; Bardetsky et al., 2007; Onate et al., 2008). Correct assessment of drill-ability of the target material can be one solution that prevent excessive bit wear (Hoseinie et al., 2008). This also can be achieved by estimating cutting tool condition while it cuts, the analysis of results of laboratory experiments, or numerical simulation (Gajewski and Jonak, 2006).

Bit wear causes changes in bit shape. Due to changes of the rake angle and the clearance angle, and the bluntness of the bit tip, the efficiency of rock chip production will decrease. There is a need for clear cut description of the wear process. Theoretical drag tool wear types are described by Deketh (Deketh, 1995). There were several basic wear mechanisms: (1) adhesion-adhesive material transferring from one surface to another, (2) abrasion - material failure by abrasion (micro-ploughing, micro-cutting, micro-fatigue, micro-cracking), (3) tribochemical reaction - rubbing contact wear processes by removal or formation of reaction layer, and (4) surface fatigue - repeated loading, crack propagation and chipping generation. There are limited theoretical works on this topic, which have not been widely used in actual practice.

In practice, bit wear can be predicted by its location on the drum or machinery by prediction of geometry changes in the given environment. Heikemoglu suggested that wear depended on the offset angle(or skew angle) which is the angle from the bit axis to the cutting line (Hekimoglu, 1998). He also proposed that bits in a single cutting track had better resistance to wear than those in multiple tracking, due to lower penetration, and lower applied forces. In single tracking, the bit may have a shorter life but the overall production per bit is higher compared to multiple tracking designs.

However, sometimes this optimal wear does not occur for several reasons. One of the most dominant problems in using the conical bit is that the rotation of the bit is hindered or stops. This could happen due to a build-up of material (fines) between the bit holder and the bit shank.

Thus the bit attacks the rock on the same face and will be subjected to non-uniform wear. In such conditions, the bit loses its efficiency very rapidly and need to be replaced very frequently. There are also other potential causes for inefficiency in the cutting process. This includes loss of the tungsten carbide insert or tip loss by premature failure of the brazing between the bit tip and bit body. Another issue is the steel wash out which refers to the wear of the bit steel body by abrasive material. When the steel body of the bit is gradually removed, rendering the tip (carbide) without support. In this case, the bit tip also falls and is lost. The later scenario can to some extent be mitigated by using of the cap style tip.

Additionally, appropriate static or dynamic friction between the bit and cutting materials (Brian Armstrong et al., 1994; Irfan and Prakash, 2000; Liu et al., 2007) could lead to less wear and long bit life by reducing friction (Hoseinie et al., 2008). Reduction of friction could be achieved by appropriate material selections depending on cutting materials. Another implication of this concept is using water, surfactant, or chemical mixture fluid in cracks (Staroselsky and Kim, 1997; Ostermeyer, 2003) considering right spray location and rust of bit body.

2.6 Cutting force and bit rotation

Before the 1980s, force analysis on cutting tools was two-dimensional. Due to the simple configuration of the wedge cutter, two dimensional forces were enough. However, from 1980s, complex shapes of point attack tools have been widely used and there was a need for three dimensional forces analysis. Hurt and Evan analyzed the force of the point attack tool and calculated force trigonometry of the groove and the bit tip shape(Hurt and Evans, 1981). From this effort, normal force, side force, and drag force are conventional forces in analysis on cutting force (Figure 2-7). These forces might lead to bit rotation.

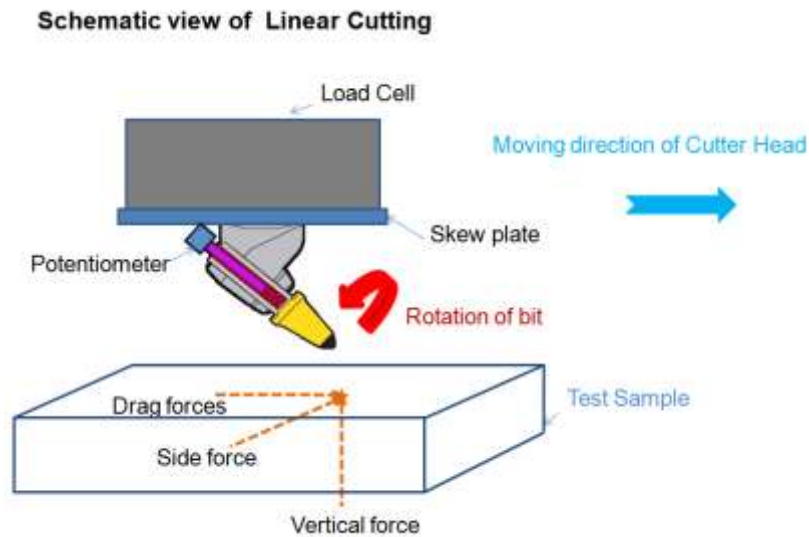


Figure 2-7 Example of three direction of forces with schematic view of Kennametal Inc system

Even though there are many studies dedicated to cutting forces, there are only few studies that briefly mention bit rotation and its impacts on bit cutting efficiencies. Some researchers assumed that bit rotation induced uniform wear, or uniform bluntness of conical bits (Hurt and Evans, 1981) and hypothesized that the type of rock, the clearance angle of bit, and the skew angle (angle from the line of cut) could be important factors used to determine bit rotation. Some researchers reported observations of conical bit rotation and presumed that the bit rotation might be induced by torque at the contact point, but not during the whole cutting process (Hekimoglu, 1998).

Other researchers proposed that a new type of bit. The “Frustum bit”, is a trial bit with concave tip shape that was intended to rotate during the cutting process and was suitable for surface grinding and cutting of material such as metals, polymer, and composite material (Kim et al., 2009). The initial trials have proven that the cutting forces and the specific energy of these bits are much higher than regular conical bits. There is no mention of bit rotation in the published

material on this bit. Currently they are not used on mining and construction machinery, and the results of trials of this bit were not supporting their successful use in rock cutting(Asbury et al., 2001). Overall, the review of the literature shows that there is no published work on the process or mechanism of bit rotation or any direct measurement of bit rotation in lab testing or field experiments. It should be noted that the study of the conical bit rotation is of importance for the mining and Earth works group within Kennametal Inc and they have sponsored the current study to seek means of improving bit rotation and thus conical bit life and performance in various applications.

Chapter 3

Linear Cutting Experiment Setting

3.1 Instrumentation and installation

In order to objectively study rotation of the conical bits, a system of measuring bit rotation was needed to allow for monitoring of bit rotation under various cutting conditions. To study parameters impacting bit rotation it was decided to examine the issue in a laboratory environment, since field testing involves a time-consuming and costly process, meanwhile for lab testing, full scale cutting tests had to be used to show the actual bit cutting and the rotation while cutting rock, since scaling is known to be ineffective in rock excavation. A handful of laboratories are capable of performing full-scale rock cutting tests. One of these facilities is at Kennametal Inc's complex located in Latrobe PA.

The full-scale linear and rotary cutting test for investigating conical bit rotation took place at Kennametal Inc (KMT). This facility is appropriate for performing the tests needed for this dissertation. This facility has been used in some of the previous projects, such as a low-energy planetary excavator cutterhead (Kim et al., 2009/2010 Rostami et al.2009).

The rock cutting facility had to be reconfigured to allow for measurement of conical bit rotation. The Kennametal rock cutting test fixture is a sizable piece of equipment that allows for mounting rock samples up to 1.5 x 2.4 x 0.6 m (5' x 8' x 2') on the table and excavating the sample by cutter heads of up to 1.2 m (4") in diameter. The machine allows for control of the position of the cutterhead in 3D, and the rotational speed of the head is controlled by a Variable Frequency Alternative Current (AC) drive. The motion of the cutterhead and table is controlled by a Programmable Logic Controller (PLC). Also, this facility already possesses that most of

instruments required for this study. This includes load cells to measure cutting forces, a power transducer to measure power consumption of the drive unit, and a proximeter to monitor cutterhead rotation.

The test system consists of several components: a supporting beam, side movement rails, concrete supporting walls, a mounting flange for the cutterhead, a dust collector, and a sample table (Figure 3-1). The supporting beam has one rail that guides the cutting drum in a longitudinal direction. A mounting flange for the cutterhead has a proximeter sensor, which detects the position of the cutterhead.

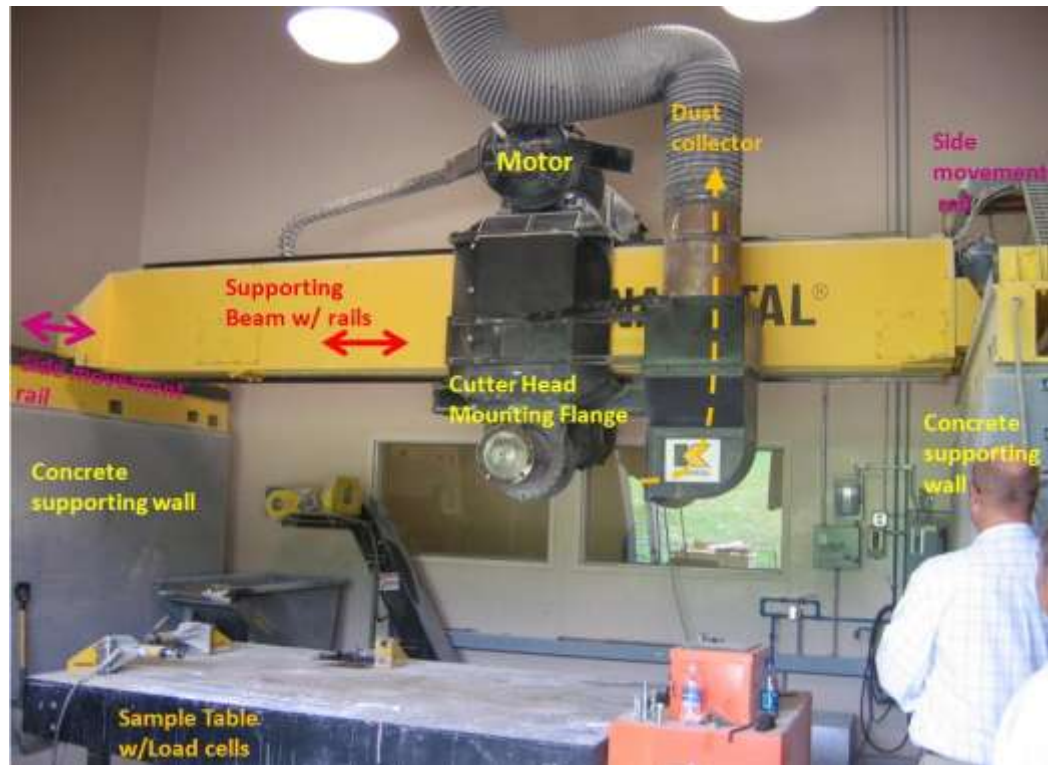


Figure 3-1 Picture of cutting test fixture in Kennametal cutting lab

The sample table holds the rock samples with four vertical posts and two horizontal hydraulically actuated jacks. The hydraulic jacks can move the table up and down in the vertical

direction. Six load cells are embedded under the sample table, two in horizontal directions and four in vertical directions at the four legs of the table.

The dust collector is in front of the cutterhead. The suction pump can collect dust particles during the cutting and deliver them to a container through the dust conduit. Load cells are set up to measure cutting forces in three orthogonal directions including normal, side, and drag (Z, Y, and X direction on the table). Load cells(9167A) are primarily Piezoelectric accelerometers/made by Kistler. For linear cutting test the load cell was mounted on a gear box of the machine for higher rigidity. However, for rotary cutting tests, the load cells were mounted on a 50.8 cm radius by 50 cm long heavy duty steel drum and the data was transmitted to the data acquisition system via an antenna.

The data acquisition system (DAS) using for data collection is a Yogokawa WE 7000 with WE7271/WE7272 modules which can achieve maximum 100kHz sampling rate when it analyze single channel (Kistler brochure) . This system monitored 20 channels at a sample rate of (200Hz) and has signal conditioning capabilities. The system was configured to monitor four load cells under the table in vertical directions, two load cells mounted on the table in horizontal direction, spatial location of the bit (X, Y, Z) and a 3D load cell mounted under the bit, in addition to cutterhead power, and the proximate to track cutterhead rotation if needed. The travel speed in the x direction and the RPM of the cutterhead were controlled by PLC of the rock cutting fixture.

3.2 Conical Bit Instrumentation

The approach for this study was to develop a simple electronic device mounted on the bit, to measure bit rotation at various cutting conditions. Figure 3-2 shows a schematic drawing of the instrumentation plan used for measurement of the rotation. The potentiometer was connected to

the bit through an axial insert which allows for the free movement of the bit in the bit holder, along the bit axis as well as rotation in the bit block. This arrangement allowed for measurement of rotation in both directions and can be refined based on the initial testing results to obtain proper measurement resolutions for the given set of parameters.

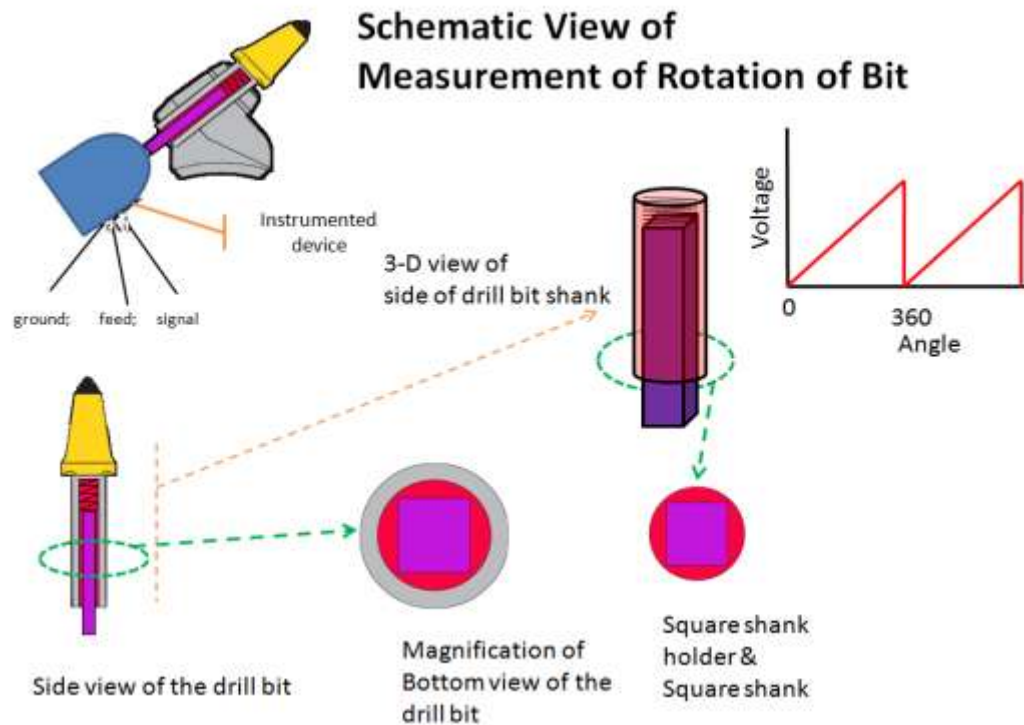


Figure 3-2 Schematic view of measurement of bit rotation.

With the instrumentation of the bit rotation in place, testing of the bits under various working conditions in linear cutting or rotary cutting tests could be performed. The preliminary design of the circuits for bit rotation measurement started in the fall of 2008. Subsequently, two bit blocks and some conical bits were selected by KMT mining and construction group for testing. These sets were delivered to PSU for the assembly of the bit rotation instrument. The bits/blocks selected for the initial testing included the AM 470 and the U765 mining bits, and the RZ24 construction bit from Kennametal standard production line. These bits were selected to

represent the most popular bits used in the mining and construction industry, and are considered to be of a moderate size among mining and construction products. The shank size for the mining bits is 1" (25mm) and for the construction bit it is 0.76" (19 mm) which is the middle of the road for each group. Also these bits are respectively used in 50° and 45° rake angles which are within the range of widely accepted the optimum rake angle (Evans and Pomeroy, 1966).

The bits and bit blocks were machined at the Earth and Mineral Science (EMS) machine shop at Penn State University (PSU) to mount the selected rotary potentiometer in order to measure bit rotation without adding any obstacles or additional loads, which would prevent bit rotation (Figure 3-2). In other words, the designed measurement system allowed free rotation of the bits. The system was designed to be mounted on the back end of the bit block and connected to the bit shank through a hinged shaft, which allows for minor out of axis movement of the bit and limited axial motion. This allows for mounting assembly of the bit on the blocks as they are normally used in the field while protecting the rotation sensor. The measurement circuit included a Wheatstone bridge to measure electrical signals from the potentiometer. The initial testing on the potentiometer showed the perfect saw-tooth signal, representing a linear variation of the voltage with bit rotation.

A special bracket was designed and fabricated by KMT to allow mounting of the load cell on the gearbox of the drum. This was considered to be advantageous in two ways; first is the added rigidity of the system, and secondly direct wiring to join the load cell to the data acquisition system. Additional cables were pulled through the cable conduits and a connection box allows for simple mounting and running of the load cell from the new location. After installation of modified bracket, the PSU-KMT team assembled the bits and bit blocks and the rotation sensing system (Figure 3-3). A new mounting system capable of changing bit skew angle was designed and fabricated by Kennametal in order to allow for variation of the skew angle. The skew plates allow for the rotation of the bit at 3° increments between 0° and 15° on each side

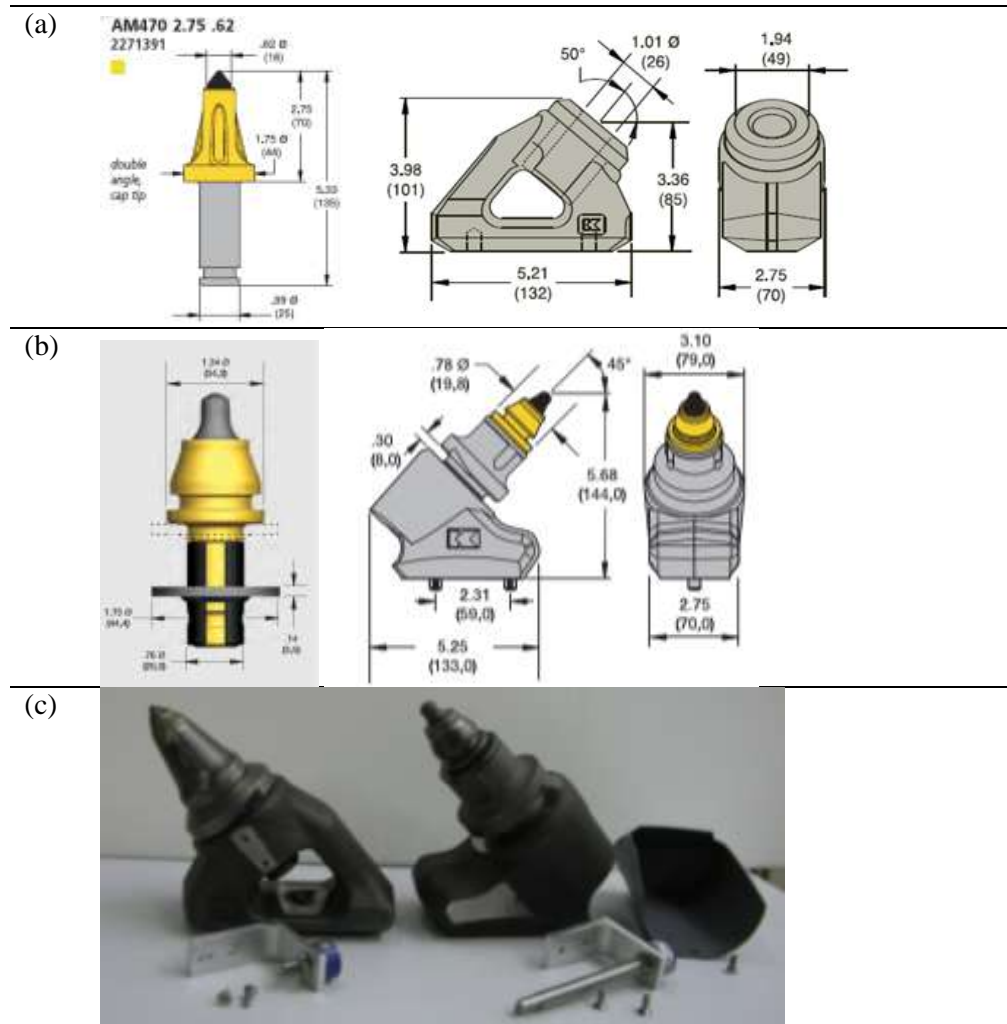


Figure 3-3 Pictures of selected bits :(a) AM 470 bit and K25S block (b) RZ 24 bit and KPF301 block (c) instrumented U 756 bit and KPF 301 block; RZ 24 bit and R25s bit block.

Five additional lines were directly connected to the DAQ system to install the customized bits and preserve the configuration of the present data acquisition system. This allows for switching between the load cells when used in a fixed position or when a load cell is mounted on the rotary drum. The load cell is connected to the charge amplifier by a standard 9 pin connector and to the data acquisition system via different cables. The new cables also connect the rotation sensor to the DAQ system (Figure 3-4).



Figure 3-4 Pictures of (a) test set up with load cell mounted on the gear box using the new bracket
(b) AM 470 bit ready for testing with the bit rotation sensor

Calibration and data analysis programs were set up to reflect the new configuration of the data channels and the sequence of information from various instruments. The system was initially set up with the AM 470 bit for linear cutting tests (Figure 3-4b). The linear cutting tests were started in fall 2008.

3.3 Linear cutting test in limestone

The experimental program for this study involved full scale linear cutting tests where various bits were used to excavate the rock while measuring bit rotation (Figure 3-5) (Kim et al., 2009).



Figure 3-5 Picture of rock surface with different cut spacing during the linear cutting tests (Kim et al., 2009)

This machine is supported by two concrete walls and a system of steel guide rails which allows cutterhead and drum to move in a horizontal plane covering two orthogonal directions (X and Y). The table that carries the sample can move up and down and covers the required movement in the vertical direction (Z-direction) and control the depth of cut. The testing of conical bit rotation started with full scale linear cutting tests on a sample of Salem (Indiana) limestone, a commonly referenced rock type. Physical properties of the limestone sample can be found in Table 3 - 1 [Kim et al, 2009]. The sample block dimension was 1.8 m x1.2 m x0.6 m (6 ‘x 4’ x2’).

Table 3-1 Physical properties of Indiana Limestone [Kim et al, 2009]

Rock Properties	Value
Unconfined Compressive Strength	50 (MPa)
Young’s Modulus	17.3 (GPa)
Indirect Tensile Strength	3.1 (MPa)
Direct Shear Strength	3.9 (MPa)
Poisson’s Ratio	0.25
Specific Gravity	2.2
Flexural Strength (3-point loading)	7.3 (MPa)

Measurement and instrumentation system including the load cells and bit rotation device as well as the machine motion sensors were calibrated at the beginning of each day. This calibration verified the linearity of the system and developed calibration factors for the forces and the data acquisition system (Figure 3-6). Once the calibration results showed the repeated and linear responses, actual testing was commenced.

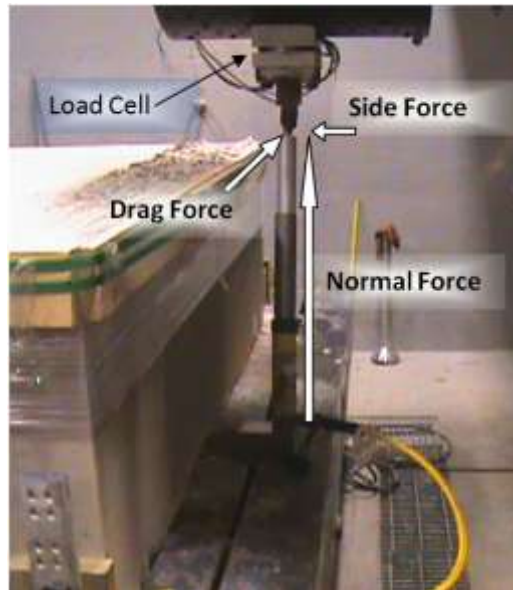


Figure 3-6 Calibration of load cells which are embedded on the sample tables and behind the bit(Kim et al., 2009)

3.3.1 Linear cutting test design in limestone

In total 908 lines of cut were performed; 582 lines of cut for AM 470 and 326 lines of cut for RZ 24 bit. There were four variables that made up the test matrix:

- Bit type (AM470 and RZ24)
- Skew Angle (0, 3, 6, 12, and 15 degrees)
- Penetration Depth (2.54 mm, 5.08 mm, and 7.62 mm)
- Cut Spacing (25.4 mm, 38.1 mm, 50.8 mm, and 63.5 mm)

At the 7.62 mm penetration depth, high forces were experienced and deemed a bit risky with the current capacities of the machine. A decision was made to limit the depth of penetration to 5 mm. The detailed summary of the test matrix and testing parameters for the linear cutting tests is provided in Table 3-2

Table 3-2 Test matrix for linear cutting tests with the AM470 and RZ24 at various skew angles. Each set (as shown in each row) was repeated at least twice.

Bit Type	Skew angle (degree)	Penetration (mm)	Spacing (mm) (repetition #)
AM 470	0	2.54	25.4(8), 38.1(8), 50.8(6), 63.5(6)
AM 470	0	5.08	25.4(8), 38.1(8), 50.8(6), 63.5(6)
AM 470	0	7.62	25.4(8), 38.1(8), 50.8(6), 63.5(6)
AM 470	3	2.54	25.4(8), 38.1(8), 50.8(6), 63.5(6)
AM 470	3	5.08	25.4(8), 38.1(8), 50.8(6), 63.5(6)
AM 470	6	2.54	25.4(8), 38.1(8), 50.8(6), 63.5(6)
AM 470	6	5.08	25.4(8), 38.1(8), 50.8(6), 63.5(6)
AM 470	6	7.62	25.4(8), 38.1(8), 50.8(6), 63.5(6)
AM 470	12	2.54	25.4(8), 38.1(8), 50.8(6), 63.5(6)
AM 470	12	5.08	25.4(8), 38.1(8), 50.8(6), 63.5(6)
AM 470	15	5.08	25.4(8), 38.1(8), 50.8(6), 63.5(6)
RZ 24	0	2.54	25.4(8), 38.1(8), 50.8(6), 63.5(6)
RZ 24	0	5.08	25.4(8), 38.1(8), 50.8(6), 63.5(6)
RZ 24	6	2.54	25.4(8), 38.1(8), 50.8(6), 63.5(6)
RZ 24	6	5.08	25.4(8), 38.1(8), 50.8(6), 63.5(6)
RZ 24	12	2.54	25.4(8), 38.1(8), 50.8(6), 63.5(6)
RZ 24	12	5.08	25.4(8), 38.1(8), 50.8(6), 63.5(6)

Note:

- i) All the tests listed in this table have been conducted on Indiana Limestone.
- ii) Each pass comprises 8 lines of 25.4 mm spacing, 8 lines of 38.1 mm spacing, 6 lines of 50.8 mm, and 6 lines of spacing 63.5mm.
- iii) Bracket deflection due to high forces at 7.5mm depth of cut with a higher spacing with skew angle 6° on AM 470 bit.

At the 7.62 mm penetration depth, high normal, drag, and side forces were experienced and a decision was made to limit the depth of penetration to 5 mm. At each penetration, with the same skew angle, four different spacing were laid out on the sample and tested in each path. Often the sample was cut at the same depth more than once to add to the number of the data lines and assure that tests were replicated enough to yield good results. Length of the cuts was around 1.8 m (6 ft) or cutting along the longest dimension of the sample. Figure 3.7 shows the layout of the cuts on the limestone sample.

After completing limestone cutting tests, additional tests were performed in a softer sample which was 10Mpa (1500 psi) engineering grout to verify the impact of deeper cuts and higher depth of penetration. This additional test could simulate the action of the bits in coal mines or softer rocks. It also allowed for closer examination of the effect of deep cuts on bit rotation when forces distribute differently over more of the bit and cutting area. Due to the machine capacity and rigidity, tests were only performed within the range of 5-10 mm in 10Mpa grout.

3.3.2 Preparation for experiment condition setting in limestone

The test matrix for full scale cutting test on the conical bits for the monitoring of bit rotation was designed to provide a wide range of information for subsequent analysis. Testing included several different parameters such as the bit type, skew angle, depth of penetration, cut spacing, and in the subsequent tests, various cutting medium such as rock type and samples of engineered grout blocks with given compressive strength.

A new mounting system capable of changing bit skew angle was designed and fabricated by Kennametal in order to allow for variation of the skew angle. The skew plates allow for the rotation of the bit at 3° increments between 0° and 15° on each side. At specific skew angles, cutting tests were performed at various cut spacing and penetration. Thus, depth of cut, penetration, was performed in 2.54 mm and 5.08mm (0.1”and 0.2”). At each depth of cut, which constituted a pass across the surface of the sample, the cut spacing varied from 25.4 mm, to 38.1 mm, 50.8 mm, and 63.5 mm (1”, 1.5”, 2”, and 2.5”) (Figure 3-7). Length of the cuts was around 1.8 m (6 ft) or cutting along the longest dimension of the sample. Often more than one path was cut at a certain depth of penetration to generate sufficient number of cut lines for subsequent analysis.

In this experiment, the deeper depth of cut, 7.62mm, could not be performed. One test was performed at 7.62 mm at 0° skew angle and the system showed potential deflection on connector between machine and rail system due to excessive load over than machine normal capacity. Thus, to prevent any further accident and to protect the current system from any damages, tests more than 7.62mm depth of cut were not performed.

The selected skew angles for testing included the following; 0°, 3°, 6°, 12°, and 15°. These angles cover the range of common skew angles used on various cutterheads (0° -10°). Test of the RZ24 bit was limited to 0°, 6°, and 12° skew angles to minimize the number of tests.

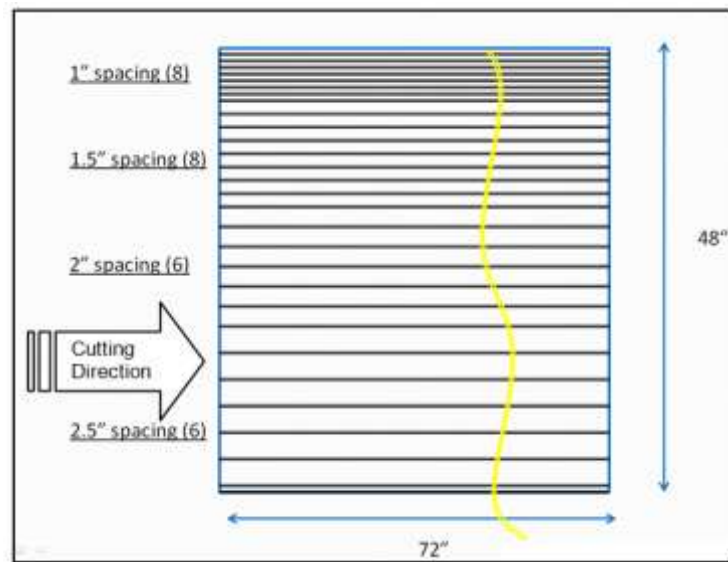


Figure 3-7 Test matrix of the 2.54 mm, 5.08mm, and 7.62mm (0.1", 0.2", and 0.3") depth of cut with 0°, 6°, 12° skew angles in Indiana limestone

3.4 Linear Cutting Test in Grout

After completing limestone cutting tests, additional tests were performed in a softer sample which was 10Mpa (1500 psi) engineered grout to verify the impact of deeper cuts and

higher depth of penetration. This additional test could simulate the action of the bits in coal mines or softer rocks. It also allowed for closer examination of the effect of deep cuts on bit rotation when forces distribute differently over more of the bit and cutting area. Due to the machine capacity and rigidity, tests were only performed within the range of 5-10 mm in 10Mpa grout.

The linear cutting tests on the grout test aimed to examine the effect of deep cuts on bit rotation when point of effect of the side and drag forces (possibly the frictional forces against bit body) are closer to the bit shoulder. The layout of cuts on the grout sample for linear cutting test at higher depth of cut is illustrated in Figure 3-8. Due to the machine capacity for lateral/drag forces, cutting tests in lower strength grout (~1500 psi) were limited to the range of 5-10 mm (0.2"- 0.4") depth of cut.

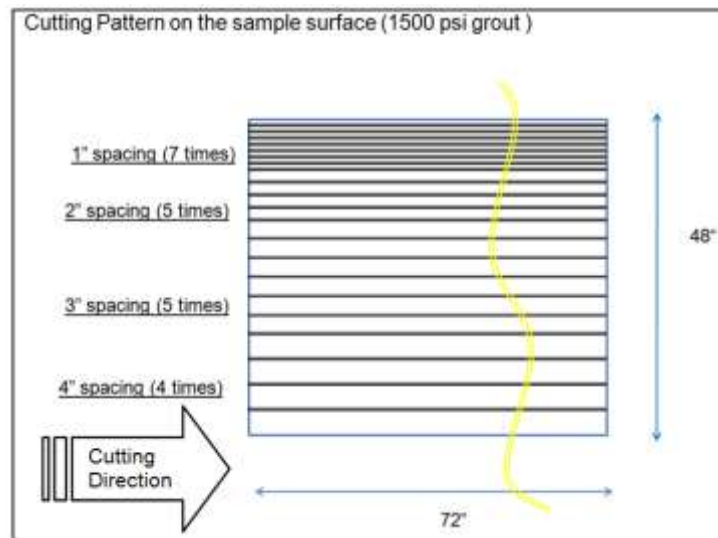


Figure 3-8 Test matrix of the 5 mm, 10 mm & 15 mm (0.2", 0.4" & 0.6") depth of cut with 0°, 6°, 12° skew angles.

A total of 531 were performed and analyzed in grout sample: 291 cuts with AM 470 bit and 240 cuts with RZ 24 bit. The surface of the sample was divided into various spacing sets

from 25.4 mm through 101mm (1", 2", 3", & 4"). Other important parameters included skew angle (0, 6, and 12 degrees), penetration depth, 5.08 mm, 10.1 mm, and 16 mm (0.2", 0.4", & 0.6"). Testing for each set of parameters was repeated several times to assure the accuracy of the measurements and to provide sufficient data for subsequent analysis. The test matrix and the number of cuts at each spacing are summarized in Table 3-3.

Table 3-3 The test matrix for full scale linear cutting tests in 10 MPa (1500 psi) grout using AM470 and RZ24 bits. Each set was repeated at least two times.

Bit Type	Skew angle (deg)	Penetration (mm)	Spacing (mm)
AM 470	0, 6, & 12	5.08, 7.62, & 10.16	25.4, 10.16, 76.2, & 101.6
RZ24	0, 6, & 12	5.08, 7.62, & 10.16	25.4, 10.16, 76.2, & 101.6

* randomized the sequence of cutting within same test set to see the impact of cut sequence

Chapter 4

Data Analysis on Linear Cutting Tests in Limestone and Grout

4.1 Data Analysis Program

To analyze collected data, an Excel spreadsheet was designed with Visual Basic macro program. The program allows users to import the data into a template and combine the data as required to observe various parameters (i.e. combining data from various load cells to estimate forces acting on the bit). The program uses the pertinent calibration factors to estimate bit location, cutting forces, and bit rotation from measured voltages. Other features of the program include the visual aid for the observation of the cutting parameters and for development of charts, in which the user can see the variations of the forces, select a window for zooming to observe the variations, and perform analysis within selected region of data with calculation of mean, median, min, and max for each parameter.

4.2 Test Results and Data Analysis in Limestone

4.2.1 AM 470 bit in limestone

Figure 4.1 shows a typical data line for cutting in limestone. This includes the measured forces and bit rotation. In these figures, the dashed line indicates the range of the data (window) for data analysis of cutting. The data before bit engagement with the rock was used as the initial reference points, which are considered to be the load cell read out before contact, or simply the zero level. Once the data lines were analyzed, they were grouped and averaged for each setting

(given spacing, penetration, and skew angle). The summary reflects the measured forces and measured rotation for each test setting.

The preliminary results showed some sporadic rotation of the bit but no systematic rotation when cutting with AM 470 bit. This is true even at 0°, 3°, 6°, 12°, and 15° skew angles. This simply means that running the bit with various skew angles does not seem to impact the rotation of the bit.

There was a limited variation of bit rotation signal (green line) observed in most of the tests. One possible scenario is that this small vibration occurs by stick-slip behavior of lock and release motion of the bit. It could also occur due to motion of impacting and hitting of the bit on the rock surface either at the beginning of the cut or when large chips are formed, where the bit re-engaged the rock. The observed bit rotations were small and arbitrary, instead of a systematic bit rotation in a specific direction. Even with various skew angles, no systematic rotation was observed.

To find any potential general trends for parameters, normal force, drag force, side force, and bit rotation were plotted with different depth of cut, spacing and skew angle with box-plot in MINITAB 14®. Generally, normal force and drag force tended to increase with increment of depth of cut and cut spacing which are generally found in literature review (Barker, 1964), while normalized rotation (rotation of the bit for the entire line of cut divided by the length of the cut to yield deg/meter) seems to be inconsistent and not showing any trends. As mentioned earlier, due to the machine capacity, the set of 7.62 mm depth of cut was not completed and eliminated from analysis of test results. Under given depth of cut, normal, drag, and side force are shown in Figure 4-2a through Figure 4-2c (Kim et al., 2010). Interestingly, normal force and drag force does not show any response with respect to increment of skew angle (Figure 4-2a and Figure 4-2b). Normal, drag, and side force are increased with increased depth of cut and spacing. In most cases, the side force tends to increase with skew angle (Figure 4-2c).

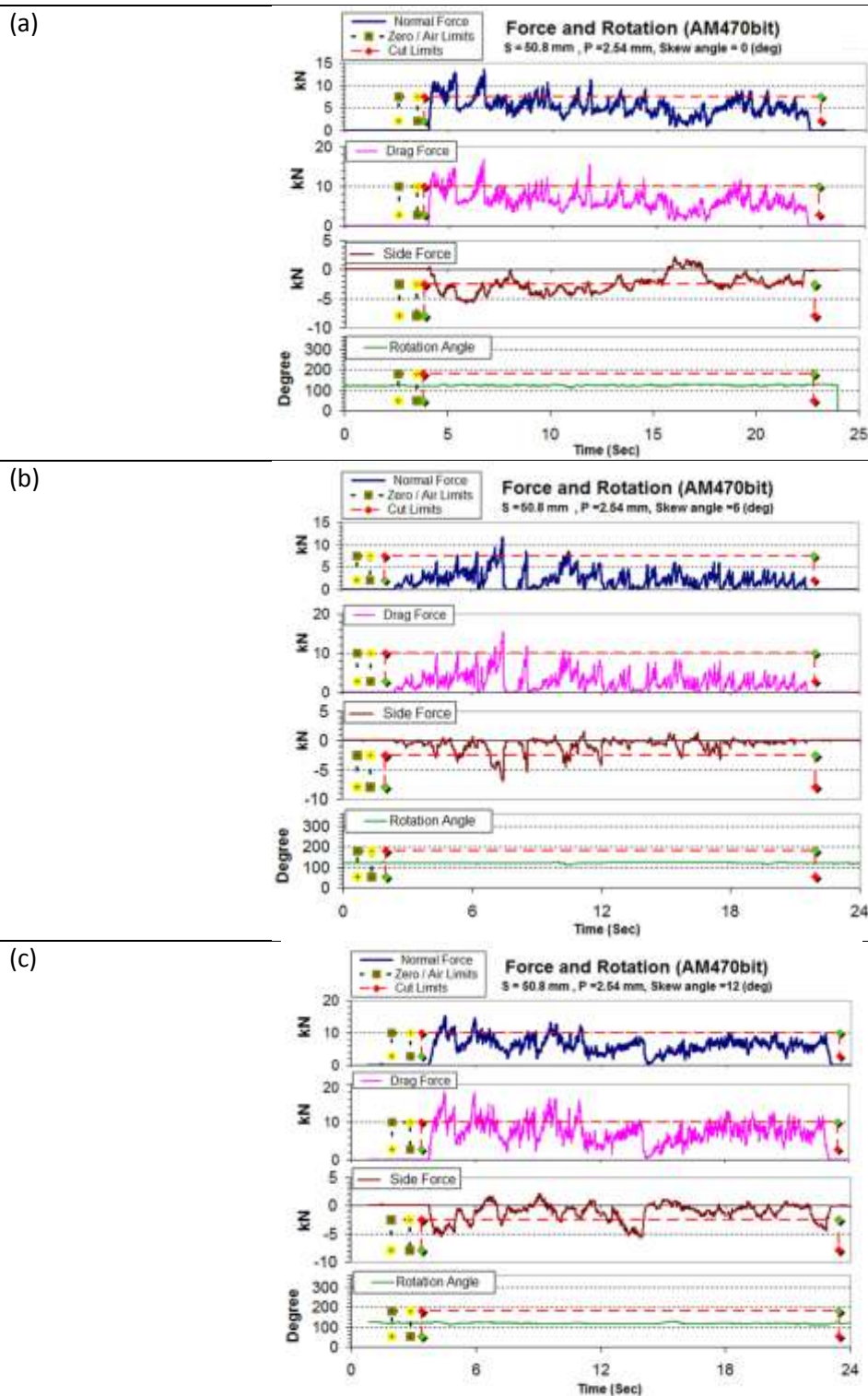


Figure 4-1 Plot of forces measured by load cells on bit and rotation measured by instrument versus time: (a) AM 470 bit at 0° skew angle (b) the AM 470 bit at 6° skew angle (c) the AM 470 bit at 12° skew angle

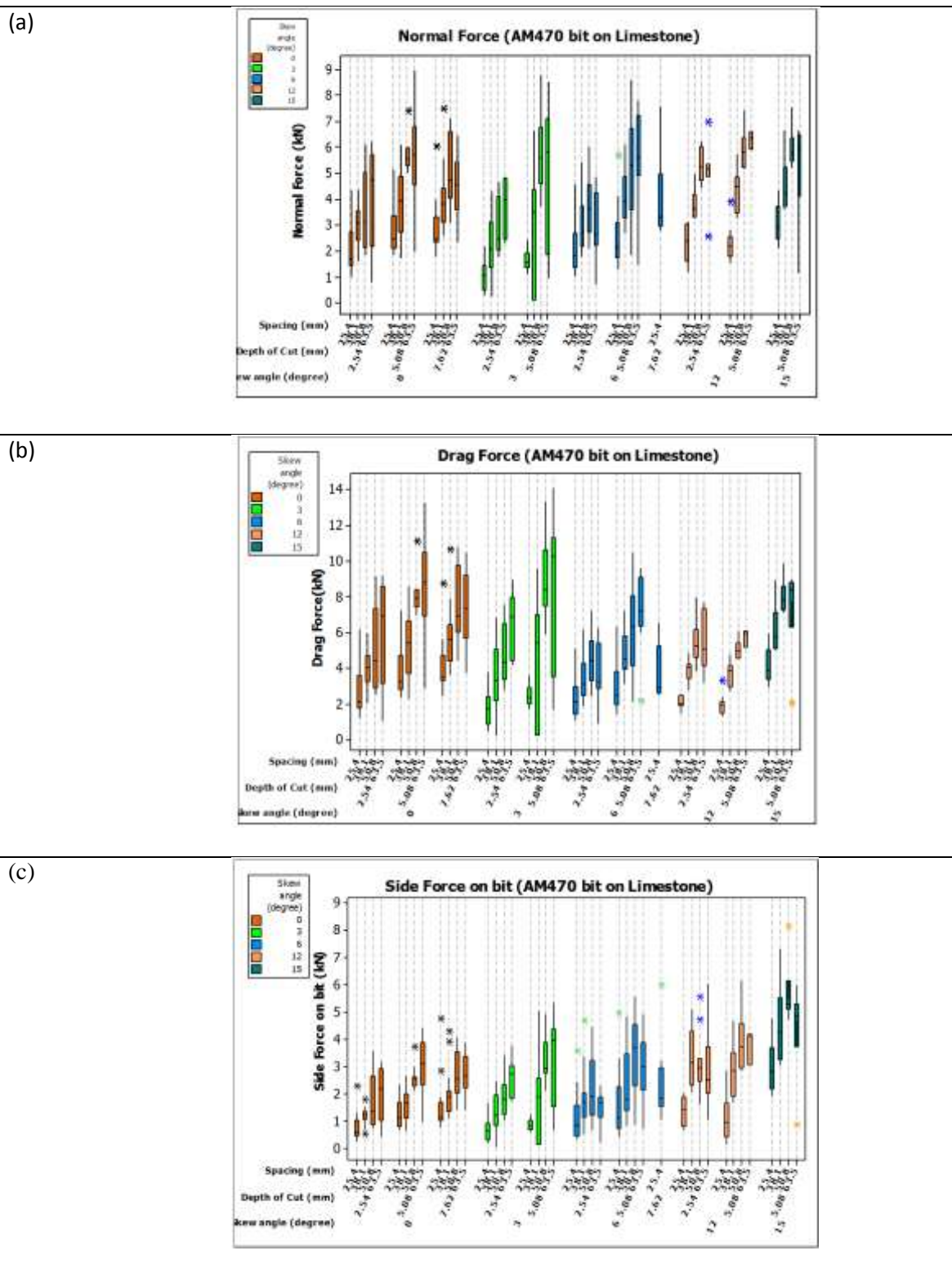


Figure 4-2 Plot of forces for various skew angle, depth of cut, and spacing of AM 470 in limestone (a) normal forces (b) drag forces (c) side forces.

Specific energy (SE) tends to decrease with increase in spacing and penetration as anticipated, indicating higher cutting efficiency (Tiryaki and Dikmen, 2006) (Equation 1). Optimum specific energy can be expressed relative to Spacing to Penetration (S/P) ratio and for Indiana Limestone, the optimum S/P ratio is around 4-5. This SE value needs to be complemented with observation of the cutting surfaces to assure that there is no ridge build up between the cuts. Specific energy of cutting was calculated from the measured cutting forces and cutting geometry as follows:

$$SE = K \frac{F_d}{S.P} \quad (\text{Eq.1})$$

Where SE = Specific Energy in kw-hr/m³ or hp-hr/yd³

F_d = Drag force in (N, or lbs)

S = Spacing of the cut (mm, or inch)

P = Penetration (mm, or inch)

K = coefficient of conversion equal to 277.8 for SI unit (or 1.96E-3 for English units).

This allowed for evaluation of the cutting efficiency and determination of the optimum cutting geometry.

Naturally, occurrence of the high ridge created by excessive spacing for the given penetration prevents the accurate calculation of SE. Thus, some non linear trend or irregularity in SE with increment of spacing was observed due to forming of ridges at higher spacing. In general, SE tended to decrease with increased penetration (depth of cut) (Figure 4-3).

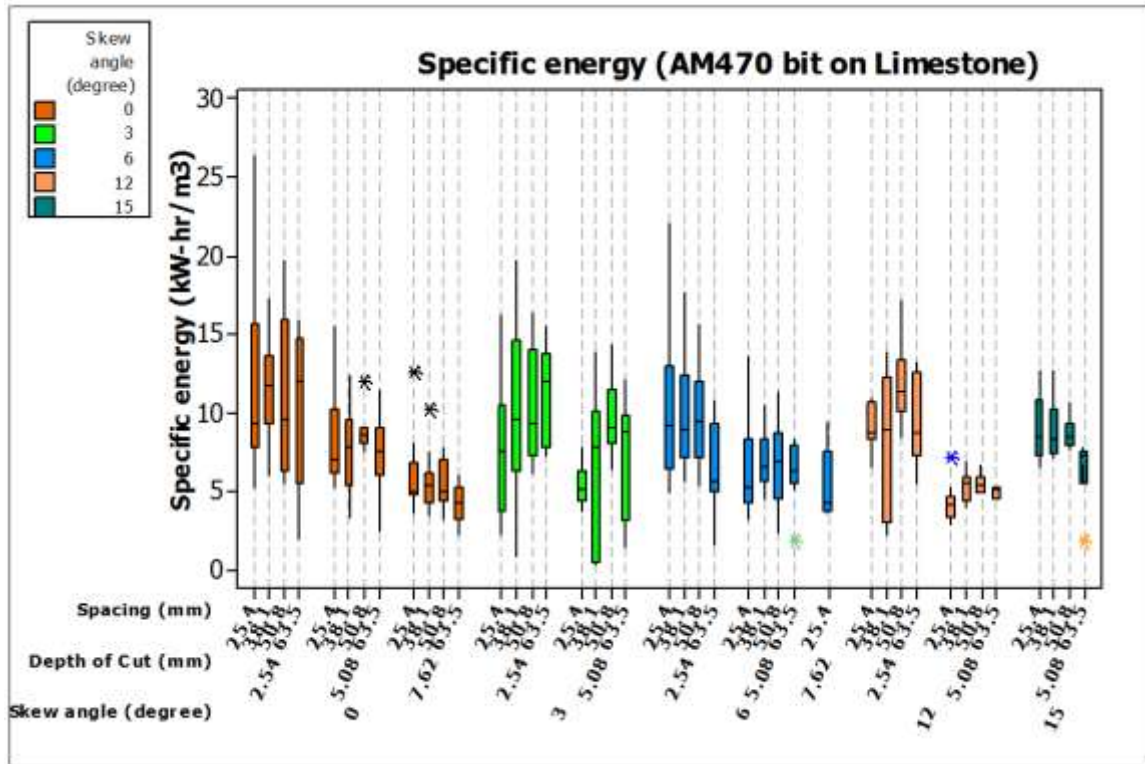


Figure 4-3 Plot of specific energy as a function of skew angle, depth of cut, and spacing for AM 470 in limestone.

Figure 4-4 shows the plots of the average rotation of the bit for the line of cut versus other cutting parameters. The initial observation is that the increment of skew angle does not affect the bit rotation. Interval plots show that the general trend of rotation is less than 1 degree during cutting. These results are too small and within the margin of instrument sensitivity but it still allows for concluding that no systematic bit rotation could be anticipated while cutting along the lines with bits fully loaded and engaged with the rock. The graph also indicates that in some cases the rotation rate per one cutting line can reach up to 0.07 degree per centimeter, but this does not mean that with increased length of cut (or in operational cases on a full face machine), it would result in a number of full bit rotations.

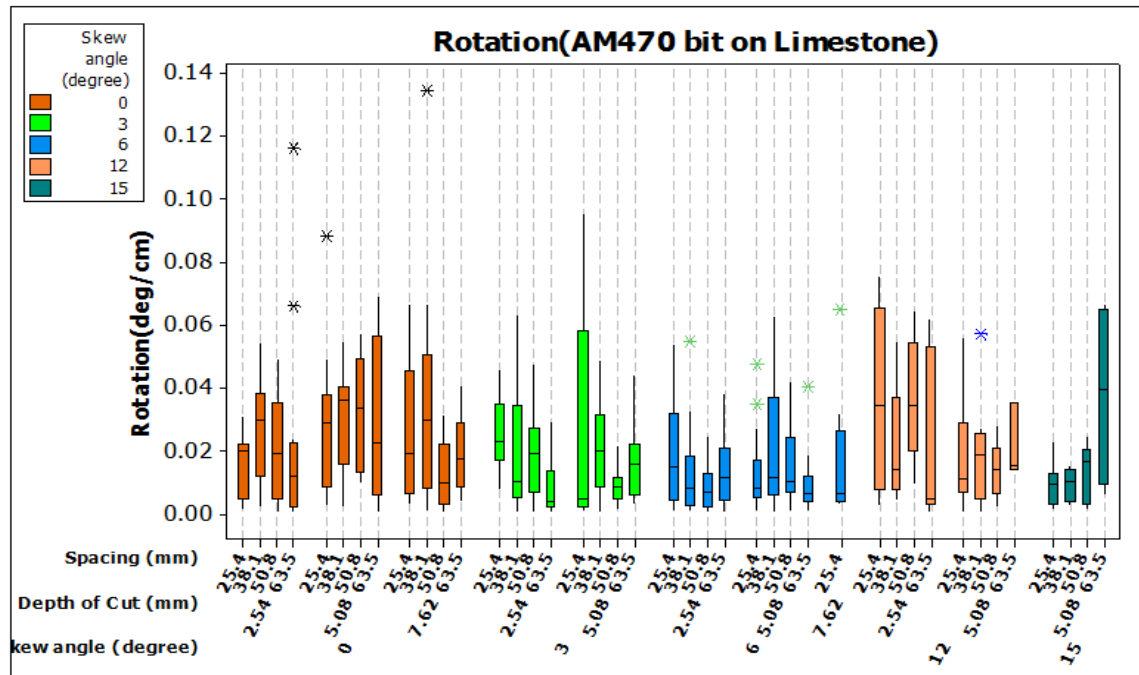


Figure 4-4 Plot of normalized average bit rotation (degree/centimeter) for AM 470 bit in limestone.

4.2.2 RZ 24 bit in limestone

Measurement of bit rotation was also made on the RZ24 construction bit under the same testing conditions and same cutting parameters as AM-470 bit. Figure 4-5 shows the traces forces and bit rotation for a typical tests using RZ-24 bit. Most of cases in RZ24 bit show no systematic rotation and flat bit rotation signal like Figure 4-5a. In Figure 4-5a, there was very small rattling of bit rotation signal (green line). Limits (window) for data analysis of cutting lines is shown in the force traces. Some small variations in bit rotation curve could be caused by stick-slip behavior (or lock and release motion) of the bit. Alternatively, it could occur due to the motion of the impacting and hitting of the bit on the rock surface either at the beginning of the cut or when large chips are formed, where the bit re-engages the rock. Overall, bit rotation did not show any particular trend with cutting geometry.

Rarely, large bit rotation was observed in a limited number of cuts. These few cases seem to be occurred by physical engagement between rock ridges and bit body. These are rare cases in this experiment. For example, full 360° rotation was observed along a few of the cuts as shown in Figure 4-5b. The saw tooth track shows continued rotation of the bit along the cut, while sometimes the bit engaged in partial rotation like Figure 4-5c and Figure 4-5d in each direction. The full cycle bit rotations on the RZ-24 were not a systematic or usual bit rotation trend, but rather isolated incidents that could be attributed to the fact that bit shoulder rubbed against the side ridges.

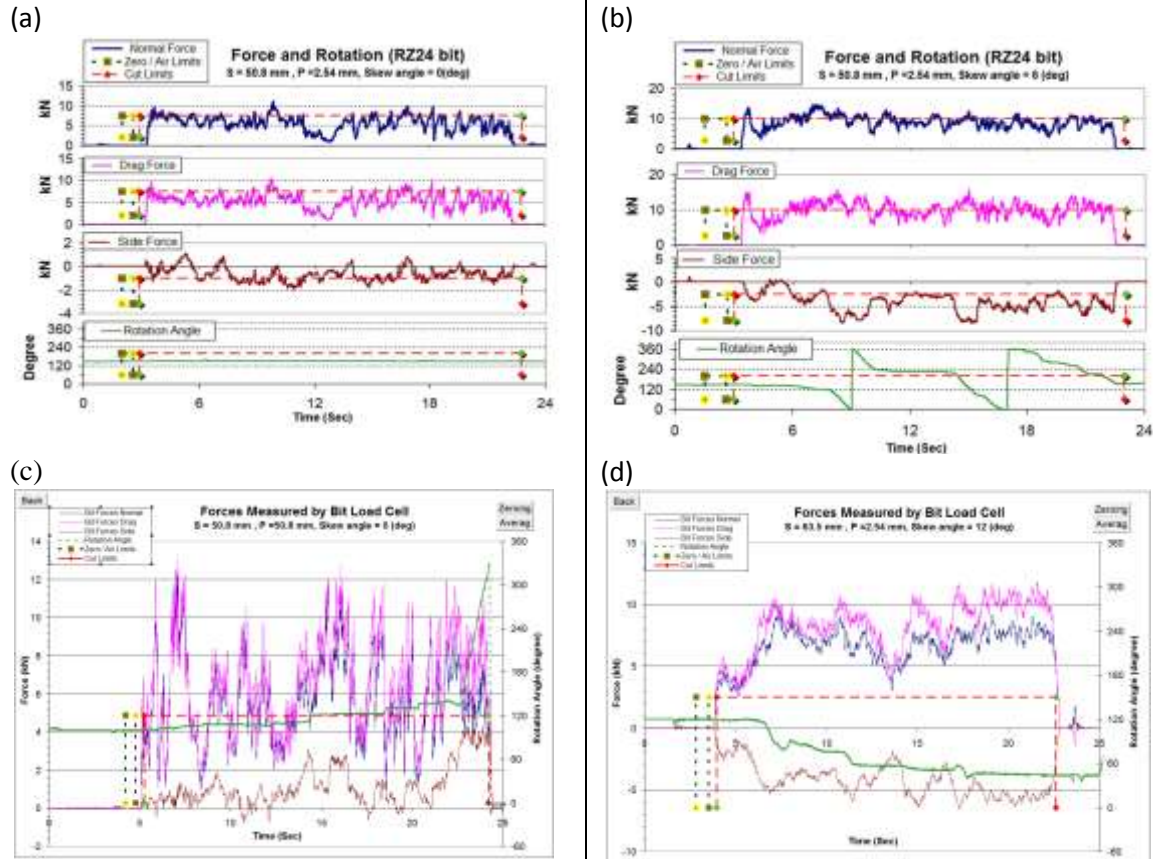


Figure 4-5 Plot of forces and bit rotation for RZ 24 bit: (a) no rotation with 0° skew angle (b) several full 360° rotations 6° skew angle (c) partial rotation with 0° skew angle (d) partial rotation with 0° skew angle.

The RZ 24 bit rotation in limestone did not show any sensitivity to the skew angle, depth of cut, or spacing (Figure 4-5a). A few rotations of the RZ24 bit observed in the testing were discovered with a couple of full (360°) rotations in one direction (Figure 4-5b). However, these incidents were not the usual case during the testing and were most likely caused by the bit body rubbing against the high ridge of un-cut material between the cut at higher spacing. Also the observed full rotations were rare and sporadic and not a routine phenomenon for the testing with RZ24. This condition should not happen in a normal cutting (body of the bit hitting high ridges).

Normal, drag, and side forces increased with spacing and depth of cut as observed in Figure 4-6a-c as anticipated. SE decreased at higher depth of cut (Figure 4-7). No particular trend was observed on the pattern of bit rotation or on normal and drag forces regarding to skew angle changes when cutting with RZ 24 bit. Specific energy seems to be insensitive to skew angle as well.

While testing the RZ 24 bit, more bit rotation was observed compared to the AM 470. Bit rotation was not related to the skew angle or depth of cut or spacing (Figure 4-8). A few high spikes in Figure 4-8 were caused by few full systematic rotations in that set, which was explained before. This kind of bit rotation was most likely caused by the shoulder of the bit running against the high ridge created by excessive spacing for the given depth of penetration. The observed full rotations were sporadic and not a routine phenomenon for the testing with RZ24. This leads to the conclusion that these rotations are not related to the side force or skew angle, or any other parameters.

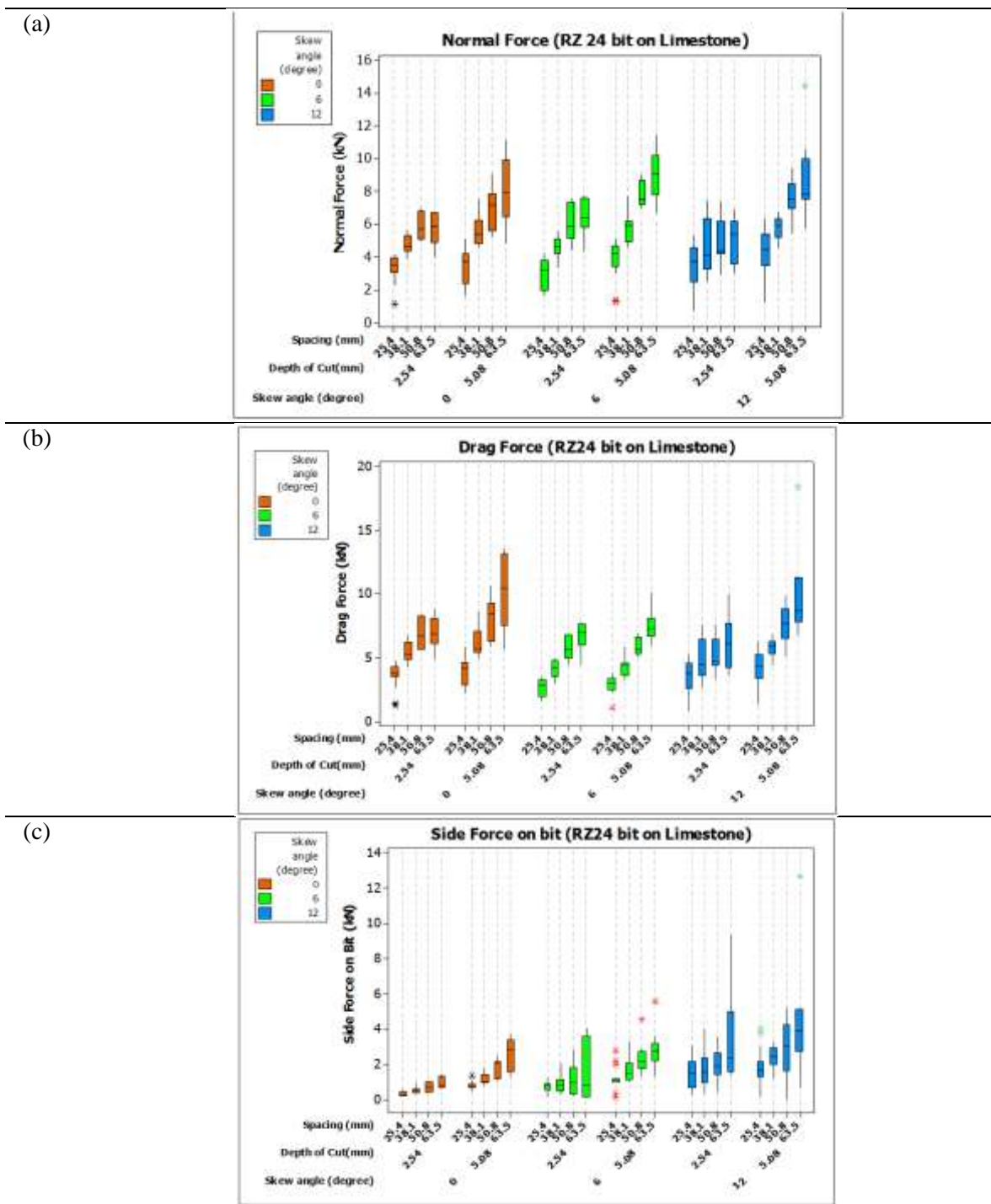


Figure 4-6 Plot of forces for RZ24 bit in limestone sample regarding skew angle, depth of cut, and spacing: (a) normal forces (b) drag forces (c) side forces (Kim et al., 2010)

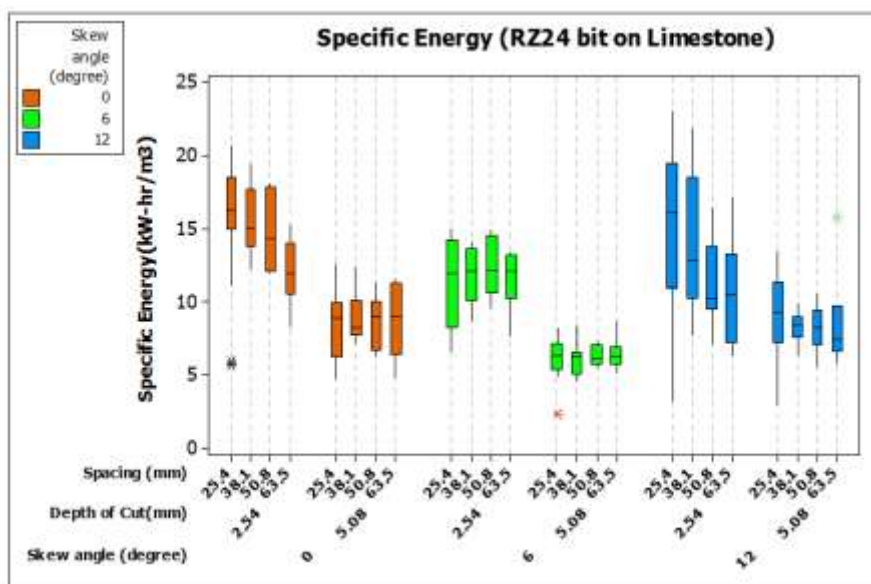


Figure 4-7 Plot of specific energy for RZ24 bit in limestone sample as a function of skew angle, depth of cut, and spacing.

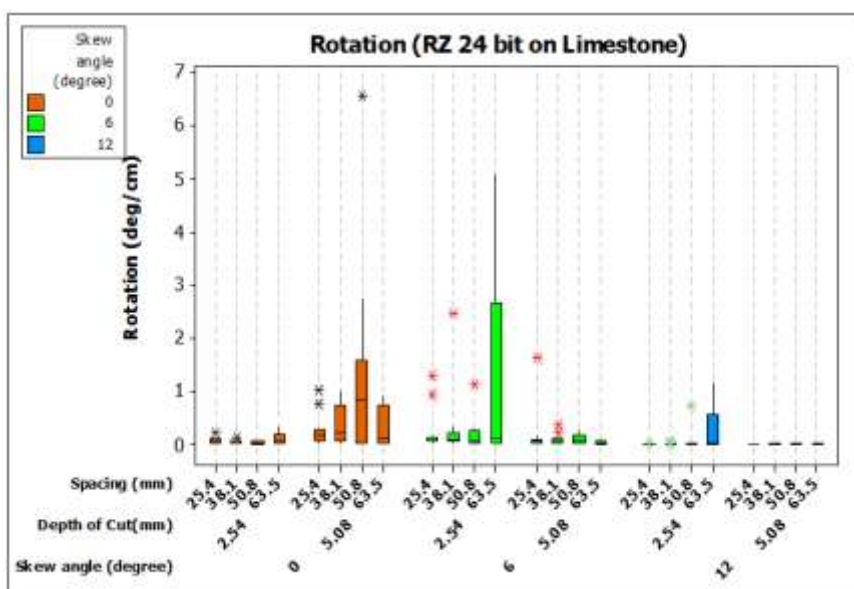


Figure 4-8 Plot of rotation (degrees/meter) for RZ24 bit in limestone sample regarding skew angle, depth of cut, and spacing.

4.3 Test results and Data analysis of linear cutting test in grout

4.3.1. Review of Linear Cutting Test Results for AM470 bit in grout

The results of linear cutting tests using the AM 470 bit in grout were analyzed and the summary of the analysis is as follows. A total of 291 data lines were analyzed for observing bit rotation and possible trends with test testing parameters and cutting conditions. The results show that normal force, side, and drag forces tend to increase with increment of depth of cut (penetration), spacing, and skew angle (Figures 4-9a-c). The observed trends support the accuracy of measurements and experiments. Figure 4-9d is the summary of the measured specific energy of cutting for AM-470 bit cutting the grout at various spacing and penetrations.

Only results at 0°skew angle and 5.08 mm depth of cut showed the anticipated trend where specific energy decreased with increment of spacing and penetration (depth of cut). Other test settings did not follow the anticipated patterns of SE values perhaps because they required additional testing to establish the true cutting pattern and breakouts. This is especially true for wider spacing since some ridges were built up and the expected cut geometry did not clear up the rock between the cuts. Therefore, while SE measurements are a good indicator of cutting efficiency in general, in this particular testing it should be validated by actual cutting pattern observation to assure the material clearance between the cuts. Like before, there was no systematic bit rotation in this series of tests and the details of observed bit rotation are explained later part.

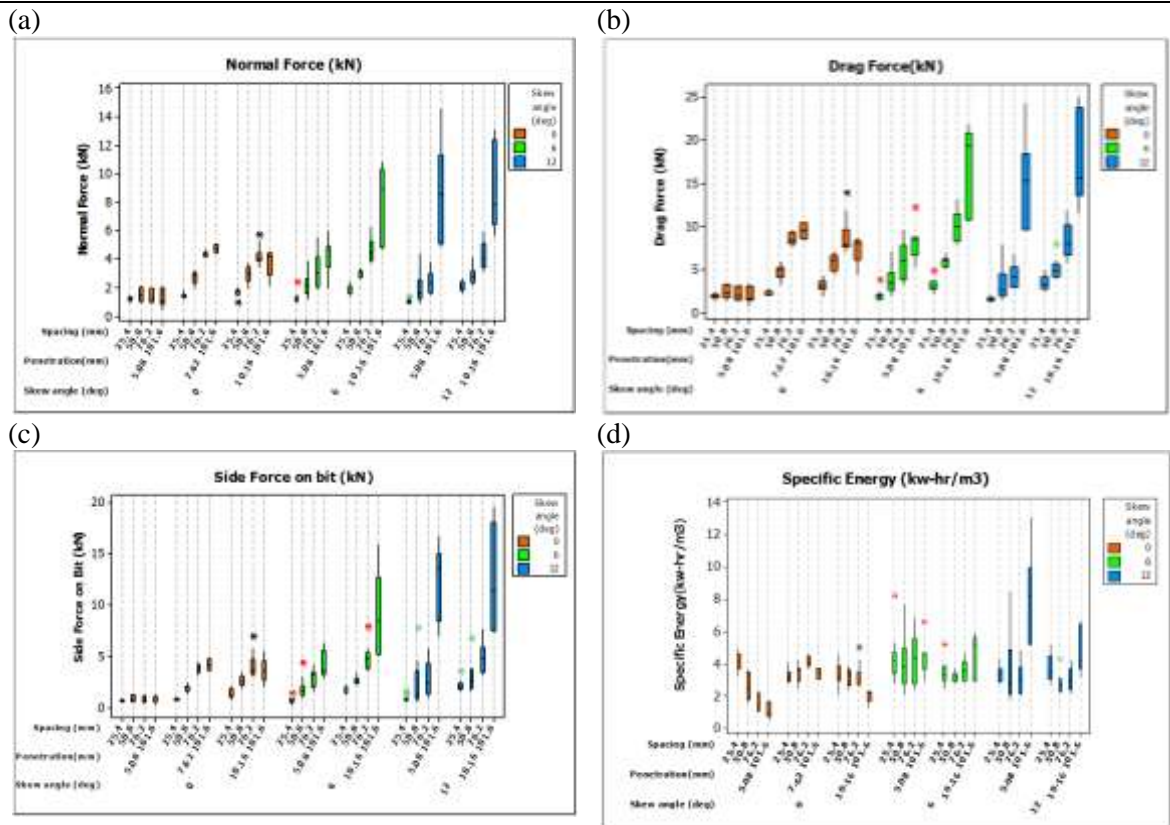


Figure 4-9 Box-plot of data of AM-470 bit in grout regarding skew angle, depth of cut and spacing (a) normal forces (b) drag forces (c) side forces (d) specific energy

4.3.2 RZ24 bit in grout

The RZ 24 bit was also tested in grout samples using the linear cutting test set up. After initial screening of data, 240 data lines were analyzed with a special program in spreadsheets and subsequently by Minitab 14. Collected RZ24 bit data were analyzed to obtain normal, drag, and side forces, and specific energy (Figure 4-10a through d). Normal, side, and drag forces were increased with increased spacing and penetration (depth of cut) as anticipated.

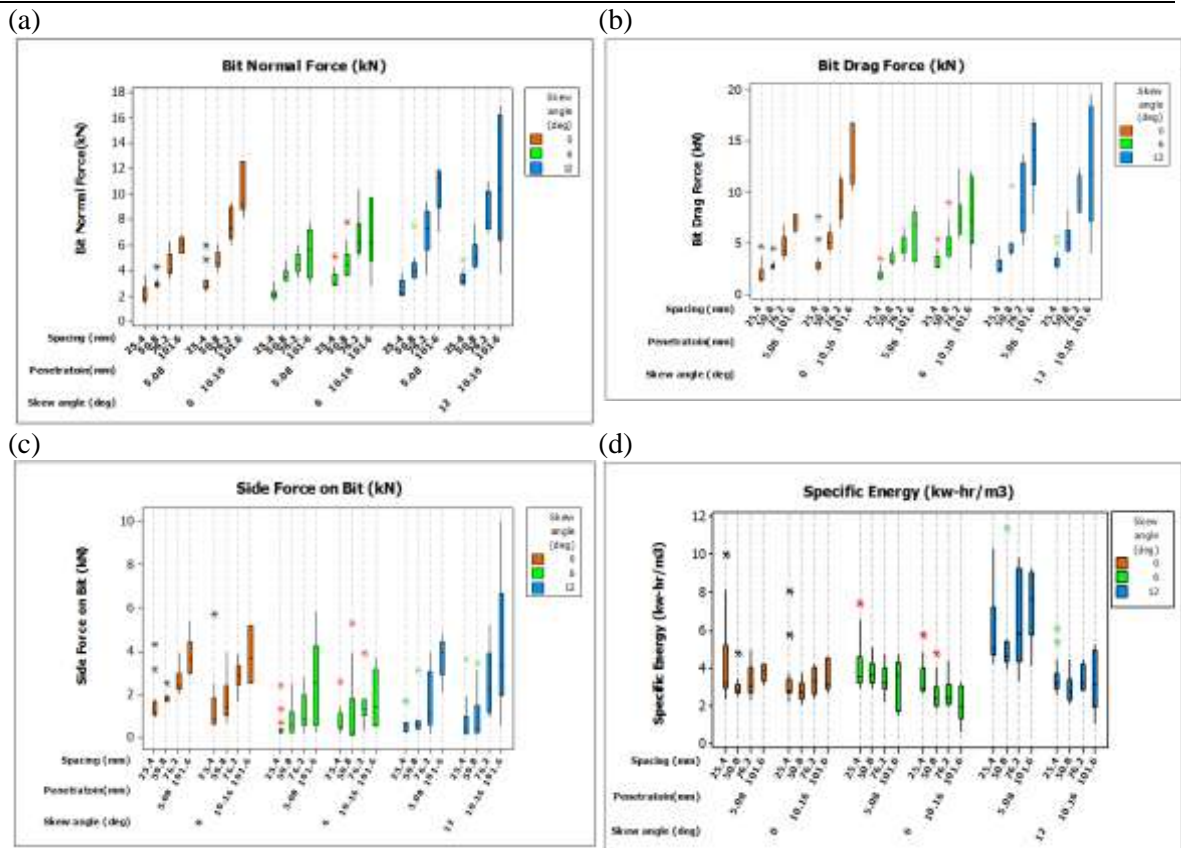


Figure 4-10 Box-plot of testing RZ 24 bit in grout regarding skew angle, depth of cut and spacing. (a) normal forces (b) drag forces (c) side forces (d) specific energy

It seems like the increase in penetration (depth of cut) affected specific energy (Figure 4-10d) in a negative way. This could be explained by the shape of the bit body and that at higher penetration the bit body was taking load and thus increasing the specific energy.

4.3.3 Comparison of measured rotation of the bits in limestone and grout sample RZ24 bit in grout

Overall, it was hard to see any bit rotation in the linear cutting tests, regardless of the material used in testing (the limestone and grout samples), or the cutting test parameters. Bit rotation trends of AM 470 and RZ 24 in limestone sample bits are shown in Figures 4-11 through

4-12. Direction of bit rotations seems to be arbitrary (Figure 4-11). Bit rotation of RZ 24 bit in limestone, was also very sporadic and spotty except for a few incidents (Figure 4-12) where the body of the bit was rubbing against the high ridges. In most cases, there was no systematic rotation at linear cutting tests in the limestone.

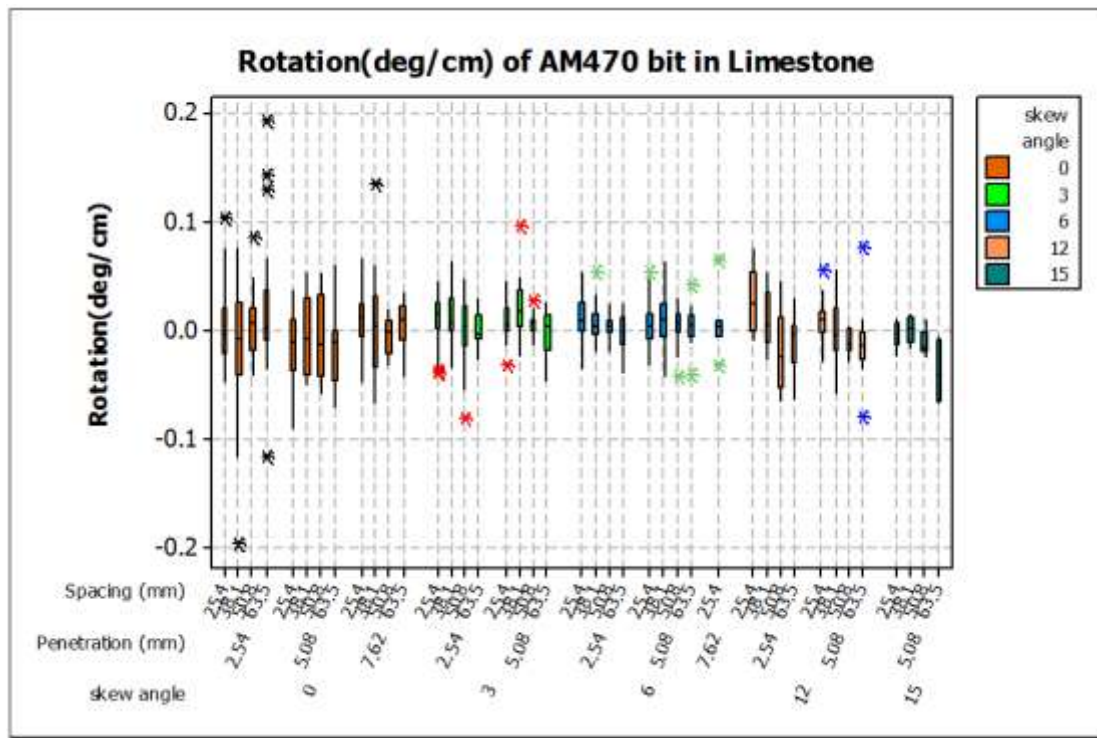


Figure 4-11 Box-plot of the rotation with AM 470 bit in limestone regarding skew angle, depth of cut, and spacing

The cutting sequence in grout samples with the AM470 bit was controlled in half of the experiments to examine the impact of varying cutting speed in various lines in the sequence of cut. This was implemented from the final set of 0° to 12° skew angles. The reason for randomization was to see the effect of changing speed in adjacent cuts on the bit rotation.

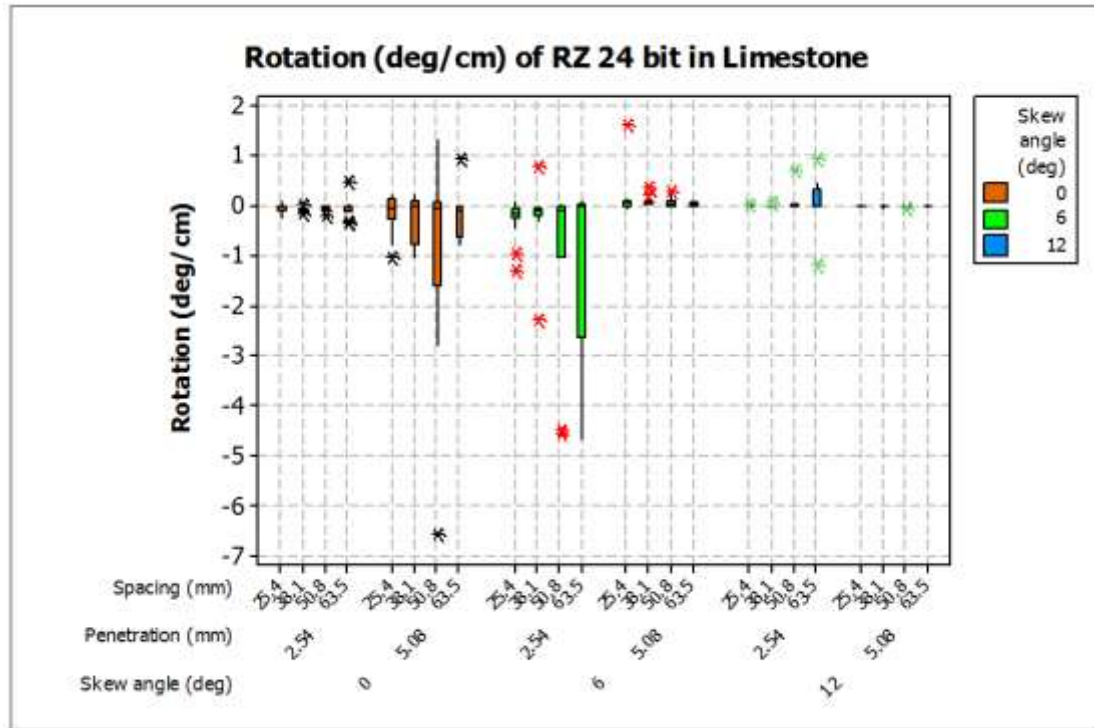


Figure 4-12 Boxplot of bit rotation for RZ24 bit in limestone regarding skew angle, depth of cut, and spacing

As can be seen in Figure 4-13, the measured bit rotation was typically hovering around the 0 deg/cm and does not seem to follow any particular trends. Furthermore, the magnitude of the AM 470 bit rotations in grout sample was smaller than those of AM470 bit rotations in limestone sample. Overall it appears that there is a greater possibility of bit rotation at 0° skew angle and at lower spacing where the magnitude of axial load is lower (Figure 4-13). The bit rotations were almost random, arbitrary, and smaller with deeper cuts, perhaps due to higher loads at deeper penetration.

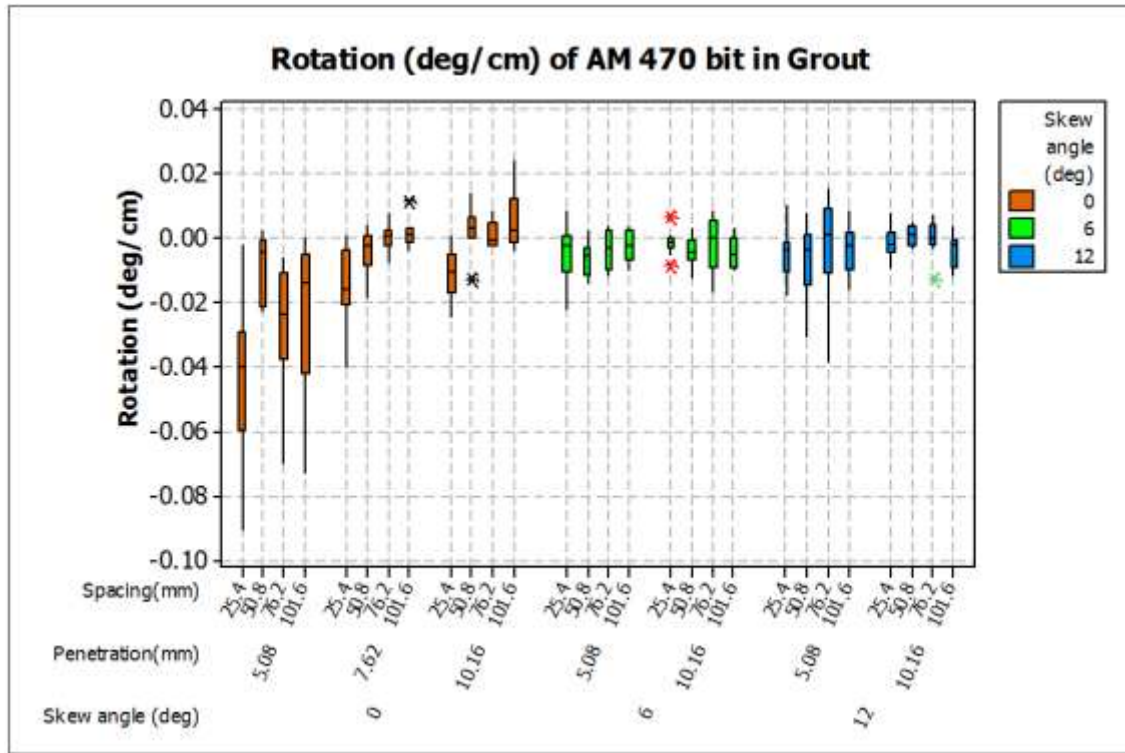


Figure 4-13 Box-plot of bit rotations for AM470 bit in the grout sample regarding skew angle, depth of cut, and spacing

Bit rotations of the RZ 24 bit were also measured in linear cutting tests in grout. Cutting sequence of RZ 24 bit in grout was fully controlled to make a better observation of the cut sequence impact on the test results. In most cases no bit rotation was observed except few isolated incidents (Figure 4-14). These incidents were related to partial bit rotations at the 10 mm (0.4'') depth of cut but very low spacing, meaning the presence of a relieve cut on one side and a ridge on the other. The overall measured average or normalized bit rotations in the linear cutting tests with the RZ24 in grout were close to zero. No full bit rotation like the testing of the RZ24 bit in limestone was observed. This could be attributed to harder ridges in the limestone compared to those of the grout sample as a platform of bit rotations.

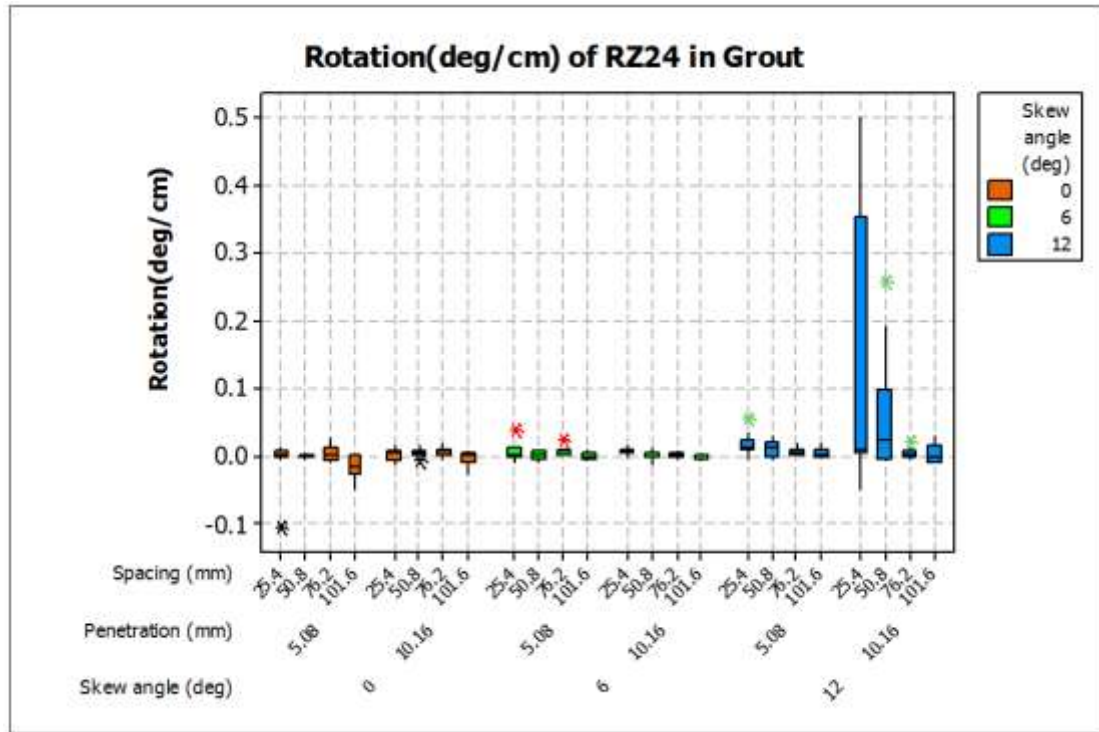


Figure 4-14 Box-plot of the bit rotation for RZ 24 bit in the grout sample regarding skew angle, depth of cut, and spacing

Overall, no systematic pattern or trend nor any specific trigger was found to induce bit rotations in linear cutting tests. Few full rotations were observed when cutting limestone by the RZ-24 under circumstances that are not expected to occur in normal conditions (hitting high ridges). As a next step, rotary cutting tests followed the linear cutting to see the effect of variable cutting depth along with cutterhead drum revolution, and the cutting geometry that is typical of bit application including dynamic loading on bit rotation. This is a better representation of the working conditions of conical bits since cutterhead drums are usually used in mining and construction applications.

4.4 Summary of Conclusions for linear cutting tests

Full scale linear cutting tests using conical bits in Indiana Limestone and grout blocks were used to examine the impacts of cutting geometry (skew angle, depth of cut, and spacing) and configuration (AM 470, and RZ 24 bits) on bit rotation. The results show no systematic bit rotation when bits were fully engaged and were under load. The linear cutting tests provide observation of the cutting forces and bit rotation under controlled conditions and allow experiments to isolate the impact of individual parameters due to the simplicity of the test. The linear cutting experiments showed that normal, side, and drag forces had a tendency to increase with increased spacing, depth of cut, and skew angle. However, bit rotation did not show any trends relative to these parameters.

Linear cutting is a rare cutting condition where conical bits are used in the industry. The linear cutting condition is implemented to the conditions where conical bits are in constant contact with the face, i.e. the back reamers in directional drilling, conical bits in full face machines, or occasional usage on micro-tunnelling machines or augers.

4.5 Simulation of Bit Rotation with Analytical and Numerical Methods

4.5.1 Analytical solution of conical bit rotation

A limited analysis of the forces acting on the bit was performed to calculate the amount of torque needed to induce bit rotation and to examine the possibility of generating such torques via friction between the rock and the bit tip while cutting. For this purpose, the forces were resolved in various coordinate systems including a normal Cartesian coordinate system which coincides with the X, Y, and Z direction of the cutting machine (Spencer, 1992). The forces measured by the table load cell and the bit load cell are in this direction. These forces then can be

projected in a new coordinate system where the side force is the same (X direction) but normal and drag (Z and Y direction) are projected onto bit axis force (Y'- bit Axis) and perpendicular forces (X'- and Z' – orthogonal to bit axis) (Equation.2). The transformation matrix for the projection of the measured forces to the desired coordinate system (axis of the bit) is as follows. The α and β angles in transformation matrix are the same as the attack angle (α) and skew angle (β).The schematic drawing of the forces and the coordinate systems is illustrated by using the projection of the reference cutting forces onto a bit axis coordinate system. (Figure 4-15)

$$\begin{aligned}
 [R_z] &= \begin{bmatrix} \cos \beta & \sin \beta & 0 \\ -\sin \beta & \cos \beta & 0 \\ 0 & 0 & 1 \end{bmatrix} \\
 [R_x] &= \begin{bmatrix} \cos \alpha & 0 & -\sin \alpha \\ 0 & 1 & 0 \\ \sin \alpha & 0 & \cos \alpha \end{bmatrix} \\
 [R] &= [R_z][R_x] \quad \text{-----} \quad \text{(Eq.2)}
 \end{aligned}$$

R: indicate Rotation Matrix

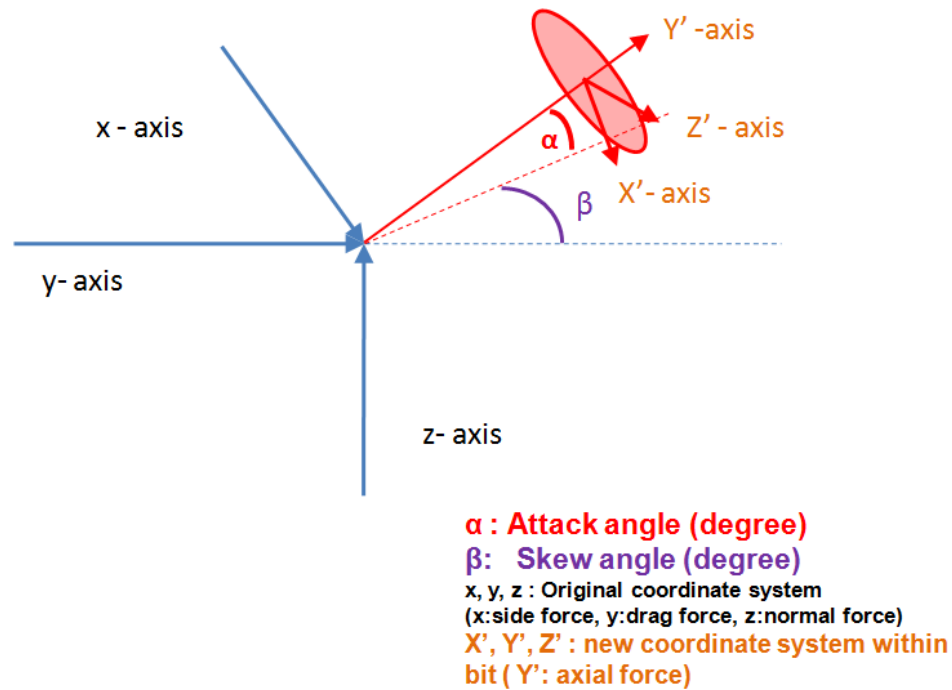


Figure 4-15 Schematic view of the coordination transformation.

Using the axial force and the coefficient of friction between the two bodies, the frictional forces between the bit block and the bit shoulder can be estimated. This force multiplied by the offset from the center of the bit axis constitutes the main component of torque that needs to be overcome for bit rotation. Using the value of resistance torque as a baseline value, the torque more than this baseline should be generated to make the bit rotate on the bit body. There are two parameters to constitute this torque: distance from centerline axis of the bit and the magnitude of force acting on the bit tip. When combined, the moment arm of the acting force or the rotational torque of the force can be determined. Thus, force can be calculated from the given distance (moment arm) or distance can be calculated for given forces to get torque that overcomes the resistance torque for bit rotation. In this study, required force for turning the bit was calculated at the assumed position or point of effect where the force would be applied.

The assumption used in this analysis was that the turning force will be applied on the bit at the half of depth of cut. This means that the distance from the bit tip to the point of effect of force along with bit axis is half of the depth of cut. Thus, the moment arm was estimated using the bit profile. In each case, the moment arm (d) was half diameter of bit which is distance from the centerline of bit axis to the point of effect. Calculation results show that the force needed on the side of the tip to overcome the resistance torque is at least one order of magnitude higher than the axial force applied on the bit. This indicates that the rotation of the bit does not occur when the bit is under loading simply by applying a load at the tip, where the friction force on the side of the bit is assumed to cause rotation. This holds through for a range of frictional coefficients assumed for steel-steel and steel-rock¹.

Resistance force (F_{resis}) is equal to μ multiplied by normal force (F_{normal}), where μ is friction coefficient factor. The calculated resistance force was converted into an equivalent resistance force which was assumed to be applied at the middle point of annulus shape contact area. With this resistance force, the moment (M) was calculated by the equation $M=F_{\text{resis}}*d$, where d was the distance from the center of the bit axis to the location of the exertion of force. From this calculation, the resistance torque and the expected force to overcome the resistance torque can be calculated using the distance of point of effect as explained before. From this exercise, the expected force to overcome the resistance force at a specific penetration of bit was estimated.

This calculation was performed for the transformed forces from measured force during the cutting tests and the results are illustrated in Table 4-1. As one can observe, the magnitudes of calculated forces were up-to 40 times higher than measured drag forces. It should be noted that

Static Resistance coefficient was found in the literature. Coefficient of static Steel (hard) on steel (hard) is 0.78¹¹ Steel on concrete is 0.57 *Journal of Structural Engineering*, Vol. 111, No. 3, March 1985, pp. 505-515

the typical cutting forces recorded for the test setting were in a range of around 10 kN (4400 lbs) as compared to the estimated range in this analysis that is around 100 kN (44000lbs).

4.5.2 Numerical simulation on conical bit rotation

To better interpret and expand the results of the full scale cutting experiments, numerical modeling was used to simulate the forces needed to rotate the bit under certain loading conditions. The laboratory experiment can be limited due to the restricted capacities to sense all of the forces acting on the bit and find their action points. This is to say that the load cell can only sense the forces at the base of bit block but cannot indicate where and what compositions of forces come into play. Sometimes, it is easy to make mistakes by observing apparent responses under limited experimental settings. Thus, to support results of the of laboratory experiment cutting tests, computer simulation was used and the result of the computer simulation were cross-checked with analytical solutions. In this dissertation, the commercial computer simulation software ANSYS was used to simulate the forces and stresses within the components of the bit/bit holder and the pressures between moving parts. Since the rotation of the bit was assumed to occur due to the torque generated by a force at the interface between the bit tip (or shoulders) and the rock, 3D models of bit and bit blocks were built and known sets of forces and boundary conditions were given to the model.

For modeling purposes, the geometry of the AM 470 bit was used and the model was constructed based on the bit profile. This geometry in model consisted of two parts; the first being the conical bit and the second being the bit block which was built as a hollow cylindrical holder with the SOLID 92 element which has properties of u_x , u_y , u_z displacement in 3-D and 10 node tetrahedral structure solid. This element is one of the appropriate elements that can simulate the behavior of bit which has the real properties of the actual bit material. This allows for an accurate

representation of the behavior of the bit and bit holder and realistic set of stress distributions within each body. Displacements and hence the parts were constrained at the end of the bit holder in 3-directions and at the end of shank of the bit in the z-direction (along the axis). A coupled force was applied at 0.15 cm (0.06") from the tip of the bit since it was assumed that at this point penetration was 0.34 cm (0.12"). The areas of contact between the bit shoulder and bit block were generated using special elements on two different surfaces; the first contact was between the shank and inside of the holder, and the second was the annulus shaped flange contact between the bit shoulder and the face of the holder. In these contact areas, surface to surface contact pairs were generated with a coefficient of friction of 0.7. A normal force was applied at the tip of the bit. The contact area between the bit shoulder and the face of bit block experienced normal loads which were measured in the range of 4.5, 6.2, and 8 kN (1000 lbs, 1500 lbs, and 1800 lbs) used for normal force (Figure 4-16). The simulation of the contact area was made to ensure that the normal load was distributed across the entire area of the ring of contact between the bit shoulder and bit block.

Schematic model in ANSYS

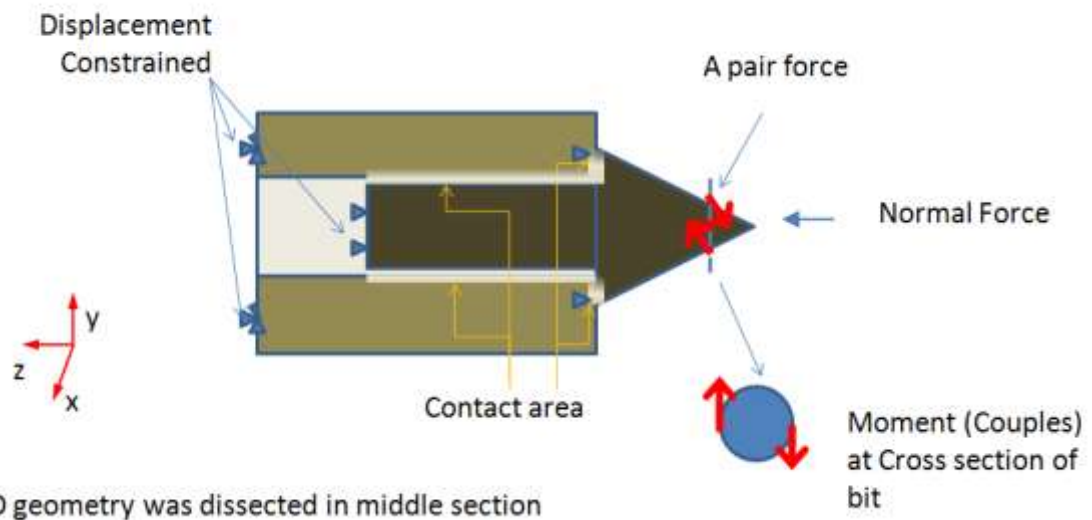


Figure 4-16 Schematic view of ANSYS program: constraints of displacement and load and a pair of forces assigned for AM 470 bit geometry.

Under different levels of normal force, a paired force (couple) was applied at a given point of effect, which as described before, was within the area of contact between the bit tip and the rock (Figure 4-17). The point of effect of the force action location was selected as explained before. With the geometrical setting and prescribed material properties, the simulation was run until it converged and provided a solution to the force displacement equations. The objective in this numerical simulation was to find the initial force needed to initiate bit rotation. To identify the bit rotation, after simulation process, post processing file which contained the x- and y- displacement was examined. In this process, several different magnitude sets of forces were applied until distinct color bands on the surface of bit were formed, which implied that bit rotation had been occurred in the model. Each distinct color band represents a specific displacement value ranging from negative direction to positive direction. However since the bit is rotating, the magnitude of the maximum and minimum of displacements in the cartesian coordinate system (as in the model) are same. To find the initial point of rotation, the smallest magnitude of forces that made these distinct color bands was chosen to compare the forces with analytical solutions.

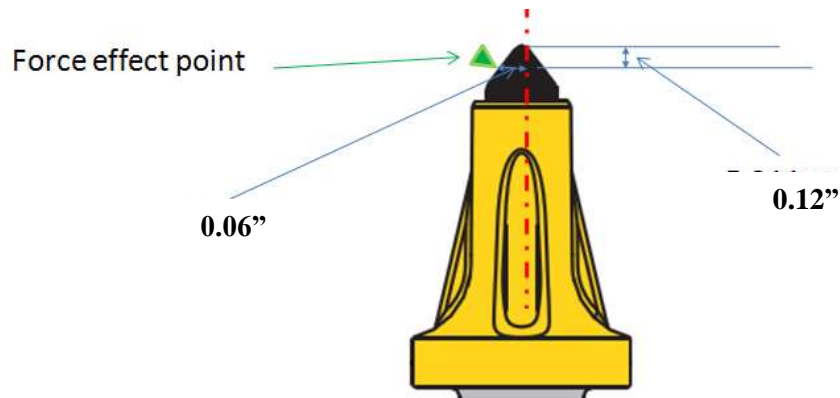


Figure 4-17 The location of the point of effect of paired forces on AM 470 bit in simulation: This same setting was used for analytical calculation to verify the simulation results.

After several sets of forces were applied to the model, the smallest force that initiated rotation or formed distinctive color band was recorded at different normal force conditions (Table 4-1). For example, when rotation occurred with an equivalent 1000 lbs normal force condition, distinctive color bands in x-, and y- directions were displayed (Figures 4-18a & b). However, there was no distinct color band in z- direction (Figure 4-18c). The normal force was distributed on the ring shape contact area between bit/bit block as well as the end of the bit and the bottom of the holder. This ensures that a force of 1000 lbs or 4448N distributed onto it distributed onto the ring shape contact area. Since this simulation deals with rotation, it was necessary to use the solver which can handle large displacements in the model. To get more precise results, the number of sub-steps in simulation was increased until the high-performance computer (HPC) at PSU reached its convergence limitation. This precision process took 24 hours, but the result was similar to the result by using a desktop computer (Dual Intel Core 2 Duo 2.26 GHz 4 GB). Thus in this study, most of simulation was performed at a local desktop computer which was sufficient for the scope of this simulation.

Finally, the simulation results were compared to analytical calculations. The difference between simulation and analytical solution is from some of the basic assumptions. The assumption of the simulation solution was based on a dynamic transient mode which can handle rebounding of the bit while it rotated or bent, while the analytical solution was based on static equilibrium of forces. Also details of the loading boundary conditions in the numerical model are little bit different to non-boundary condition of analytical solution. The boundary condition of the numerical model is to prevent errors and lack of convergence in the solutions. The numerical simulation allowed for simulation of more complex geometries similar to realistic loading condition.

As a result, these numerical results conformed to the result of analytical solution whose assumptions were the resistance force and torque on the bit. These comparisons were performed

at various levels of normal forces, which are summarized in Table 4-1. Even though rotation-initiative forces calculated by the numerical simulation were in general 1.7 times higher than those of analytical solution, the simulation solution result followed the analytical solutions results. Thus, one can simply use the analytical solution without the complicated numerical simulation to estimate the forces on the experimental settings.

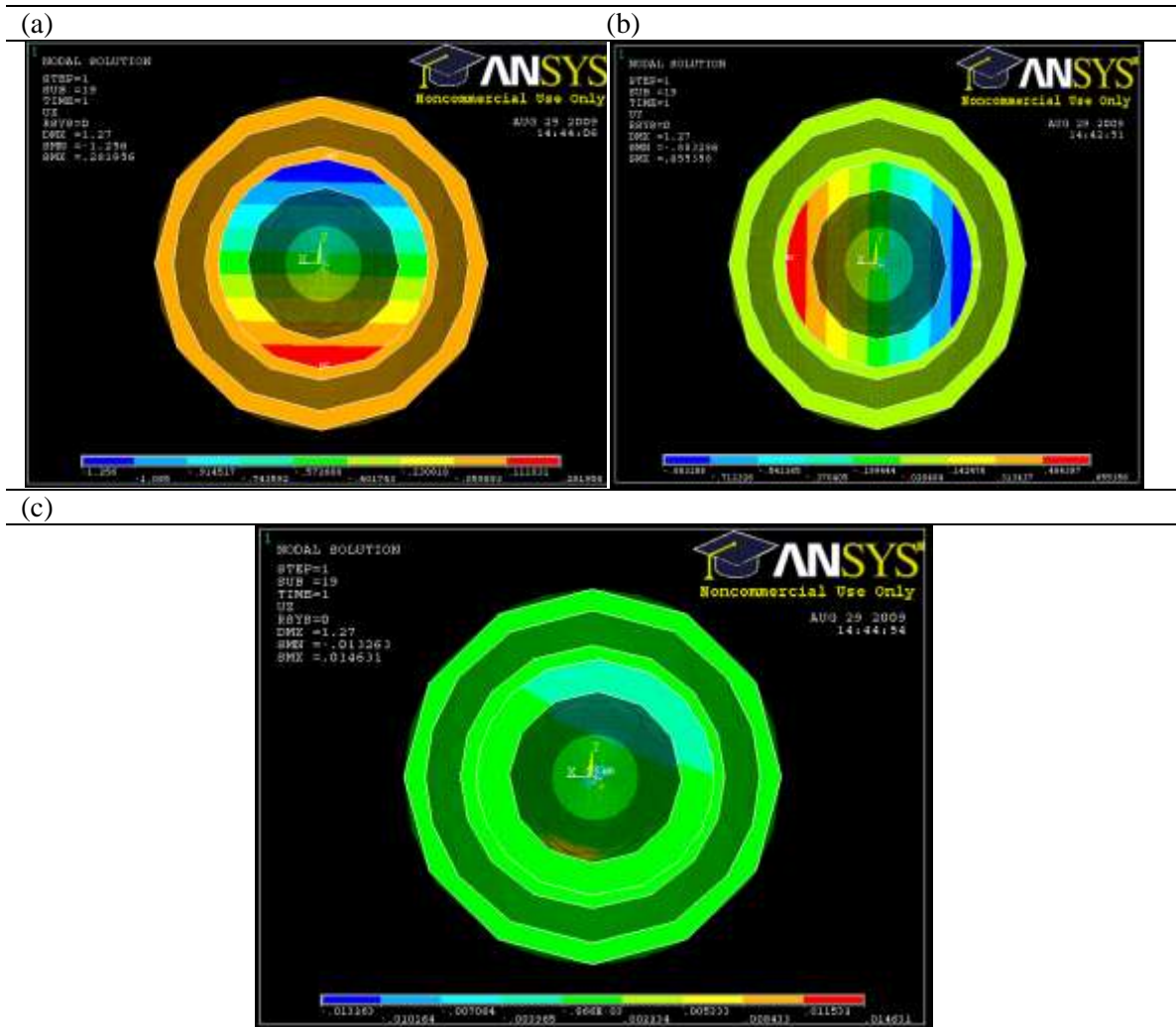


Figure 4-18 Results of displacements after force calculation which initiated bit rotation with ANSYS. (a) rotated-x direction displacement (b) rotated-y direction displacement (c) no rotation in z direction displacement

The numerical and analytical solutions in agreement showed that calculated forces were one order of magnitude larger than actual force in experiments was needed for making bits rotate. Simply this means that bit rotation cannot occur in this experiment setting.

For simplicity of analytical solutions compared to numerical solution, calculation of the forces needed for bit rotation of the RZ bit was conducted by analytical solution. The resistance forces of the RZ 24 bit were calculated using analytical torque calculation for 4.5, 6.7, and 8kN (1000 lbs, 1500 lbs, and 1800 lbs) which are representative normal forces based on laboratory test measurement. Similar to the AM470 bit, estimated forces for inducing the bit rotation were much higher than those applied on the bit thus no rotation can occur in normal conditions (Table 4-2).

Apart from the normal cutting scenario, sometimes, bit rotations were observed in the RZ24 bit when the bit body was rubbing against the ridge. To find the reason of the bit rotation in the RZ24bit, two scenarios were proposed with the RZ24 bit and set of assumed forces.

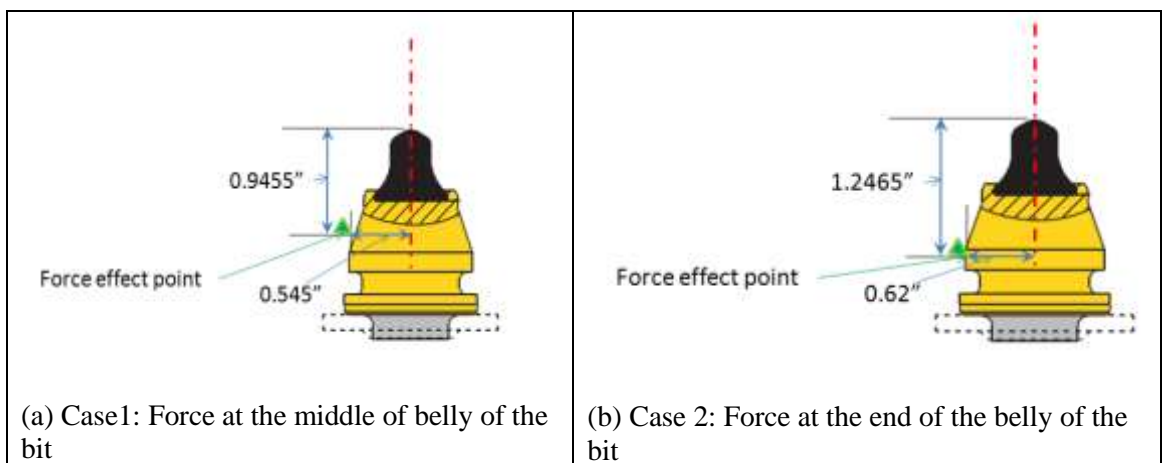


Figure 4-19 Assumed force location on the RZ 24 bit when bit rubbed against ridge in (a) & (b)

By observing the experiment process closely, there might be two different possibilities for the occurrence of the bit rotation when testing Rz-24 bits. One is that rock hitting the middle

of the bit body (Figure 4-19(a)) and the other is that hitting point is the end of bit body. (Figure 4-19 (b)). One scenario is that an equivalent resistance force was calculated in the middle of the bit belly. The other is forces were applied to the end of the bit belly. In each scenario, the point of effect of the force was at a distance of nearly 24 mm and 30 mm (0.9455" or at 1.2465") from the bit tip, where the radius of the point of effect in lateral direction is much longer than those under normal condition hitting point of the RZ 24 bit. In these scenarios, analytically calculated forces of the RZ24 bit were in the reasonable achievable range of this experiment forces measured during the experiment, or around 5.8kN and 8.5 kN (1300 lbs and 1900lbs). This is very different from normal condition of the AM470 and RZ24 bits (Table 4-3).

The summary of these numerical and analytical exercises is that it is hard to achieve rotation in the AM 470 bit and the RZ24 bit under normal cutting condition. However, rotation of the RZ 24 bit might be achieved if the body of the bit hit the ridge and it is given a long moment arm to rotate. This confirms the observations made during the linear cutting tests.

4.6 Conclusion of linear cutting tests

Full scale linear cutting tests of conical bits in Indiana Limestone have been performed to examine the impacts of cutting geometry (skew angle, depth of cut, and spacing) and tool configuration (AM 470 and RZ 24 bits) on bit rotation. The results of linear cutting tests show no systematic bit rotation when a bit is fully engaged and is under load. Linear cutting tests were performed using different types of cutting materials (i.e. limestone and engineered grout with lower compressive strength of about 10 MPa) with different cutting geometries to validate the findings of this study at higher depth of penetration. One should bear in mind that while the linear cutting test is a good way of making observations of the cutting forces and bit rotation, this linear cutting is not how the majority of bits are used in the industry.

To observe potential bit rotation in realistic conditions, one should make such measurements while bits are installed on a cutting drum and monitor bit rotation when the cutter head is rotated. Additional testing was performed to observe bit rotation while the bit was mounted on a cutter head in full scale rotary cutting tests. Meanwhile, the result of linear cutting test could be valid for bit application on full face machines such as the occasional use of conical bits on tunnel boring machines or reamers for horizontal directional drilling (HDD) applications. From the experiment, normal, side, and drag forces tended to increase with increased spacing, depth of cut, and skew angle. However, bit rotation did not show any tendency regarding to depth of cut, spacing, and skew angle.

Table 4-1 Results of estimating forces needed for bit rotation based on analytical solution of resistance force

P	Half of P		Radius*		Normal Force		Resistance Force		Torque		Analytical Sol.(An.)		Paired Force in Simulation		Single Force of Simulation (Sim)		Ratio
	(In)	(in)	(mm)	(in)	(mm)	(lbs)	(N)	(lbs)	(N)	lbs*in	N*mm	(lbs)	(N)	(lbs)	(N)	(lbs)	(N)
0.12	0.06	1.57	0.05	1.14	1000	4448	700	3114	482	54488	10717	47671	3147	14000	6295	28000	1.70
0.12	0.06	1.57	0.05	1.14	1500	6672	1050	4670	723	81732	16076	71507	4699	20900	9397	41800	1.71
0.12	0.06	1.57	0.05	1.14	1800	8006	1260	5604	868	98078	19291	85808	5665	25200	11331	50400	1.70

Note: * indicate point of effect of force relative to bit axis

P: Penetration

Table 4-2 Calculation of resistance force with the RZ24 bit with experiment settings

P	Half of P		Radius*		Normal Force		Resistance Force		Torque		Analytical Sol.	
	(In)	(in)	(mm)	(in)	(mm)	(lbs)	(N)	(lbs)	(N)	lbs*in	N*mm	(lbs)
0.10	0.05	1.27	0.2	4.90	1000	4448	700	3114	368	42189	1838	8610
0.10	0.05	1.27	0.2	4.90	1500	6672	1050	4670	551	63284	2756	12915
0.10	0.05	1.27	0.2	4.90	2000	8896	1400	6227	735	84379	3675	17220
0.20	0.10	2.54	0.2	4.90	1500	6672	1050	4670	551	63284	2756	12915
0.20	0.10	2.54	0.2	4.90	2000	8896	1400	6227	735	84379	3675	17220
0.20	0.10	2.54	0.2	4.90	3000	13344	2100	9341	1103	126568	5513	25830

Note: * indicate point of effect of force relative to bit axis

Table 4-3 Calculation of resistance force with the RZ24 bit with assumption that force was applied at the middle section of the belly of the bit

(a) Case 1: when middle of bit belly hit the ridge

P	Half of P		Radius*		Normal Force		Resistance Fric.Force		Torque		Analytical Sol.	
	(In)	(in)	(mm)	(in)	(mm)	(lbs)	(N)	(lbs)	(N)	lbs*in	N*mm	(lbs)
0.95	0.47	12.01	0.545	13.35	1000	4448	700	3114	365	41255	670	3090
0.95	0.47	12.01	0.545	13.35	1500	6672	1050	4670	548	61883	1005	4635
0.95	0.47	12.01	0.545	13.35	1800	8006	1260	5604	657	74259	1206	5561

(b) Case 2: when end of bit belly hit the ridge

P	Half of P		Radius		Normal Force		Resistance Fric.Force		Torque		Analytical Sol.	
	(In)	(in)	(mm)	(in)	(mm)	(lbs)	(N)	(lbs)	(N)	lbs*in	N*mm	(lbs)
1.25	0.62	15.83	0.62	15.19	1000	4448	700	3114	365	41255	589	2716
1.25	0.62	15.83	0.62	15.19	1500	6672	1050	4670	548	61883	883	4074
1.25	0.62	15.83	0.62	15.19	1800	8006	1260	5604	657	74259	1060	4889

Note: * indicate point of effect of force relative to bit axis

Chapter 5

Measurement of Bit Rotation in Rotary Cutting Test

5.1 Introduction

In the previous section of this dissertation, the results of bit rotation in linear cutting tests were discussed. The measurements showed no bit rotation pattern when bits were under the load in linear cutting. Thus, the logical follow up on that initial study was to look at the bit rotation while performing full scale rotary cutting tests, which are discussed in this section. This includes the experiment setting and results of full scale rotary cutting tests on two bit types and various cutterhead configurations. In this series of experiments, rotation of the drum has been taken into consideration to mimic the actual working conditions of conical bits on partial face machines such as a Continuous Miner (CM) or road milling machine in the field.

For the rotary cutting test, the rock cutting machine was reconfigured/ modified to allow bit rotation measurement with revolution of cutterhead drum. The KMT cutterhead was laced with an instrumented conical bit and bit rotation was measured during the cut with a single cutter. All rotary cutting tests were performed in grout samples (~600 psi). Various testing parameters were examined by changing variables such as skew angle, spacing, depth of cut, and travel speed. The initial testing was performed on the drum featuring a single cutter which was the instrumented bit mounted on the load cell. These tests were followed by some tests of multiple bits mounted on the cutting drum to evaluate the effect of dynamic loading and the cutterhead vibration on bit rotation while other bits interact with the rock surface by entering/cutting/exiting the contact area.

5.2 Initial setting of rotary cutting test

The existing machine for linear cutting test was reconfigured for rotary cutting test. This was done by mounting the cylindrical cutting drum on the machine and setting up the load cell and bit rotation measurement instrument to communicate with the data collection system via radio transmission. The cutting medium selected for the testing was the lower strength samples of grout to be a closer replication of the coal mining or soft ground cutting conditions. The initial set of tests were performed in the remnant grout sample that was used in the linear cutting test and after finishing the first grout sample, another grout sample was ordered and used in the testing. The strength of the grout samples used in rotary cutting test was around 4.1MPa (600 psi) within the range of strength of coal in many of the eastern and mid west coal mines. Additional testing of the concrete cylinders at the PSU concrete lab indicated that the measured strength of the samples could be lower and that the actual strength of blocks was around 3.4 - 4.1 MPa (500-600 psi). The change of the test set up and configuration of the rotary cutting machine in the rock cutting lab in the KMT facility in Latrobe started in October 2009. The set up involved installation of a proximeter to detect the cutterhead drum rotation. The signal from proximeter was used to calculate the actual rotation speed of the drum (RPM). The position of the proximeter was set to detect the bit when bit tip was located at zero degree which is the lowest point on the trajectory of bit tip in the circular path. Depending on the bit type and mounting configuration, the proximeter was adjusted to locate at the initial contact point of bit tip and the rock sample.

5.3 Experiment procedure for rotary cutting test

The retrofitted machine with cutterhead configuration were calibrated for the normal, drag, and side forces as well as the bit rotation while proximeter signals were adjusted for proper

rotation angle (Figure 5-1a-c). The actual cutting radius of the drum with the bit mounted on the load cell and the skew plates is 57.76 cm (22.75"). The proximeter was installed to detect the revolution of the cutterhead and capture the lowest position of the bit trajectory (Figure. 5-1c).

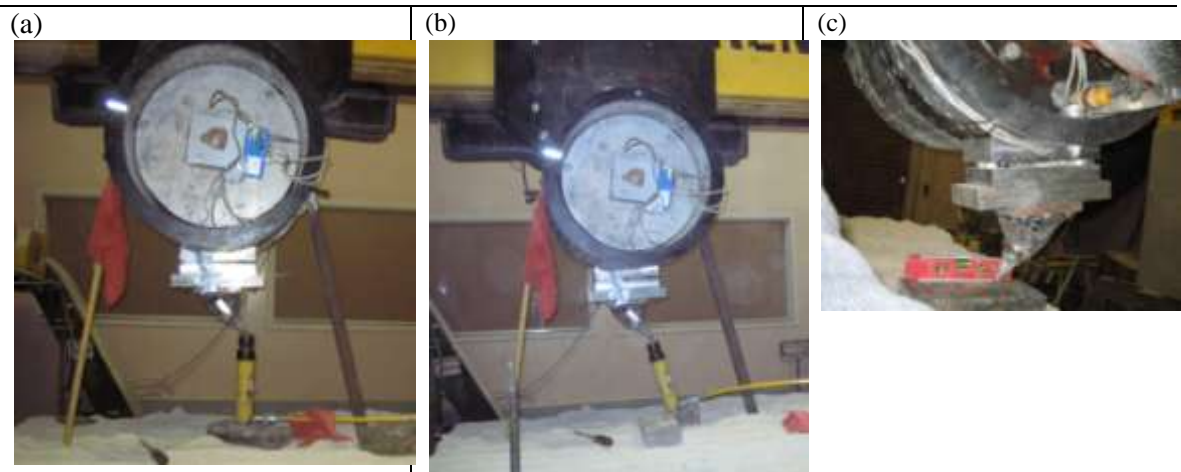


Figure 5-1 Pictures of calibration on: (a) normal force (b) drag force (c) the proximeter setting

With the machine configured for the rotary cutting tests and proximeter adjusted for the proper location, the load cell and the data acquisition system were calibrated at the beginning of each day to assure functionality of the devices and linearity of the force and bit rotation measurement systems. Once the measured signals were verified and the responses were linear and repeatable, the testing was conducted (Figure 5-2).

Overall 480 tests were performed by using single bit configuration on the cutting drum. This includes 318 lines with AM-470 bit and 162 lines with RZ-24 bit. Various approaches were used for quantification of bit rotation (details are explained in the later part in this chapter). The test matrix used in the rotary cutting experiments is summarized in Table 5-1. Testing for each set of cutting parameters was repeated at least 3 times.

Table 5-1 Test matrix for rotary cutting on engineering grout

Bit type	Depth of cut (cm)	Skew angle (degree)	Speed (m/min)	Spacing (cm)
AM470	2.54 , 5.08	0°, 6°, 12°, -6° & -12°	1.5, 3, & 4.6, (6, 7)	2.5, 3.8 & 5, (7.6)
RZ24	2.54	0°, 6°, 12°, -6° & -12°	1.5, 3, & 4.6, (6, 7)	2.5, 3.8 & 5



Figure 5-2 Picture of rotary cutting tests using a single bit on the cutting drum

To investigate the impact of cutting speed and cutterhead RPM on bit rotation, an additional set of rotary cutting tests were performed at 20, 30, 40, and 50 RPM with 1.5, 3, 4.6, and 6 (m/min) (5, 10, 15, & 20 ft/min) cutting speed. The cut spacing used in these tests was 2.5 cm (1") and depth of cut for the drum (or slice) was 2.5 cm (1"). Each setting was repeated 3 times (Table 5-2). The data for 60 RPM rotational speed of the drum was collected from the zero skew angle test data which were already conducted in previous experiment.

Table 5-2 Matrix of the test on effect of speed and RPM on bit rotation

Cutting Speed		20 RPM	30 RPM	40 RPM	50 RPM
1.5 (m/min)	5 (ft/min)	3	3	3	3
3(m/min)	10 (ft/min)	3	3	3	3
4.6(m/min)	15 (ft/min)	3	3	3	3
6(m/min)	20 (ft/min)	3	3	3	3

Various parameters were used for quantifying bit rotation. One approach was to use cumulative bit rotation while the alternative was to use bit rotation per revolution. A closer examination of the bit rotation and comparison between various representations of the bit rotation were performed. Particularly, data from the testing at 0° skew angle was a little bit ambiguous compared to other setting tests. This was due to the initial configuration of the potentiometer circuit to measure bit rotation which yielded 0.8 volts for 360° of rotation

To increase the sensitivity of the system and the magnitude of the output signal, a new circuit was used and the new configuration allowed for 8.7 V range for a full rotation of the bit. The changes allowed for easier analysis of data and the improved ability to identify the bit rotation signal since the magnitude of the signal in the new configuration was much higher than the inducted noises in the electrical circuit. The original circuit used in test sets at 0° skew angle showed relative large noise levels. It was difficult to identify the actual rotation from some of the noises while the bit rotated and traveled through the air to get repositioned for the next cut. Thus, the sets of 0° skew angle tests at 2.5 and 5 cm (1" & 2") depth of cut were repeated. These repeated tests showed the similar patterns of bit rotation with higher bit rotation value. Thus, the tests with the new circuit at zero skew angle set were performed and repeated like previous setting. The results showed similar patterns of forces and similar magnitude of bit rotation like previous repeated results with old circuit. These procedures confirmed the repeatability and reproducibility and reliability of this experiment.

5.4 Procedure of data analysis of rotary cutting test

To analyze collected data from the rotary cutting tests, a different approach and data analysis system needed to be developed. This involved separating the time frame for each revolution, and dividing each revolution time period into contact/cut times when the bit was

engaged with the rock and travel time when the bit was not engaged with the rock. Cutterhead revolution and bit position in each revolution was recognized based on proximeter signals. Using this signal as an indicator of the bit position relative to the cutting surface, the behavior of the recorded cutting forces and bit rotation before, during, and after contact/cutting were carefully analyzed. The false rotations (in air rotation) and irregular or noisy variations of the input data were rectified by the use of visual plot tool kit. The measured force/ bit rotation data for each revolution was obtained by trimming the time series based on the proximeter signal. The data for each revolution was then fed into the MATLAB, to restore signals that had been distorted in some ways. Built-in functions of MATLAB were used for digital filtering of the data. This included Fast Fourier Transformation (FFT) and elliptical digital filter employed in sequence (Mathworks, 2010). This filter is a stop-band filter that eliminates high frequency noises and is generally used for designing professional filter design and can simulate any other filters by changing variables in its filter (Smith, 1997).

Once the filters were applied to eliminate some of the known noise, the data were reprocessed to identify the series for each revolution of the cutterhead based on proximeter signals (Figure 5-3a). With given the data collection rate of 500 Hz and the typical rotational speed 60 RPM, each revolution section included 530 data points. For isolation of data for each revolution, the data points from 30 entries before and 500 entries after the detection proximeter signals were selected to represent bit rotation in given setting (Figure 5-3b). This process was repeated until every revolution of bit engagement with the rock surface in one whole cut had been taken into account.

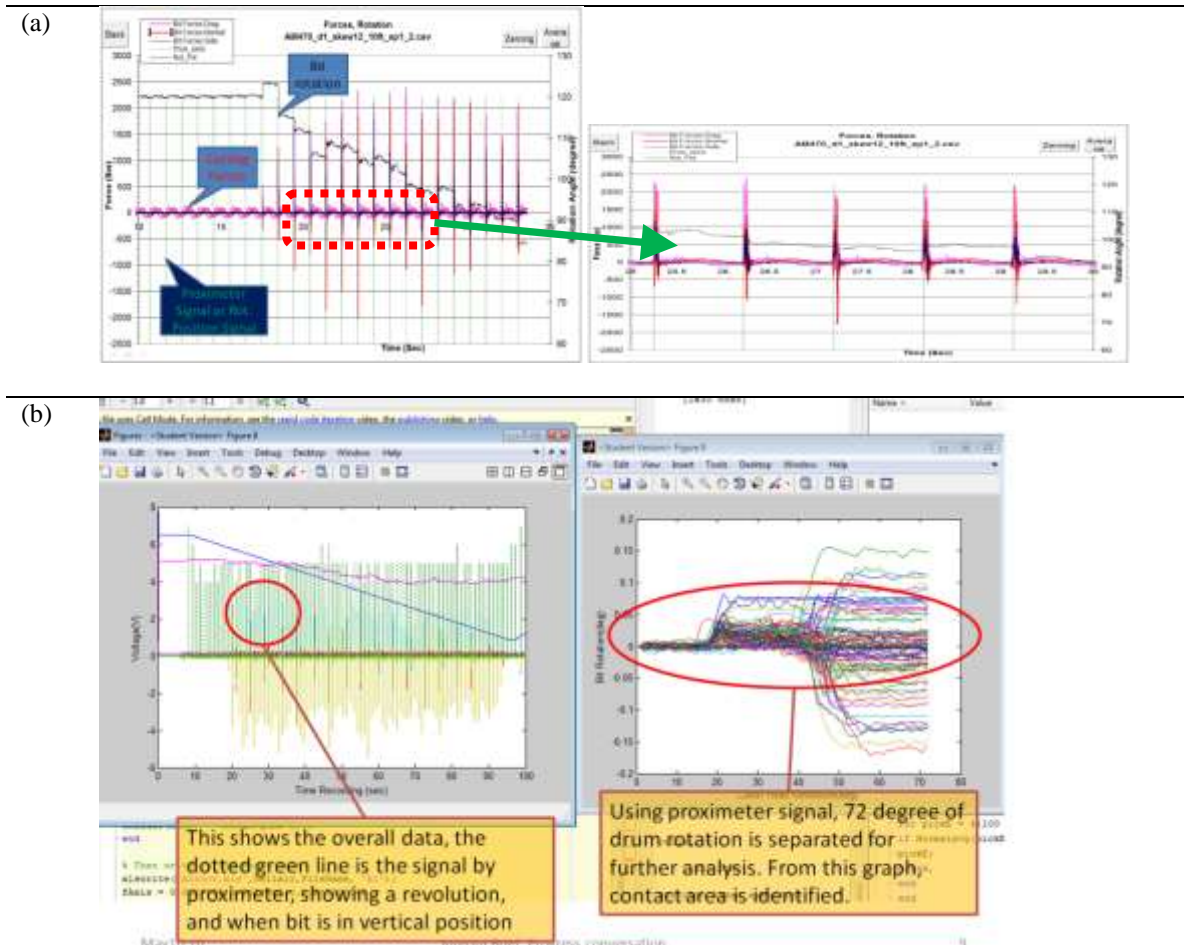


Figure 5-3 Examples of the recorded data and step by step process of the identification of each revolution. (a) typical input data (b) process of superimposing data with MATLAB

Once the data set for each revolution was identified, they were superimposed and averaged for each data entry (time/position) to create a representative set of data for a full rotation for the entire cut. In this representative signal, forces and bit rotation were calculated and the beginning and end of the cut were identified (Figure 5-4a). During this contact time, the degree of the bit rotation, normal, drag, and side forces were calculated in time series. The calculated variables were stored in an Excel file (Figure 5-4b). The behaviors of the bit as represented by the variation of the cutting forces and bit rotation within each test was examined by plotting and reviewed. These procedures were repeated for all the test settings and for each combination of

testing parameters. Then a summary table was generated based on the data. The statistical analysis performed on the results uses this summary which is discussed in the following sections.

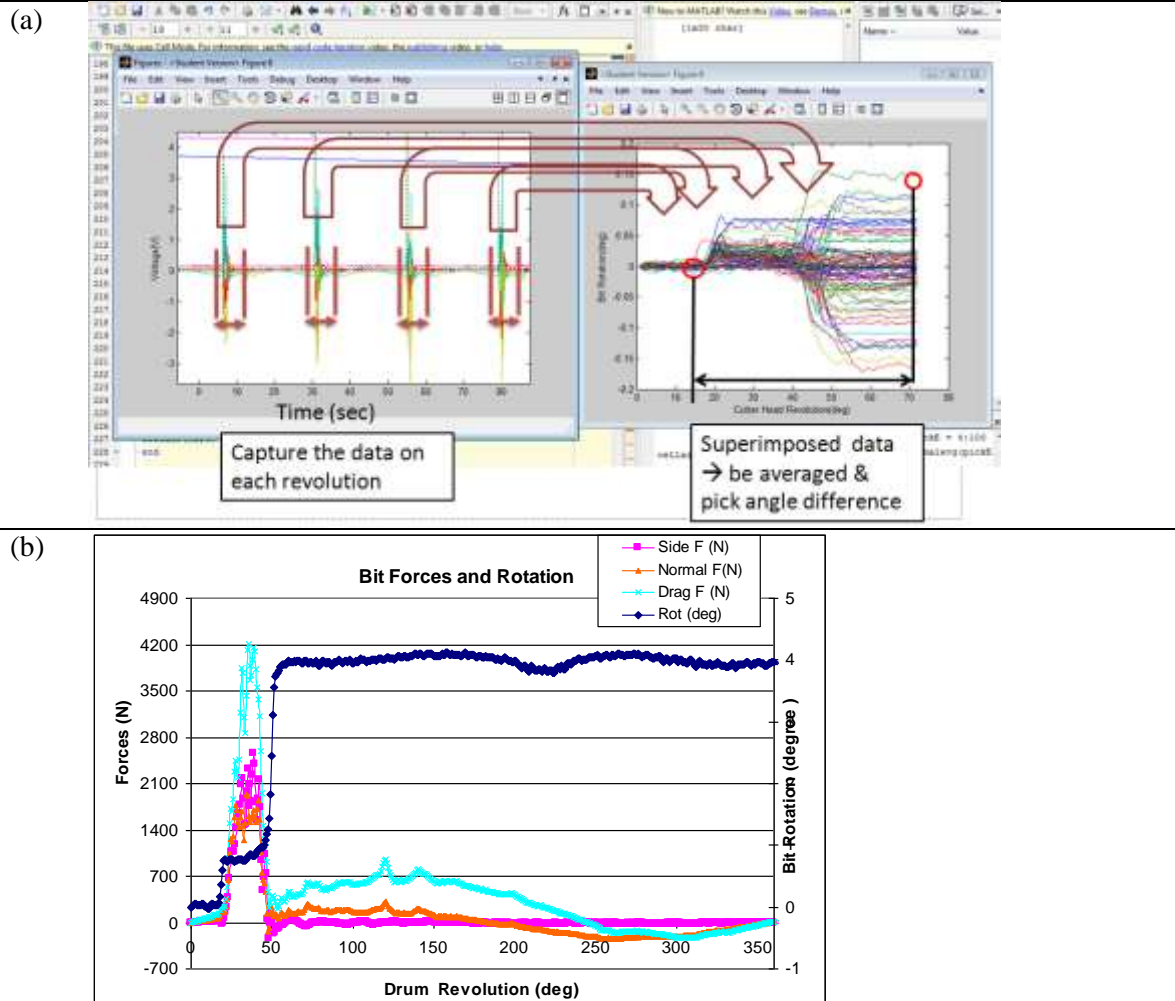


Figure 5-4 Data analysis process. (a) Snap shot of superimposed data (b) output of MATLAB process into Excel file including normal, drag, side forces, and bit rotation

Statistical analysis methods were used to find the best fits and trends in the data. All statistical analysis was performed with MINITAB16®. Data that had a unique setting was eliminated during the statistically analysis. For example, data of 6 and 7 m/min (20 & 23ft/min) travel speed and 3" spacing, and intermediate cuts were not included in the analysis. After all, number of promising variables were determined which included known essential variables such

as normal, side, and drag forces, skew angle, spacing, depth of cut, and travel speed. Just for information, linear regression (Kutner et al., 2004) was not used because this method was unsuitable for analysis and development of trends in the data set.

Analysis of variance (ANOVA) was also performed on this data set which showed the significant effect of skew angle on bit rotation. For this test, MINITAB 16® was used with respect to three independent factors; skew angle, spacing, and travel speed. Each factor had different levels: five levels on the skew angle, three levels on the spacing, and three levels on the travel speed. Before the ANOVA tests on skew angle, correlation tests on influence of other parameters such as spacing, speed, and forces onto bit rotation were performed with multivariate plot. The results show that the travel speed does not really affect the bit rotations. As a pilot test, an ANOVA test was performed regarding to skew angles only. However, this method is not reliable since it neglected the spacing effects which frequently impacted the bit rotation. Thus, it would not be an ideal method to depend on.

The last method of statistical analysis for this project was Response Surface Method (RSM) and General Linear model (GLM). The RSM was used for the analysis of RPM and speed effects on bit rotations. RSM allows observers to visually examine the response over the region of interest and enables the observers to analyze the response sensitivity to input variables and to find the interaction among the variables in the responses (Kuehl, 2000). GLM did not show any reasonable correlation between variable. Thus, solely RSM was used

5.5 Results of single bit rotary cutting test on AM-470 bit

The controlling parameters in the rotary cutting test were more than those used in the linear cutting tests. In this series of tests, in addition to spacing, skew angle and material type, other parameters such as RPM, cutting speed (or translational speed of the drum), and sequence

of cut were varied and their impact on bit rotation was studied. A number of initial experiments were performed to set up the proper procedure for developing and testing the proper test matrix. The initial test settings are illustrated in Table 5-3. The data collected from these tests were reviewed and analyzed to evaluate the best approach with determining parameters to be used in final analysis. For example, to quantify the bit rotation, a few different means of calculating the rotation was examined. The terms used through graphs and the text in this report are explained as follows:

1) “Rot_whole” represents bit rotation for one revolution, or bit rotation after one 360° revolution of cutterhead drum. This parameter was determined by the proximeter signal spike.

2) “Abs_Rot” means that absolute value of the Rot_Whole by ignoring its sign/directions.

3) “Cum-rot” is the cumulative or sum of recorded bit rotation per each individual line of cut or the sum of Rot_whole in one cut line. In other words, Rot-Whole was added up for a whole line to get Cum-Rot.

4) “Rotcum” refers to the difference between bit rotation angle at the start of a cut line and the end of the cut line. It is calculated by the end point of bit rotation angle minus the beginning point of bit rotation angle for each data file.

To determine all these parameters, separate programs were developed using MATLAB commercial software which is very powerful in handling large data sets and data matrices. Rot_whole and Abs_Rot are used for analyzing bit rotation for each test or set of testing parameters. Cum-Rot and Rot-cum were only used for checking the reliability of the data processing by the MATLAB programming. These two parameters will be similar or very close if there is no abnormal signal or behavior in data. In most case in the course of rotary cutting tests, these two numbers were almost identical.

5.5.1 Study on speed and RPM effect on bit rotation

Similar to other statistic tests, to use commercially available programs and RSM, the assumption of RSM needed to be satisfied. Two basic assumptions of RSM are normality and the equal variance. The normality was tested with 95 % confidence with 0.05 p-value. The results showed that data follow the normal distribution. The equal variance tests, Bartlett's Test and Levene's Test, showed equal variance with 95 % confidence.

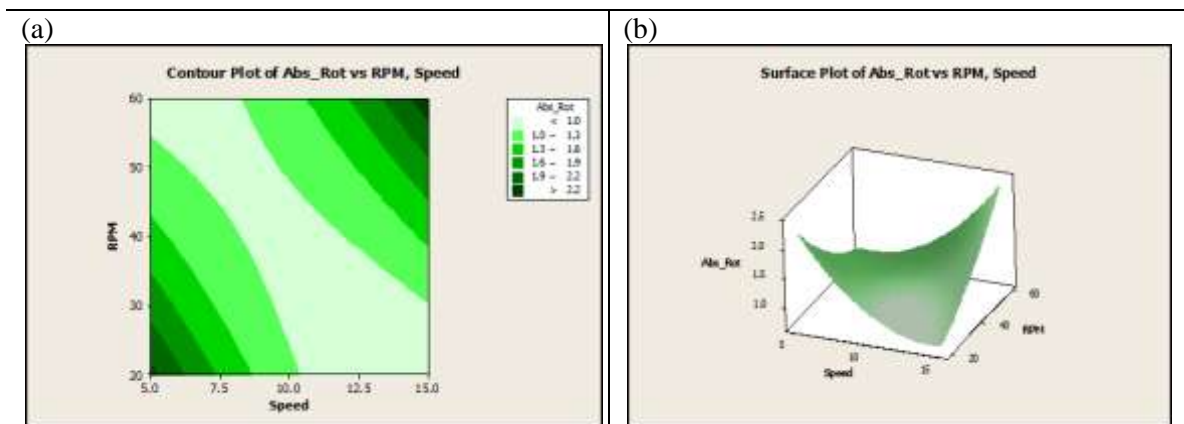


Figure 5-5 RSM of the RPM and speed relationship: (a) contour plot (b) surface plot.

RSM analysis can be used to find trends in multi-variable data sets. For example, the interaction between the RPM and speed shows that lower speed with lower RPM and higher speed with higher RPM can lead the best bit rotations as show in Figure 5-5ab. To find the best fit in the RSM analysis various functions can be used. This includes linear, linear +interaction, linear + quadratic term, and full quadratic model. These models were carefully regressed in general regression model and examined regarding variance inflection factor (VIF) which is an indicator of multi-collinearity and p-value (MINITAB, 2010). The model with lowest VIF and p-value was selected as optimum model. For example the results of RSM analysis of RPM and speed show that rotational speed of 35 ± 5 RPM and cutting speed of 3 ± 0.3 m/min (10 ± 1 ft/min) were the settings for optimum bit rotation. This means that to achieve higher bit rotation with lower RPM,

lower cutting speed should be used and vice versa. The normal, side, and drag forces were strongly related to each other and increased by increasing travel speed. Also, side and drag forces decreased at higher RPM since the higher rotational speed at the same travel speed means lower absolute bit penetration into the face.

High bit rotation was observed at zero skew angle. To prove the repeatability of the test results and for verification purposes, test at 0 skew angle with 2.5 and 5 cm (1" & 2") depth of cut were performed at different times (Dec_23_09 and June_10_10) (Figure 5-6ab). Results obtained on these different days were similar enough to confirm that higher bit rotations at 0 skew angle comparing with total average bit rotations was not random numbers or caused by signal noises.

General linear model (GLM) analysis was used to find the difference between bit rotation results of the two test sets at zero skew angle tests. This GLM included the code that distinguished the old circuit and new circuit. This analysis did not show any difference regarding circuits. Also it confirms that travel speed does not affect the bit rotation. Thus, repeatability and re-product-ability of the experimental set up and data analysis were confirmed by using GLM method. And the t-test pair system for both 2.5 cm and 5 cm (1" & 2") depth of cut were performed to find its impact on bit rotation. But this analysis did not show any significance of depth effect on bit rotation.

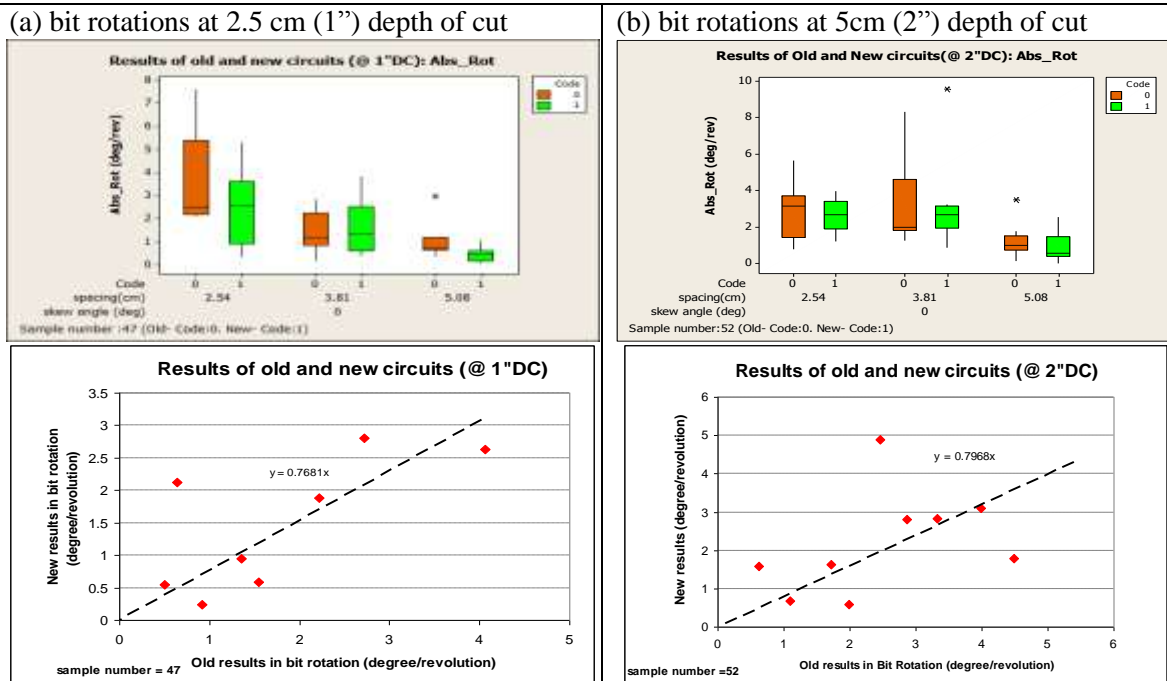


Figure 5-6 Comparison of the bit rotation data with old circuit (Dec _23_09) and new circuit (June _10_10): (a) at 2.5cm (1") (sample number = 47) (b) at 5 cm (2") depth of cut (sample number =52)

5.5.2 Results and analysis of rotary cutting tests for single bit drum using AM470 bit at 2.5cm (1") depth of cut

Summary of the rotary cutting test matrix on single bit drum using the AM-470 bit is provided in supplementary data (Table Suppl. A). Details of the test matrix in Table 5-3 included 133 different settings excluding missing data and noisy data. The data set of 2.5 cm and 5 cm (1" & 2") depth of cut were analyzed separately. This allowed for reducing the number of variables from 5 to 4 parameters to simplify the recognition of patterns and trends for influence of essential parameters on bit rotation. Multivariate plots were used for the analysis of the data to support and illustrate the actual phenomenon on bit rotation.

Overall forces and measured bit rotation are plotted to observe general trends in bit rotation versus independent testing parameters as preliminary plots before determining the important parameters. Figure 5-7ab is the plots of measured bit rotation against spacing and travel

speed respectively. Similar plots show that skew angles can impact bit rotation at higher rate compared to other parameters. Then spacing influenced bit rotation more than travel speed did. This is based on observing the mean values for each test setting. The sub-box panels in Figure 5-7 shows (a) travel speed and, (b) spacing respectively. A set of three lines in the each sub-box shows the variation of average measured bit rotation and the potential trend relative to the skew angle. In these trend lines the red lines show the variation of average bit rotation relative to (a) spacing and (b) the green dashed line for travel speed. Further analysis of pattern of variation of measured bit rotation will be discussed along with trends of normal, side, and drag forces later.

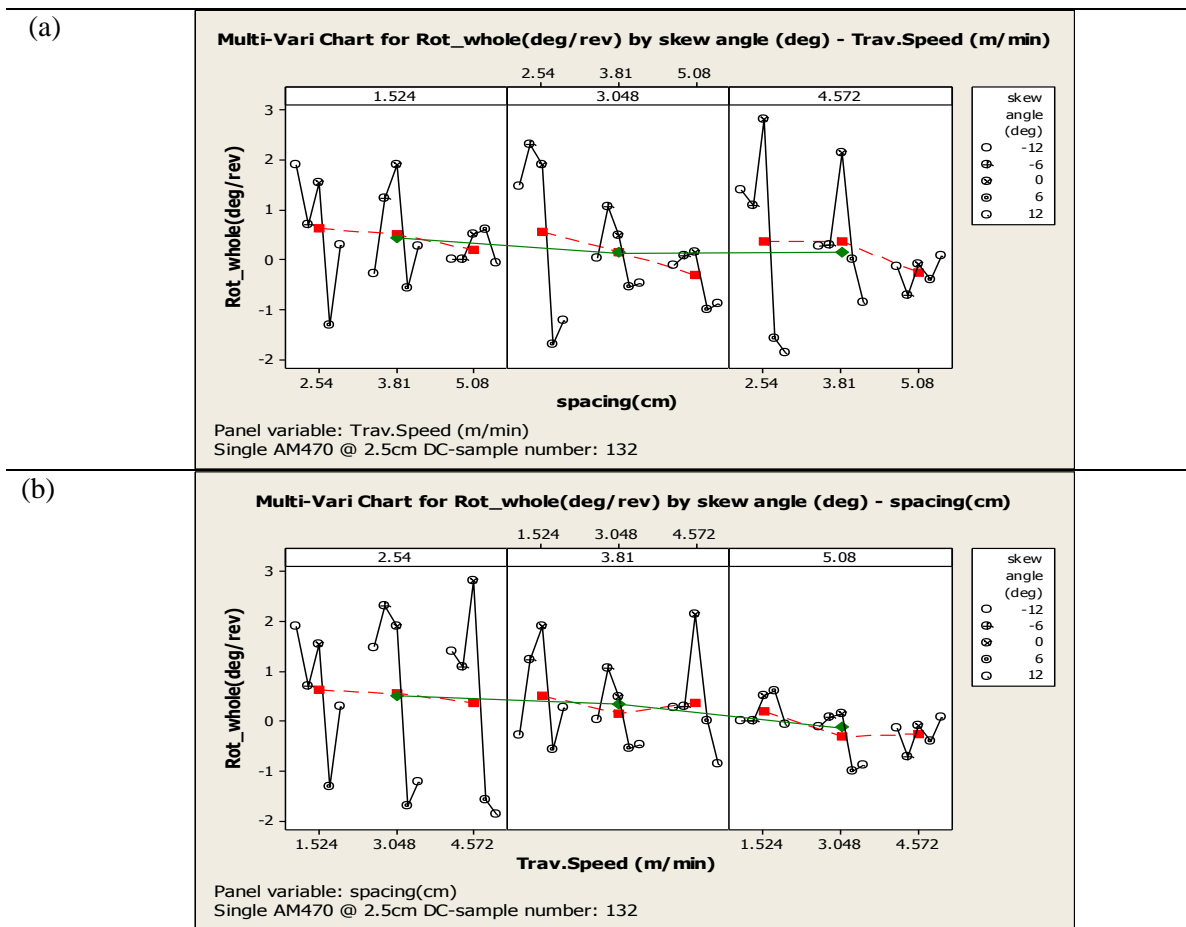


Figure 5-7 Multivariable plot of bit rotation of AM470 bit at 2.5cm (1”) depth of cut regarding skew angle, travel speed, and spacing sorted by: (a) spacing (b) travel speed

To find the relationship between travel speed (speed), spacing and bit rotation, multivariate plots were also used. As shown in Figure 5-7, the green line indicates the mean value of each box cell and the red line indicates the mean of each line in the each cell box. Not only skew angle but also spacing has significant impacts on bit rotation, while travel speed seems to have no significant impact on bit rotation.

Force analysis was performed with multivariate plots for preliminary estimation. Side forces have the direction which follows the skew angle directions. In negative skew angles, side forces were measured in the negative direction and vice versa. Normal and drag forces seem to be sensitive to increase with the travel speed (red line) in Figure 5-8. Interestingly, the trends of forces regarding skew angles are almost symmetrical relative to 0 skew angle. This trend seems to be reasonable, since positive and negative skew angle are changed by skew plate while other cutting parameters are the same.

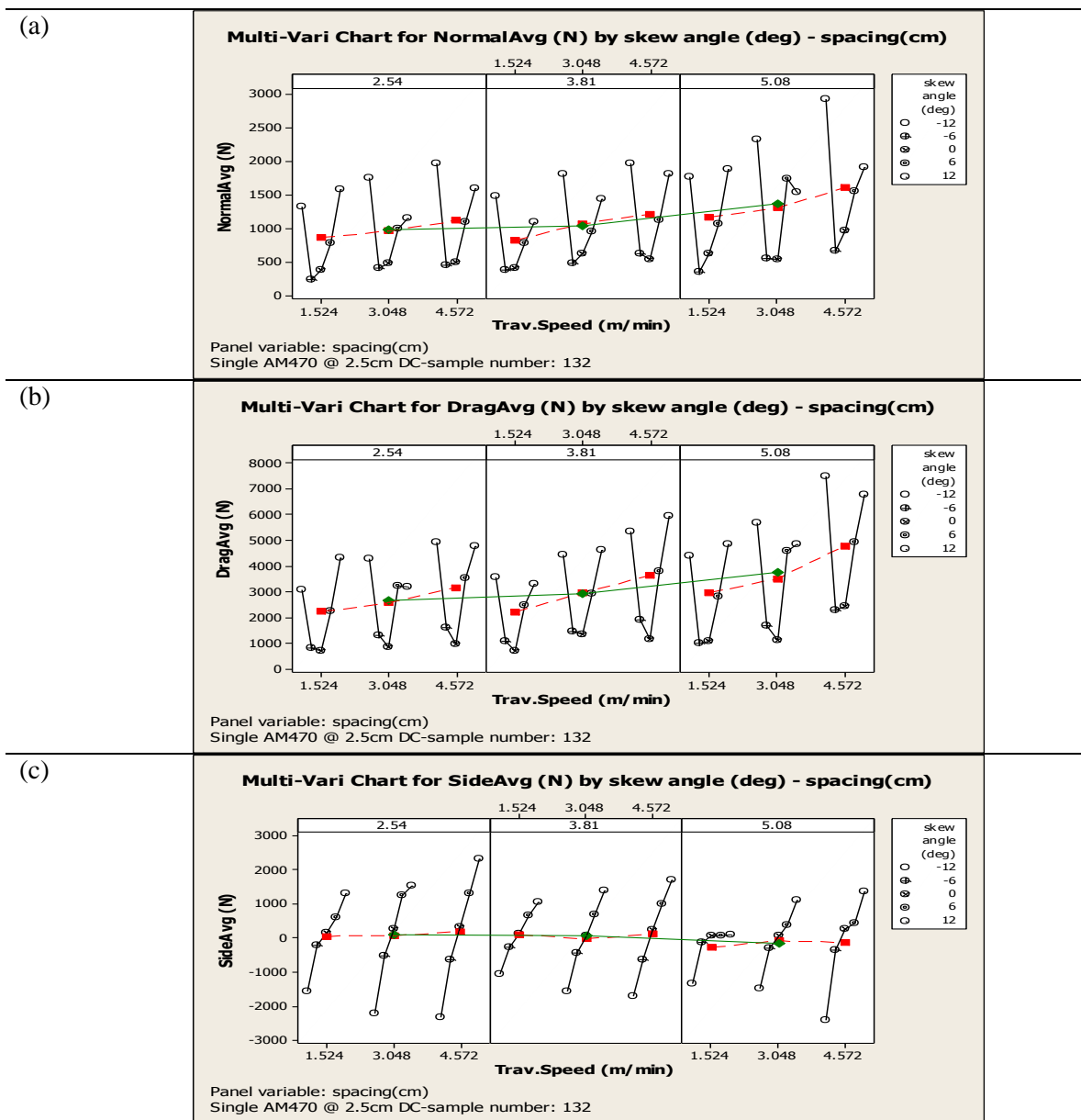


Figure 5-8 Multivariate plot of force trend at 2.5cm (1”) depth of cut regarding spacing, travel speed and skew angle in rotary cutting test: (a) normal forces (b) drag forces (c) side forces

Due to the insensitivity of bit rotation to travel speed, the data from different travel speeds were summed for each spacing to create a larger and more reliable data set for additional analysis. The combined data is plotted in the box plot for various skew angles and cut spacing. The result of analysis shows that increased spacing decreases the bit rotation and changing skew

angles affects the direction of bit rotation (Figure 5-9a). Normal and drag forces increased and side force was decreased with spacing. It seems a like large magnitude of the side force at lower spacing enhanced the bit rotation (Figure 5-9).

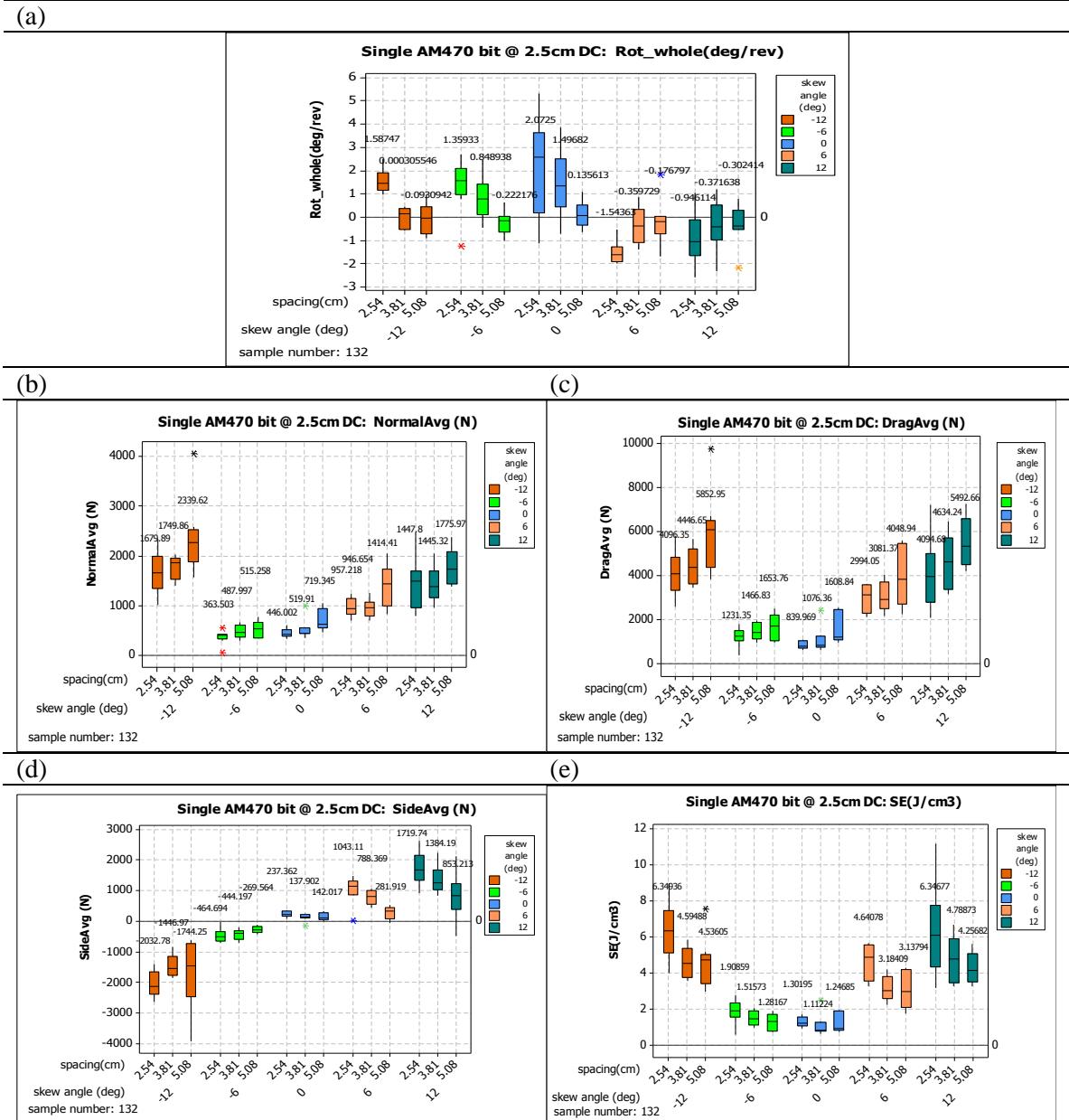


Figure 5-9 Plots of bit rotation and forces of AM470 single bit at 2.5 cm (1”) depth of cut regarding the skew angles, and spacing (outermost first): (a) bit rotations (b) normal forces (c) drag forces (d) side forces (e) specific energy

To have a closer look at the bit rotation respect to positive and negative skew angles, the concept of the positive and negative bit rotations was defined and used for finding some trends of bit rotation. Before discussion on the detail, few terms are defined: positive/negative skew angle and positive/negative bit rotation. Positive skew angle means that the bit tip is heading to the lower level on the cutting surface or previously cut line. Negative skew angle means that the bit tip is heading towards the higher level on the cutting surface. Positive bit rotation means clockwise (CW) and negative bit rotation means counterclockwise (CCW) bit rotation. From Figure 5-9a, positive skew angle showed positive bit rotation and negative skew angle showed negative bit rotation. In this graph, bit rotation signals show the positive number when the bit rotated counterclockwise which is negative bit rotation. This trend seems to be caused by the first contact of the bit tip with the cutting surface and the higher side of the cutting surface.

The largest bit rotation was observed at zero skew angle and at smallest spacing. However specific energy decreased with increased spacing/penetration as anticipated within the range of variables used in the testing. Specific energy was higher at the higher skew angles and this shows decreased cutting efficiency. Side forces decreased with spacing, as did bit rotation (Figure 5-9e).

Analysis of response optimizer suggested that largest bit rotations were observed around 0 skew angles at 3.6 m/min (11.7 ft/min) travel speed with 2.5 cm (1") spacing. Thus RSM plots were made with 2.54cm (1") spacing and 3 m/min (10ft/min) which were the closest condition that calculated optimum values. Maximum recorded bit rotation was at 2.5 cm (1") spacing for negative to positive six degree skew angle. Figure 5-10 indicates that the bit rotation was sensitive to the skew angle. Thus, in 2.54cm (1") depth of cut with single AM470 bit, we can conclude that the highest bit rotation can be achieved with 2.54cm (1") spacing among negative six to positive six skew angles. Even though travel speed did not affect the bit rotation, high travel speed was recommended to improve the productivity in real mining situation.

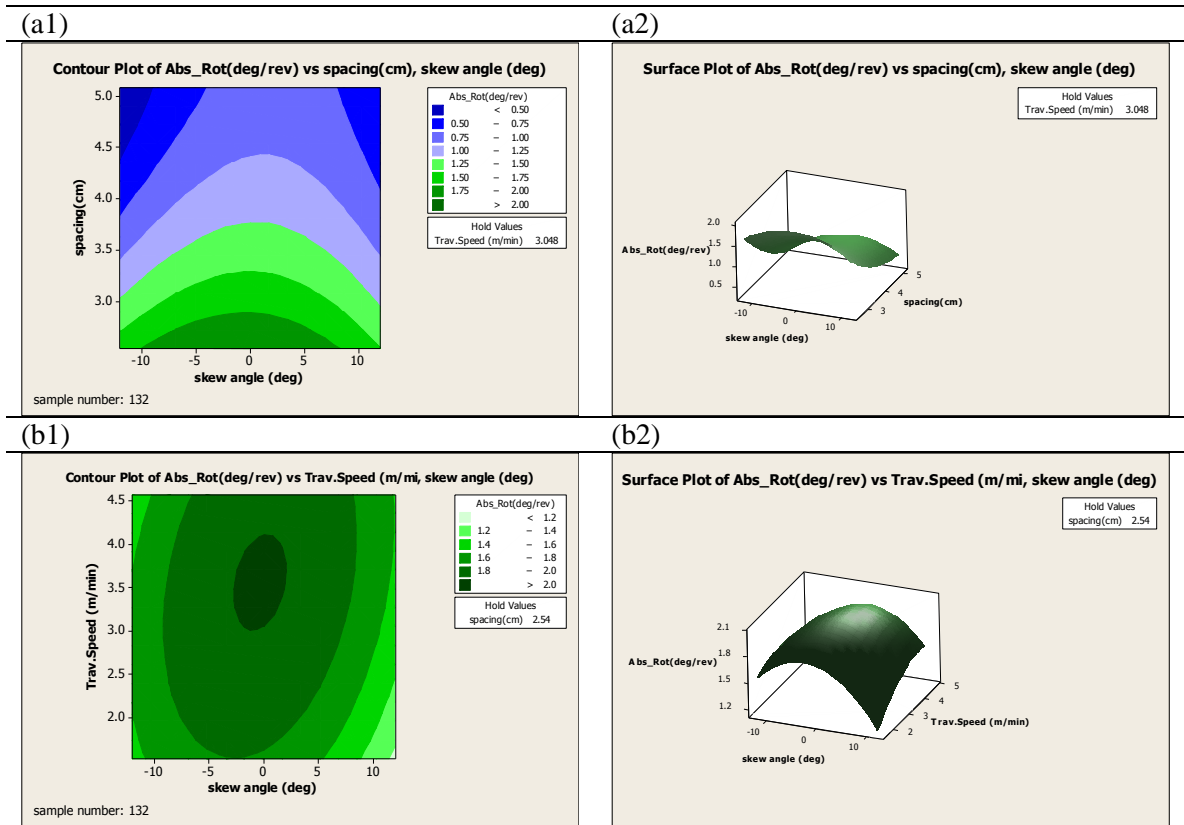


Figure 5-10 RSM plots of bit rotations of AM470 bit at 2.5 cm (1”) depth of cut regarding: **a**, skew angles and spacing at 3 m/min (10ft/min) travel speed: (a1) contour plot (a2) surface plot; **b**, skew angles and travel speed at 2.5cm (1”) spacing: (b1) contour plot (b2) surface plot

This RSM analysis supports that the effect of travel speed was not significant on the bit rotation from the observations on the previous multivariate plots (Figures 5-8). Thus, various speed data were combined and slurred into other significant parameters such as spacing and skew angles to find more significant trend of experiments.

5.5.3 Results and analysis of AM470 bit single at 5 cm (2”) depth of cut

The rotary cutting test on the drum with a single AM470 bit was continued at 5cm (2”) depth of cut and 135 cut lines were analyzed excluding missing and defective data (Table Suppl. B). The result of the testing is presented as a function of skew angle, spacing, and travel speed in

Figure 5-11. The green dots indicate the mean value of each box cell and the red dots indicate the mean values of different settings in a given cell box. Similar to 2.5cm (1") depth of cut, there was a distinctive difference in bit rotation relative to the variation of skew angle. Also, cut spacing seems to be more significant than the travel speed on bit rotation. The rest of the multivariate graphs were plotted with combined data to eliminate travel speed and to focus on the effect of spacing and skew angle.

The force trends of 5 cm (2") depth of cut are little different from those of 2.5 cm (1") depth of cut with respect to skew angle, spacing, and travel speed (Figure 5-12a-c). Normal and drag forces seem to follow the travel speed which is actually penetration of the bit into the rock face (red line). However, bit rotation seems to be insensitive to spacing mainly due to lack of full breakage at higher spacing (green line). Interestingly, the force trend relative to skew angles are different than the previous set of tests and form a S-shaped trend relative to zero skew angle.

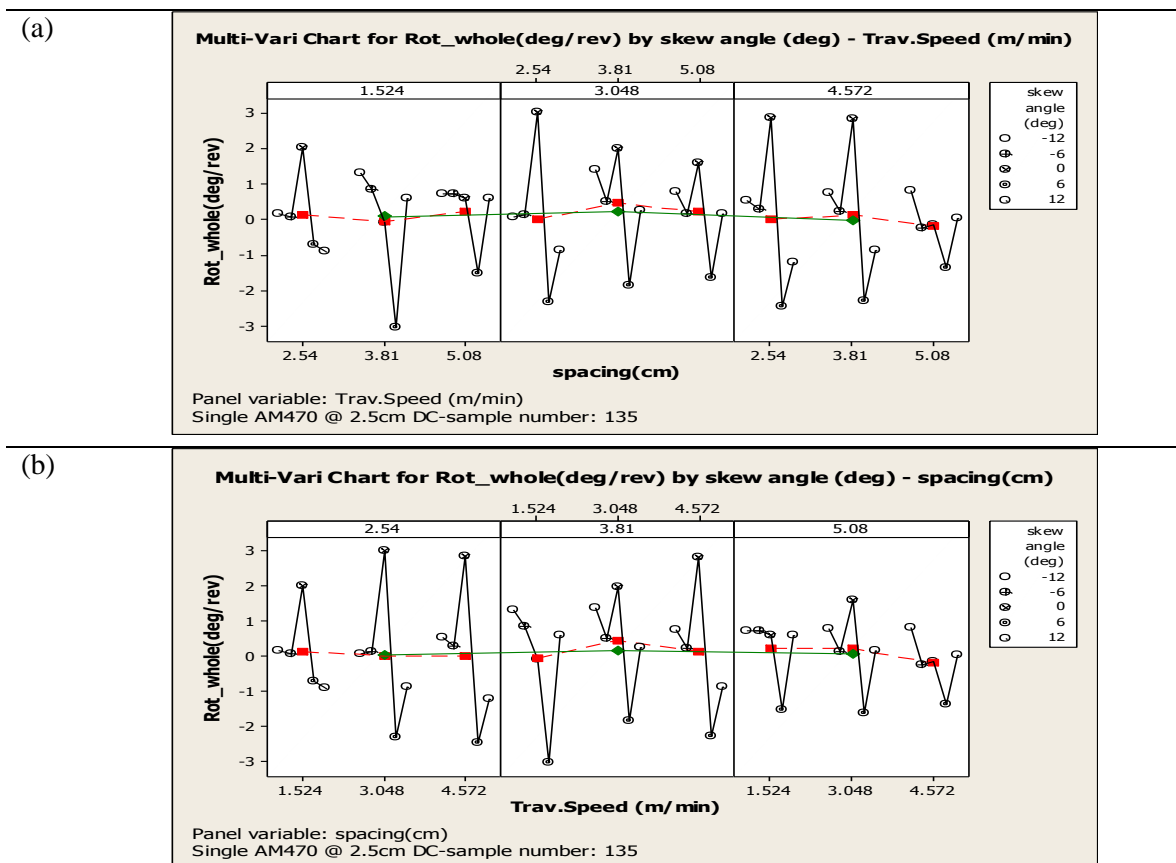


Figure 5-11 Multivariable plots of bit rotation for single drum testing of AM470 bit at 5cm (2") depth of cut as a function of skew angle, travel speed, and spacing sorted by: (a) spacing (b) travel speed

The force trends of the AM470 single bit at 5cm (2") depth of cut were different from the results of the AM 470 single bit at the 2.5 cm (1") depth of cut. Normal and drag forces increased with the increment of travel speed. However, with only multi-vari chart overall mean of side force in one cell box seems to be insensitive to cut spacing (green line) and travel speed (red line) similar to the AM 470 single bit at 2.5 cm (1") depth of cut (Figure 5-12a-c). Negative 6 degree skew angle seem to require more force than -12 degree skew angle. In the positive direction, +12 degree skew angle required more forces than +6 which is a similar trend to a previous set of tests.

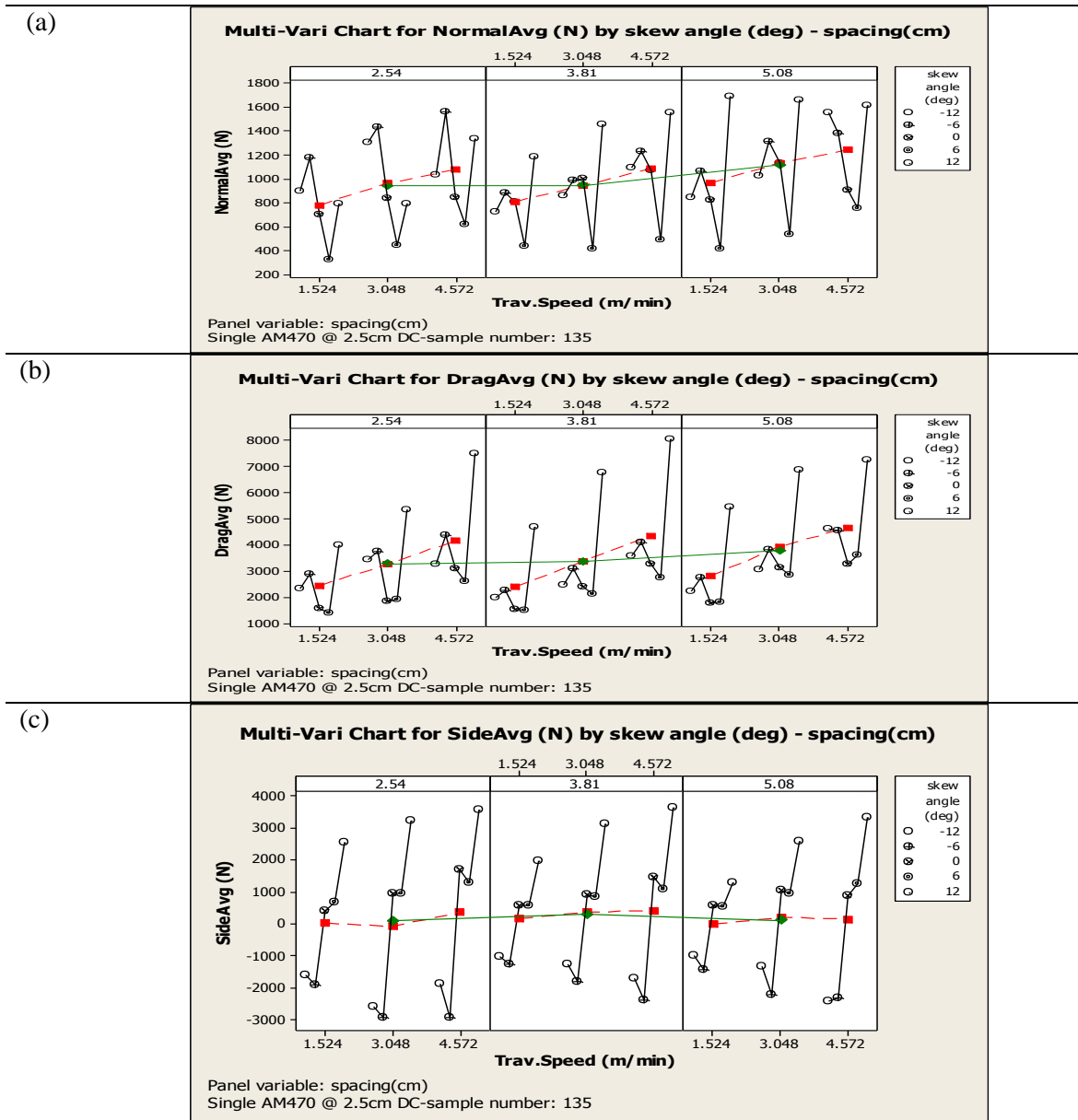


Figure 5-12 Multivariate plots of forces of single AM470 bit with 5 cm (2”) depth of cut as a function of spacing, travel speed and skew angle: (a) normal forces (b) drag forces (c) side forces

At 3.8 cm (1.5”) spacing, the highest bit rotation was observed at positive 6 skew angles (Figure 5-13a). Low normal and drag forces coincide with high bit rotation in this series of tests (Figures 5-13bc). Specific energy decreased with the increasing spacing, perhaps indicating that the optimum SP ratio could be achieved at higher spacing. (Figure 5-13e)

The high magnitude of the side force was related to the bit rotation (Figure 5-13d). Similar to previous sets of tests, higher side force magnitudes coincided with the higher bit rotation. Negative side forces induced negative bit rotation and positive side forces caused the positive bit rotation. Similar to the test results for the AM 470 on the single bit drum at 2.54 cm (1") depth of cut; positive rotation in the graph (Figure 5-13a) means the negative bit rotation. It means that the bit rotation trends were consistent and side forces were related to the bit rotation.

Zero skew angle at 2.5 and 5 cm (1" & 2") depth of cut showed the tendency to lead to the higher values of average bit rotation and were overall more advantageous to cutting efficiency. Higher skew angles lead to higher side force and higher specific energy requirement, which means lower efficiency and lower risk of bending the blocks and breaking them off the drum.

The RSM analysis for 5cm (2") depth of cut with the single bit drum using the AM 470 bit was used for examination of inter-relationship between bit rotation and other parameters. A similar trend was observed when comparing the result of RSM with that of the previous test at 2.5 cm (1") depth of cut. From 0 to +6 skew angle, high bit rotation was observed at low spacing. Response optimizer indicates that optimum bit rotation can be achieved at ~4 degree skew angle and 3 cm (1.2") spacing, and 4.6 cm (15ft/min) cutting speed. This response optimizer calculated the derivative function of the statistical equation and found the best spot for the bit rotation. Thus, these numbers were too specific to be realistic, but it can be used to get approximate conditions for real cutting settings

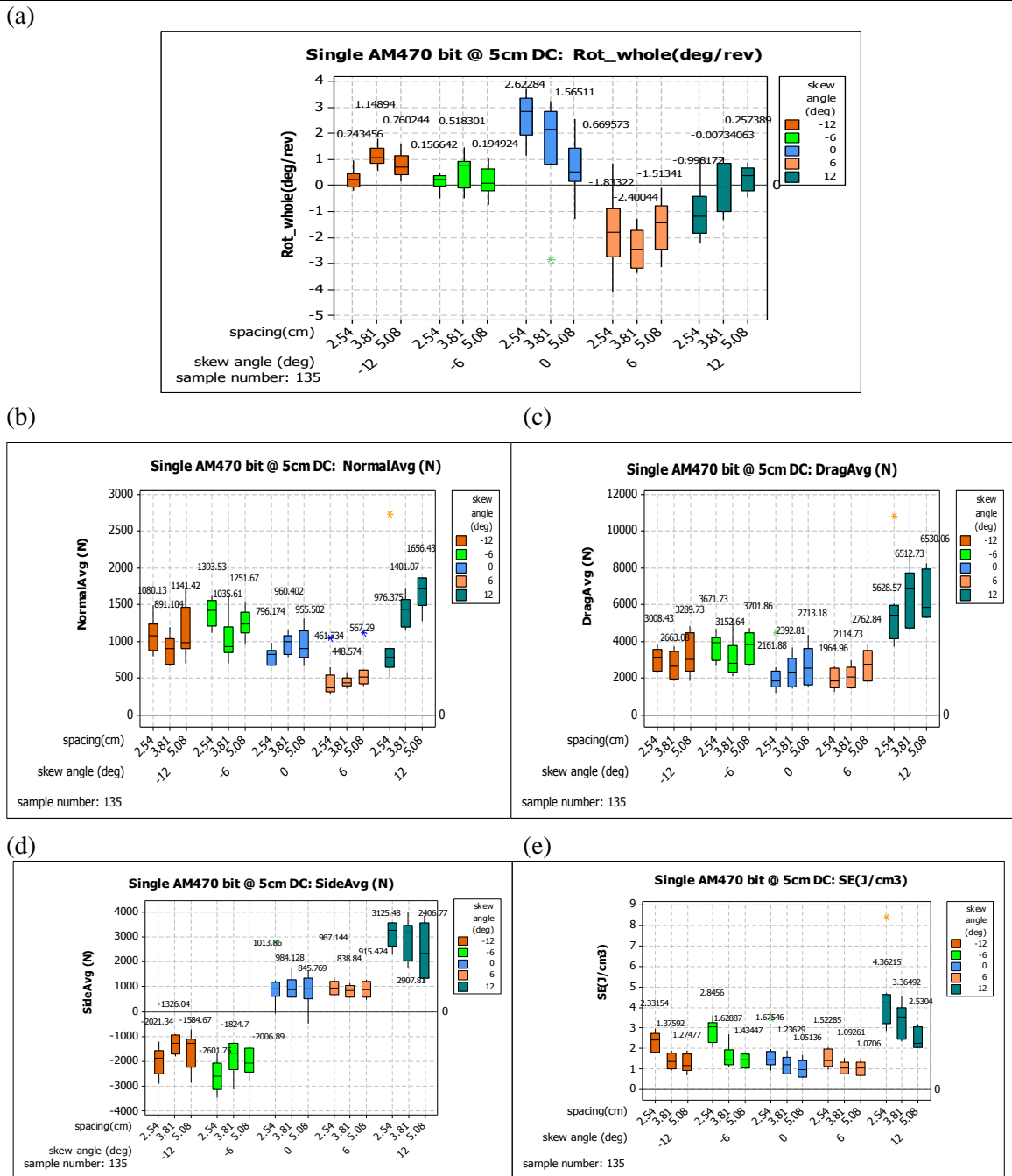


Figure 5-13 Plots of bit rotation, forces, and SE of single AM470 bit cutting at 5cm (2”) depth of cut: (a) bit rotation (b) normal force (c) drag forces (d) side force (e) specific energy

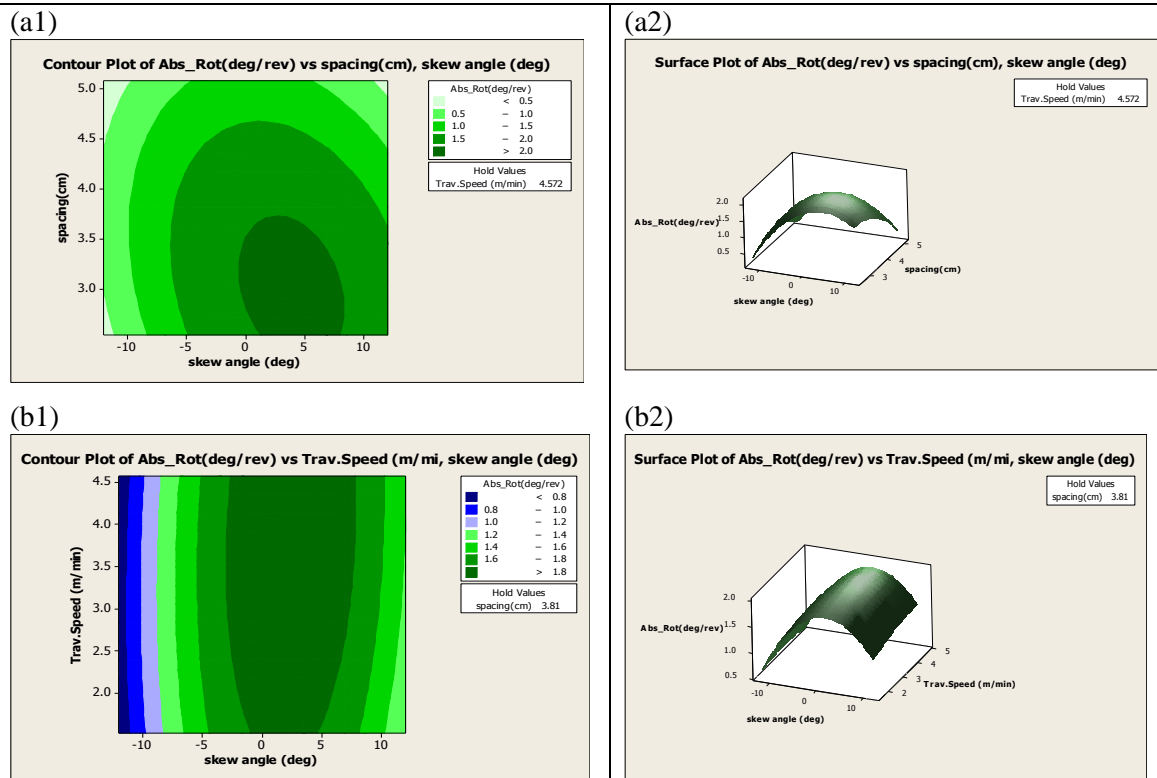


Figure 5-14 RSM plots of bit rotation of single bit drum using AM470 bit at 5cm (2") depth of cut: as a function of : a, skew angle and spacing at 4.6 m/min (15 ft/min) travel speed: (a1) contour plot (a2) surface plot; b, skew angle and travel speed at 2.5 cm (1") spacing: (b1) contour plot (b2) surface plot

Analysis showed that bit rotation is insensitive to cut spacing. The best skew angle for bit rotation was found in a range between zero and five degrees (Figure 5-14a). Results also show that travel speed does not affect the bit rotation (Figure 5-14b). In conclusion, to get the highest bit rotation in the 5.08 cm (2") depth of cut with a single AM470 bit, 0 to 5 degree skew angle seem to produce the best results.

5.5.4 Discussion of the results of single bit rotary cutting tests using AM-470

As noted earlier, there were two series of rotary cutting tests performed using a single AM-470 bit on the Kennametal drum. The tests included 2.5 cm and 5 cm (1" and 2") depth of

cut and variations of spacing, cutting speed and skew angles. The results show that normal, drag, and side forces increase linearly with spacing and travel speed within the range of parameters used in the test. However, travel speed does not affect bit rotation. At this stage, the questions of the effect of depth of cut on the bit rotation could be addressed.

To find the effect of depth of cut on bit rotation, comparison of 2.5 cm and 5 cm (1" and 2") depth of cut was performed. These data included over 267 lines of data and showed that bit rotation trends between 2.5 cm and 5 cm (1" and 2") depth of cuts were similar (Figure 5-15). It means that different depths have no significant influence on the bit rotation, but the forces have different trends. At this stage, the questions of the effect of depth of cut on the bit rotation could be not addressed with a degree of certainty.

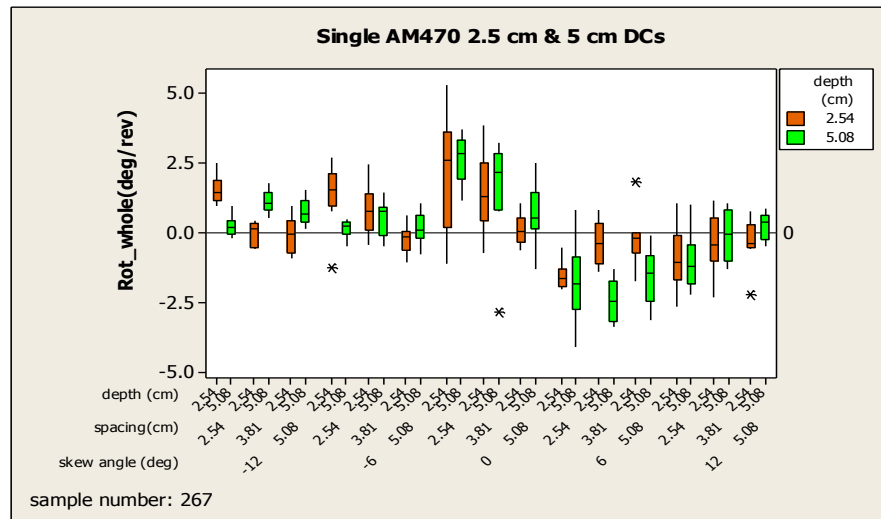


Figure 5-15 Effect of depth of cut in full scale rotary cutting test using AM470 single bit for 2.5 cm and 5 cm (1" and 2") depth of cut.

At 2.5 cm (1") depth or shallow depth of cut, wear was observed to occur in a uniform manner (Figure 5-16a). In deeper cut, 5 cm (2") depth of cut, some wear was observed in three flattened surfaces on the bit (Figure 5-16b). The simplest explanation for this different wear process is that, at low penetrations, the bit action is different than at higher penetration in terms of

normal and drag forces. Perhaps this is the penetration above which more consistent chip formation occurs, which is a desirable outcome. At high skew angle with 2.5cm (2") depth of cut, the AM470 bit seem to experience more wears than zero skew angle. High forces of 5cm (2") depth of cut at skew angles illustrated in Figure 5-16 may correlate to the wear process. Thus, in deeper cuts, it is not recommended to have a higher skew angle, due to possibility of higher bit wear and less bit rotation compared to 0 -6 degree skew angles

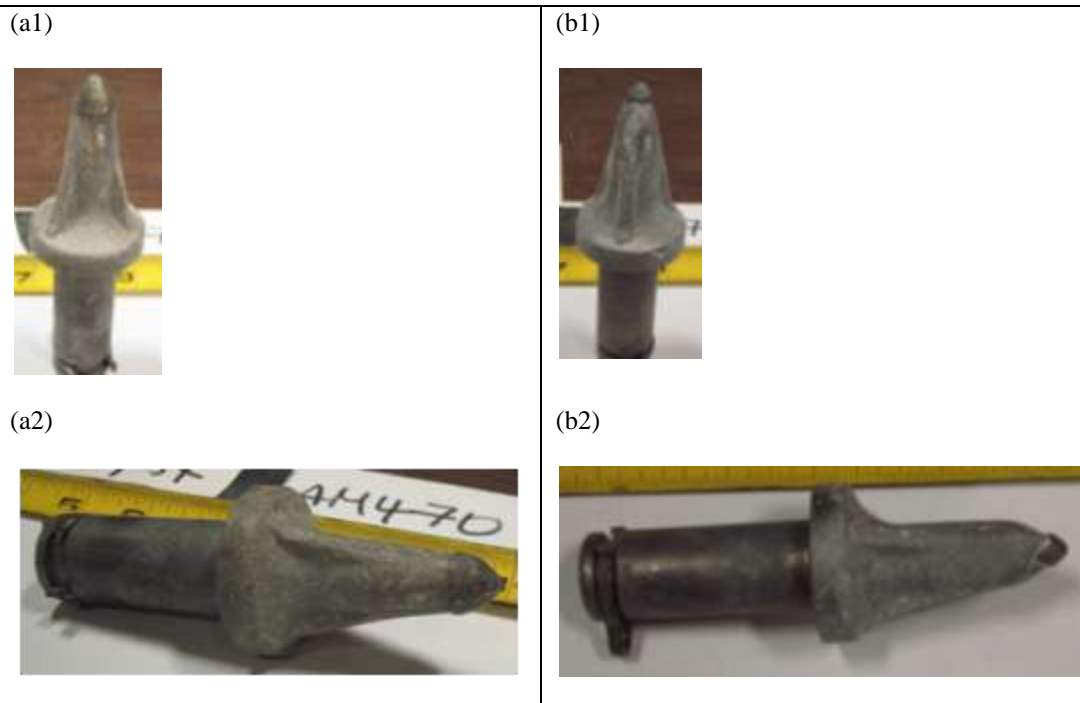


Figure 5-16 Picture of AM740 after test : **a**, after data set of 2.5cm (1") depth of cut was completed: (a1) top view (a2) side view; **b**, after data set of 5cm (2") depth of cut was completed (b1) top view (b2) side view

The finding of the testing could be summarized as follows:

- Travel speed does not affect the bit rotation.
- Normal and drag forces were affected by cutting geometries (spacing, and depth of cut), and increased with skew angle and travel speed.

- Side forces affect bit rotation and were not affected by the travel speed but by the spacing and skew angle.
- Observed bit rotations were highest at zero to slight skew angle like +6 degrees skew angle.

5.6 Analysis of RZ24 bit single cutting test

Full scale rotary cutting tests were continued by using the RZ 24 as a single bit on the Kennametal cutting drum. The skew angles tested were -12, -6, 0, 6, and 12, similar to the testing with AM-470 bit. Similarly, spacing was 2.5, 3.8, & 5 cm (1", 1.5", & 2") and the tests were run at cutting speed of 1.5, 3, and 4.6 m/min (5, 10, & 15 ft/min). Each subset was repeated at least three times (Table Suppl. C). While testing the RZ24 bit, dirt was frequently getting packed in the retaining ring, causing jamming of the bit and the retaining system (Figure 5-17). This process prevented bit rotation. Thus, during the experiments, to allow for bit rotation, the bit had to be pulled out and cleaned to remove the dirt and release the bit shank for rotation. This could indicate possible problems with these types of bits in actual operation.

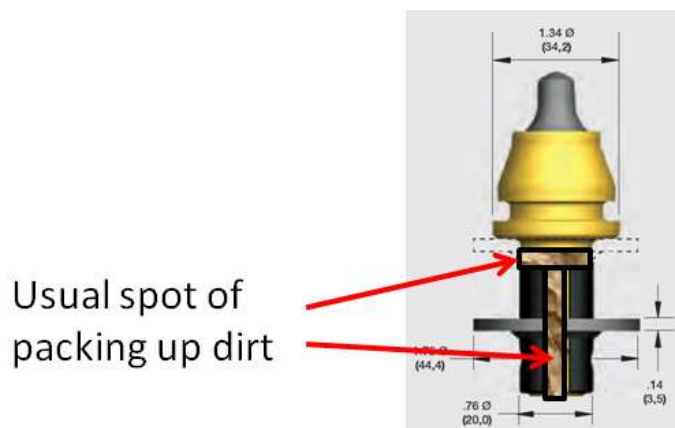


Figure 5-17 The accumulation of dirt between bit shank and the retainer rings in the RZ24 bit.

A total of 130 tests were performed and details of experimental program for this series of tests are summarized in Table Suppl. C. In testing of the RZ 24 bit the electrical connections were changed and as a result the direction of positive and negative rotation was different than that of tests with the AM470 bit. Due to the geometry of the bit and the short neck of the carbide relative to the bit body, only 2.5 cm (1") depth of cut was tested on RZ24 bits.

Figure 5-18 and 5-19 show the preliminary data trend in RZ24 bit at 2.5cm depth of cut. The bit rotation was more observed to the skew angle and followed by spacing. The forces were increased with increasing spacing and travel speed. Then, the test results were analyzed with more enhanced statistical analysis using box plots. Similar to the testing with the AM-470 bit, the results show that high bit rotations were observed at smaller spacing and that travel speeds did not have any significant impact on the bit rotation. Side forces were reduced with an increase in spacing. Normal and drag force increased with spacing as anticipated.

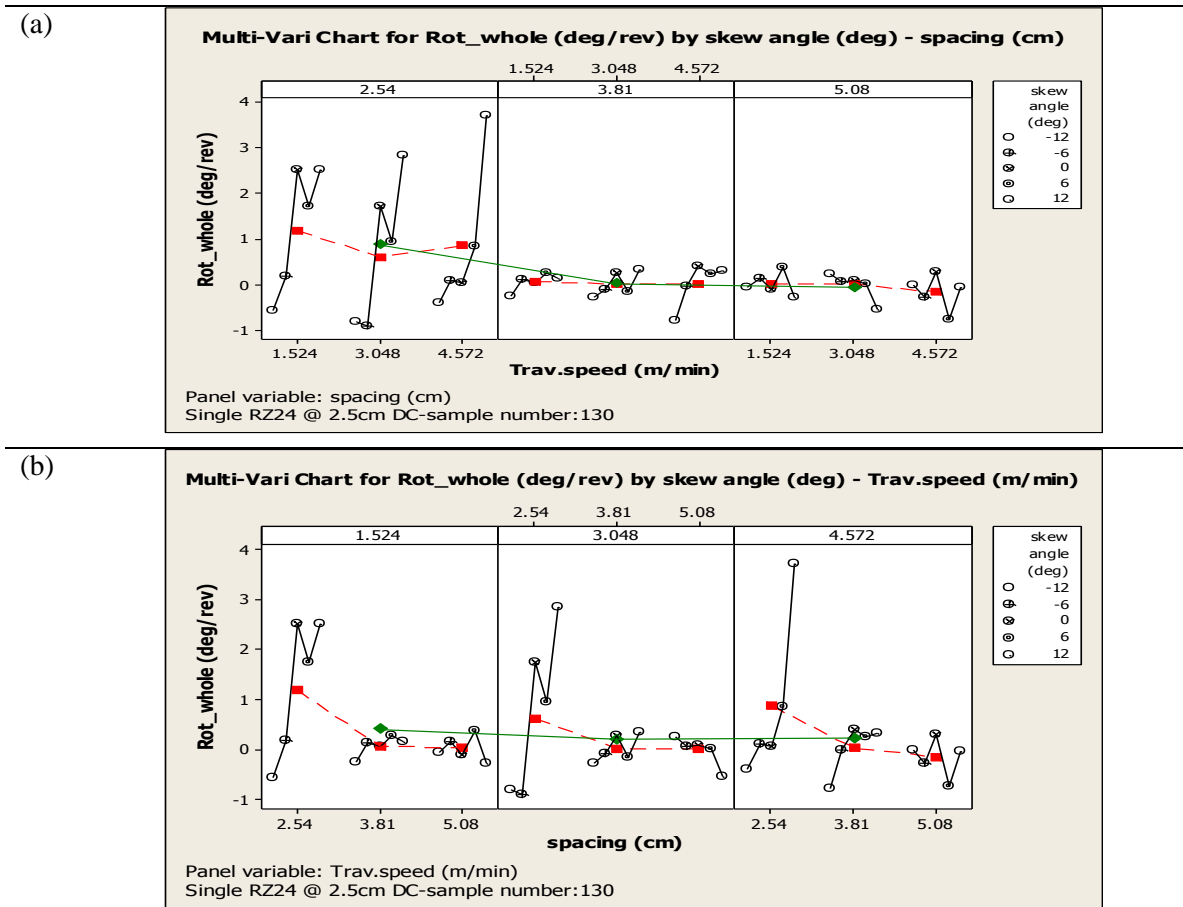


Figure 5-18 Multivariable plots of bit rotation of RZ24bit at 2.5cm (2”) depth of cut as a function of skew angle, travel speed, and spacing for testing sorted by: (a) travel speed (b) spacing

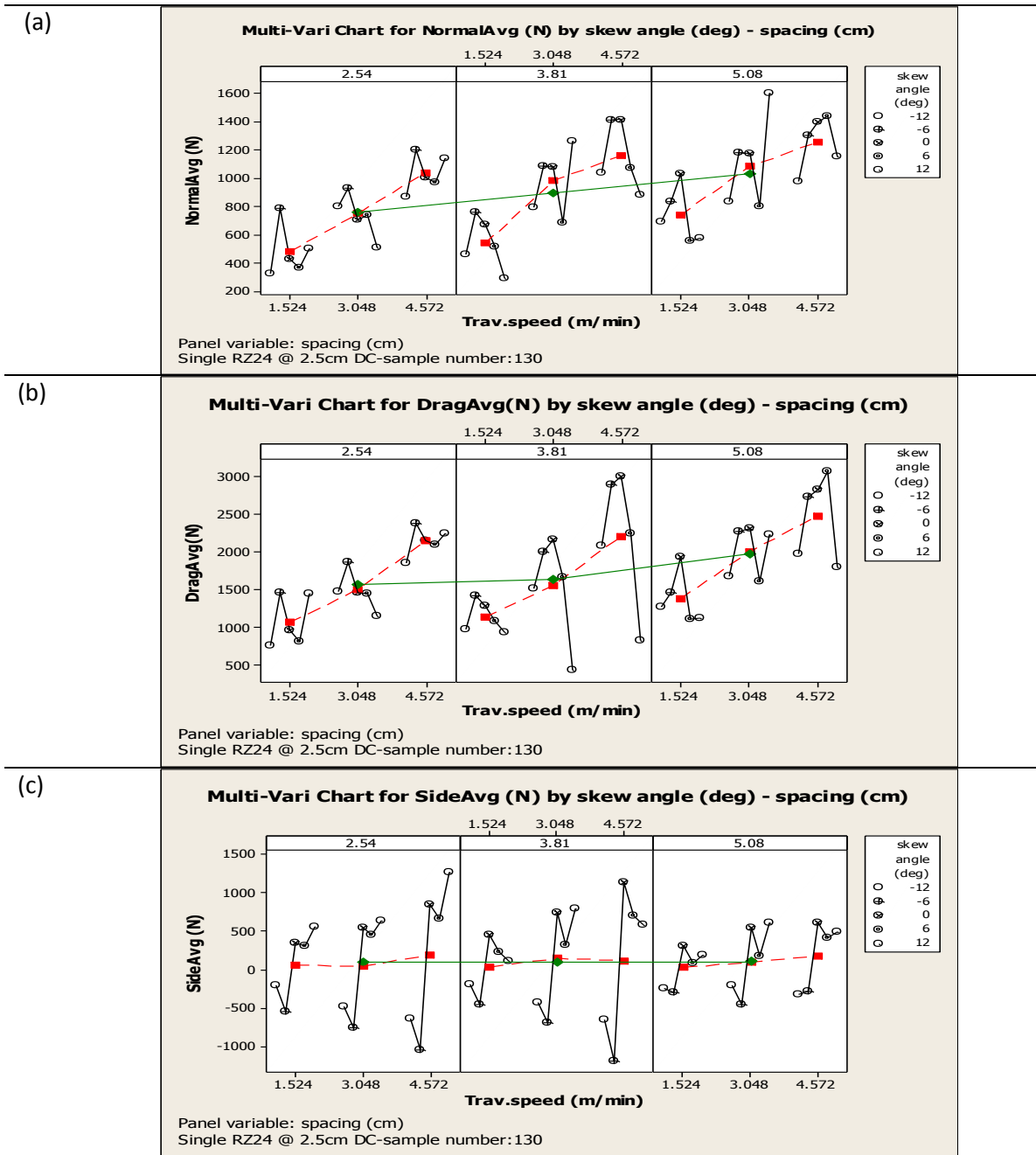


Figure 5-19 Multivariate plots of forces of single RZ24 bit with 2.5 cm (2”) depth of cut as a function of spacing, travel speed and skew angle in rotary cutting test: (a) normal forces (b) drag forces (c) side forces

Due to the insensitivity of the observed bit rotation to travel speed, the box plots were developed for varying skew angle and spacing. The plots show that increased spacing contributes

to reduced bit rotation (Figure 5-20a). Normal and drag forces were increased with the spacing. Side forces and specific energy were decreased with spacing. The higher magnitudes of side force seem to coincide with the larger bit rotations (Figures 5-20b-e). Positive skew angles lead to positive bit rotation (CW) and negative skew angle caused negative bit rotation (CCW).

General trends of the RZ24 bit can be explained by following: Bit rotation in the RZ 24 single bit at 2.5 cm (1") depth of cut; at zero degree and 12 degree skew angle had highest bit rotation at the 2.5 cm (1") spacing. The bit rotation decreased with spacing. Drag forces tend to increase with spacing increment SE tends to decrease with spacing increment, at a low to moderate rate. Side forces decrease with increment of spacing. Exceptionally 1" spacing at 12 degree skew angle showed high bit rotation, high drag force which needs further investigation on the reason of difference from typical behavior of the bit rotation trend.

RSM analysis was performed for bit rotation. The response optimizer indicated that best bit rotation can be achieved with 12 degree skew angle, 2.5 cm (1") spacing and 1.5m/min (5 ft/min) travel speed. Figure 5-21a illustrates the changes in bit rotation relative to cut spacing and skew angle at 1.5 m/min (5 ft/min) travel speed. Highest bit rotation was observed at 2.5 cm (1") spacing, from +6° to +12° skew angles. The bit rotation was not sensitive to the travel speed at 2.5 cm (1") spacing (Figures 5-21b). Regardless of travel speed, highest bit rotation was observed from +6° to +12° skew angles in RSM analysis. It seems that the high bit rotation of 1" spacing at 12 skew angle shift the general trend and control the RSM results. However, from the boxplot, 1"spacing at 0 skew angle show the highest bit rotation, too. RSM analysis has inherent usage of the regression method. Thus, if there is one of scope data, this data can dominate the analysis and alter the original trend. This is happened in this RSM analysis. However, combination of boxplot and this RSM analysis, I can conclude that still 0"skew angle is the best set for bit rotation.

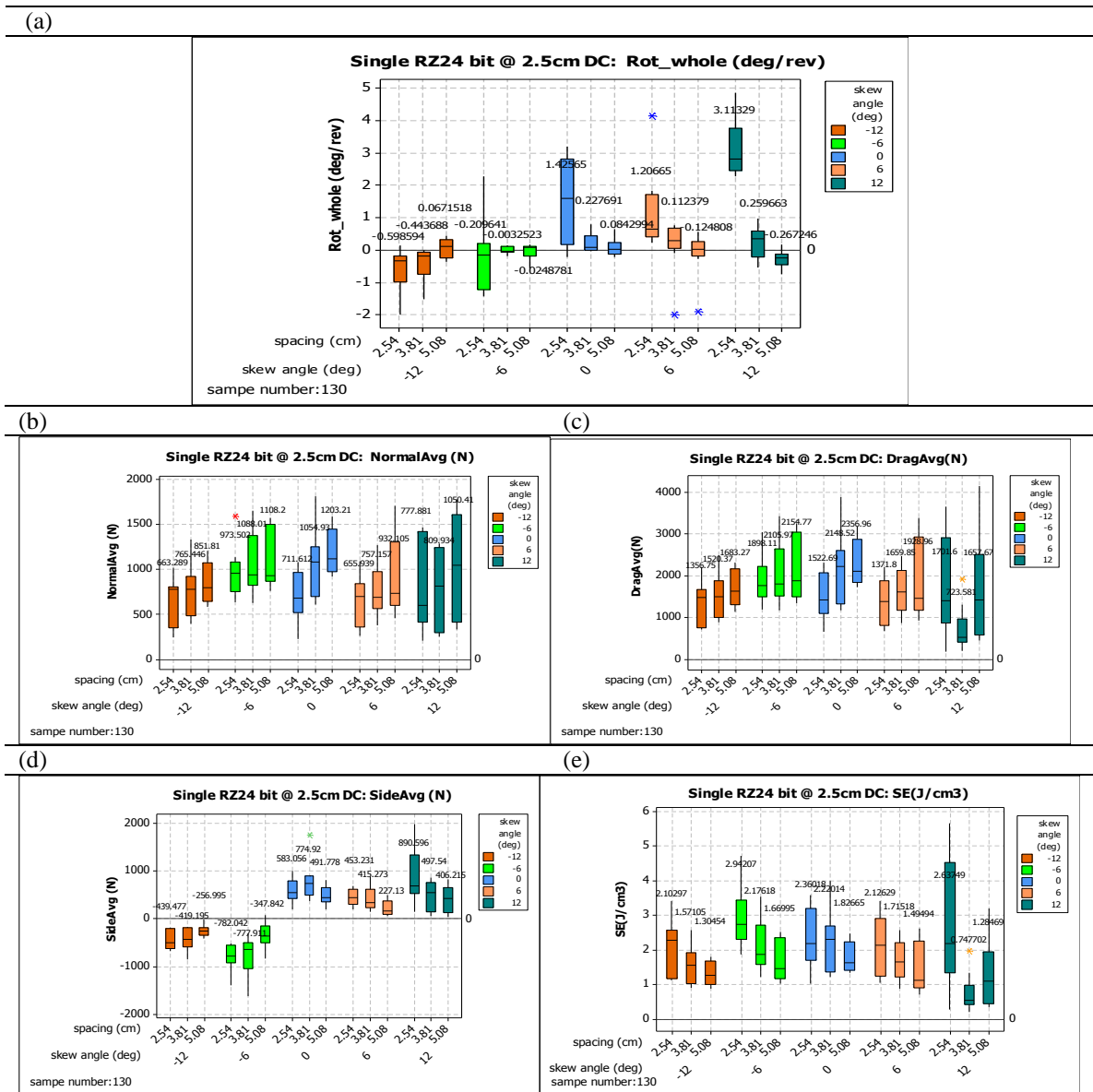


Figure 5-20 The box-plot of bit rotation, forces and SE of single RZ24 bit at 2.5 cm (1”) depth of cut as a function of skew angle spacing: (a) bit rotations (b) normal forces (c) drag forces (d) side forces (e) specific energy

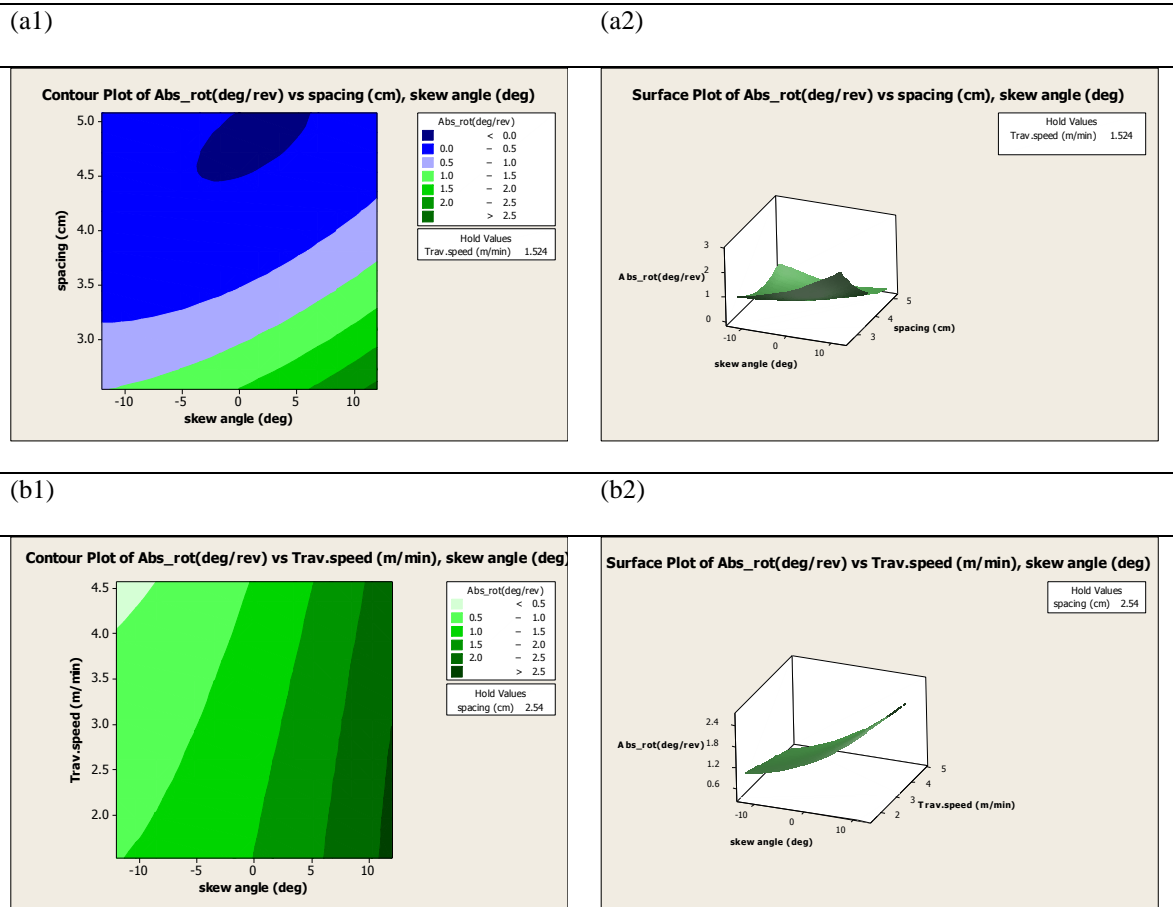


Figure 5-21 RSM plots of bit rotations of single RZ24 bit at 2.5 cm (1") depth of cut regarding :
 a, skew angle & spacing at 1.52 m/min (5 ft/min) travel speed: (a1) contour plot (a2) surface plot;
 b, skew angle & travel speed at 2.5 cm (1") spacing: (b1) contour plot of (b2) surface plot

5.7 Rotary cutting tests of the drum with multiple bit drum

Rotary cutting tests on the drum with multiple bit lacings were performed to evaluate the potential bit rotation during the cutting action due to dynamic loading and interaction with other bits on the drum. Tests were performed with the instrumented bit mounted on the skew plate for testing different skew angles, along with a few other bits at preset angular interval. Multiple bit

setting is the closest cutting conditions to the field applications. There are many papers about the optimum cutterhead lacing but none has discussed the impact of cutterhead lacing on bit rotation. It is well known that optimum lacing will lead to higher efficiency and productivity, minimum vibration, and longer bit life. For the purposes of this study, simple arrangement of multiple bits was designed to investigate the effect of bit interaction on bit rotation.

5.7.1 Experiment setting for multiple AM470 bits

The cutting drum was arranged with two lines of cuts and two bits per line, for a total of four bits, each pair at 180° and overall the four bits placed at 90° from each other (Figure 5-22). The spacing between two lines of cut was set at four inches, which is the minimum spacing that the bit blocks could be mounted considering the existing cutting drum bolting pattern. The other three bits placed on the cutterhead were not instrumented and had additional shim under the bit block to reach the same height as the instrumented bit. The testing was performed at negative 6, zero, and positive 6 degree skew angles. The skew angles in the multiple bit tests were defined based on the direction of the instrumented bit tip: The bit tip directed toward to left hand side was considered positive, where the bit faced the lower level in the cutting sequence and back of the bit was facing to the higher level of sample. When bits headed toward the right hand side of the cut lines, it was assumed to be a negative skew angle.



Figure 5-22 Pictures of multiple bit cutting drum lacing for rotary cutting test: (a) side view (b) front view

For 0° skew angle, the cutting matrix of multiple cut is summarized in Table 5-3. A total of 76 cuts were performed: 44 cuts at 2.5 cm (1") depth of cut and 32 cuts at 5 cm (2") depth of cut. This matrix was conducted at 0, -6 and 6 degree skew angles at 2.5 cm and 5 cm (1" & 2") depth of cut. Detail summary results of the multiple bit cutting tests are provided in Table Suppl. D. The 10 cm, 5cm, and 2.54 cm (4", 2" & 1") spacing cuts were performed in chronological order at the same sample height, which meant that depth of cut for 2.5 cm (1") spacing is lower than the depth of cut for the 5cm and 10 cm (2" & 4") in same given setting of depth of cut. The cutting sequence was to cut the 10 cm (4") spacing cuts first, followed by 2" spacing cut by re-aligning the cut lines with the ridges in between the 10 cm (4") original cutting lines. Finally, 2.5 cm (1") spacing cuts were conducted by placing the drum where the bits would be cutting between the 5cm (2") cut lines. This sequence created the lower depth of cut at 2.5 cm (1") spacing than expected depth of cut value. For example, the depth of cut at 2.5 cm (1") depth of cut, $4/5$ " or $5/6$ " were achieved. Thus, data of 2.5cm (1") depth of cut in 2.5 cm (1") spacing were included in the data analysis.

Table 5-3 Test matrix of cutting at 2.5 and 5 cm (1" & 2") depth of cut: number of tests were performed at particular setting.

Depth of cut (cm)	2.5 cm (1")			5 cm (2")		
Speed (m/min)	1.5	3.0	4.6*	1.5	3.0	4.6*
Spacing (cm)						
2.5(cm)	5	6	8	5	6	8
5.1(cm)	3	5	4	3	5	4
10.2(cm)	5	4	4	5	4	4

* Testing at 4.6m/min (15ft/min) cutting speed has not been performed in +/- 6 degree skew angles due to shortage of the sample and interruption in testing due to equipment breakage.

However, when cutting at 2.5cm (1") spacing with 5 cm (2") depth of cut, the height of cut was reduced to the 2cm (4/5") which was much less than the expected depth of cut. This lower depth of cut was caused by the interaction between two cuts at 5 cm (2") spacing. For this reason 2.5 cm, (1") spacing cuts of 5cm (2") depth of cut were excluded in the data sets for analysis. Thus, total 108 cut lines were analyzed.

The variation of skew angles included zero, positive and negative six degrees. The completed tests so far includes 1.5 and 3 m/min (5 and 10 ft/min) cutting speed at -6, 0, & +6° skew angles. Following is the analysis for 2.5 and 5 cm (1" & 2") depth of cut. Figure 5-23 and 5-24 show the preliminary trends of the measured bit rotation and cutting forces. Bit rotation in multiple cutting tests was sensitive to the skew angle but it did not show any particular trend regarding the spacing and travel speed, even though forces were increased with spacing and travel speed.

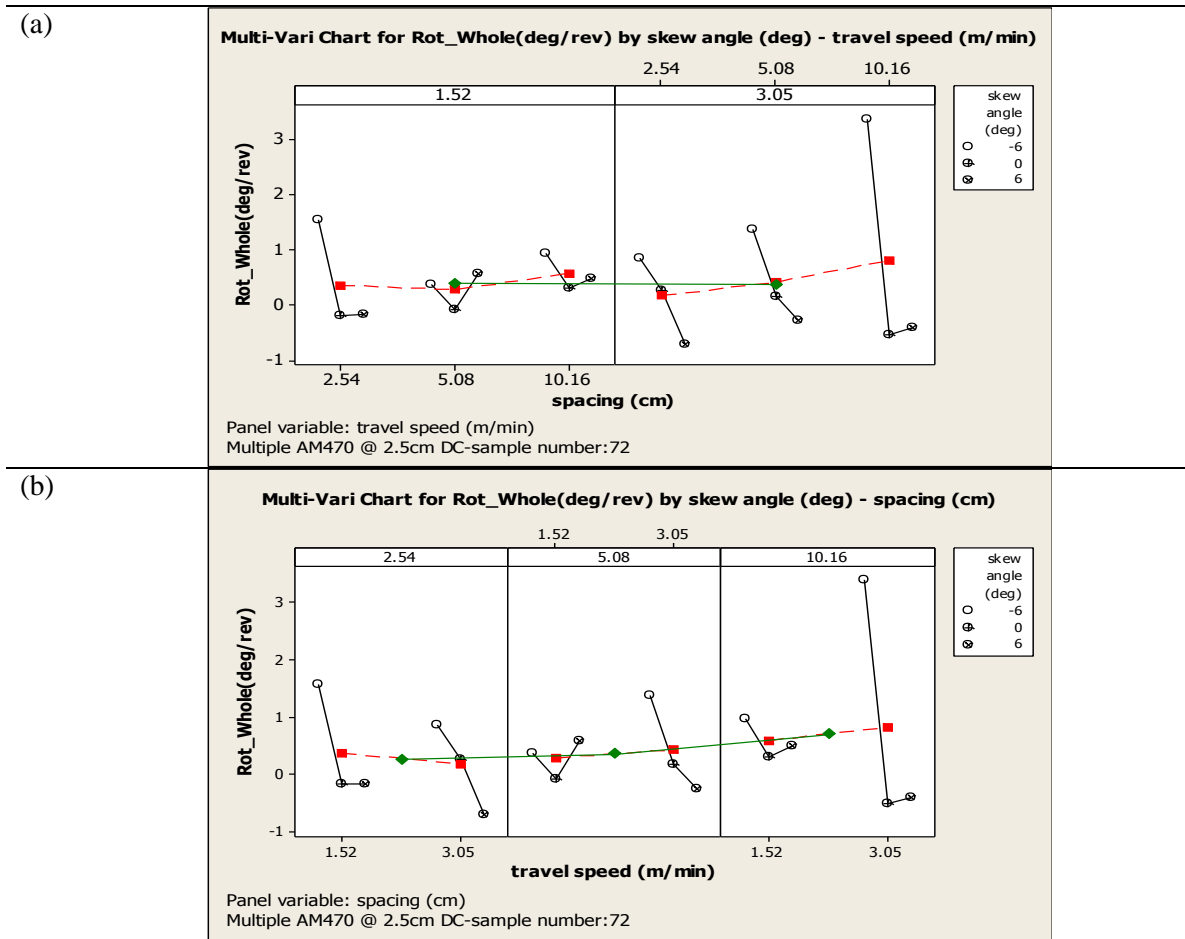


Figure 5-23 Multivariable plots of bit rotation of multiple bit drum using AM470 bit at 2.5cm (1”) depth of cut as a function of skew angle, travel speed, and spacing sorted by: (a) travel speed (b) spacing in each box

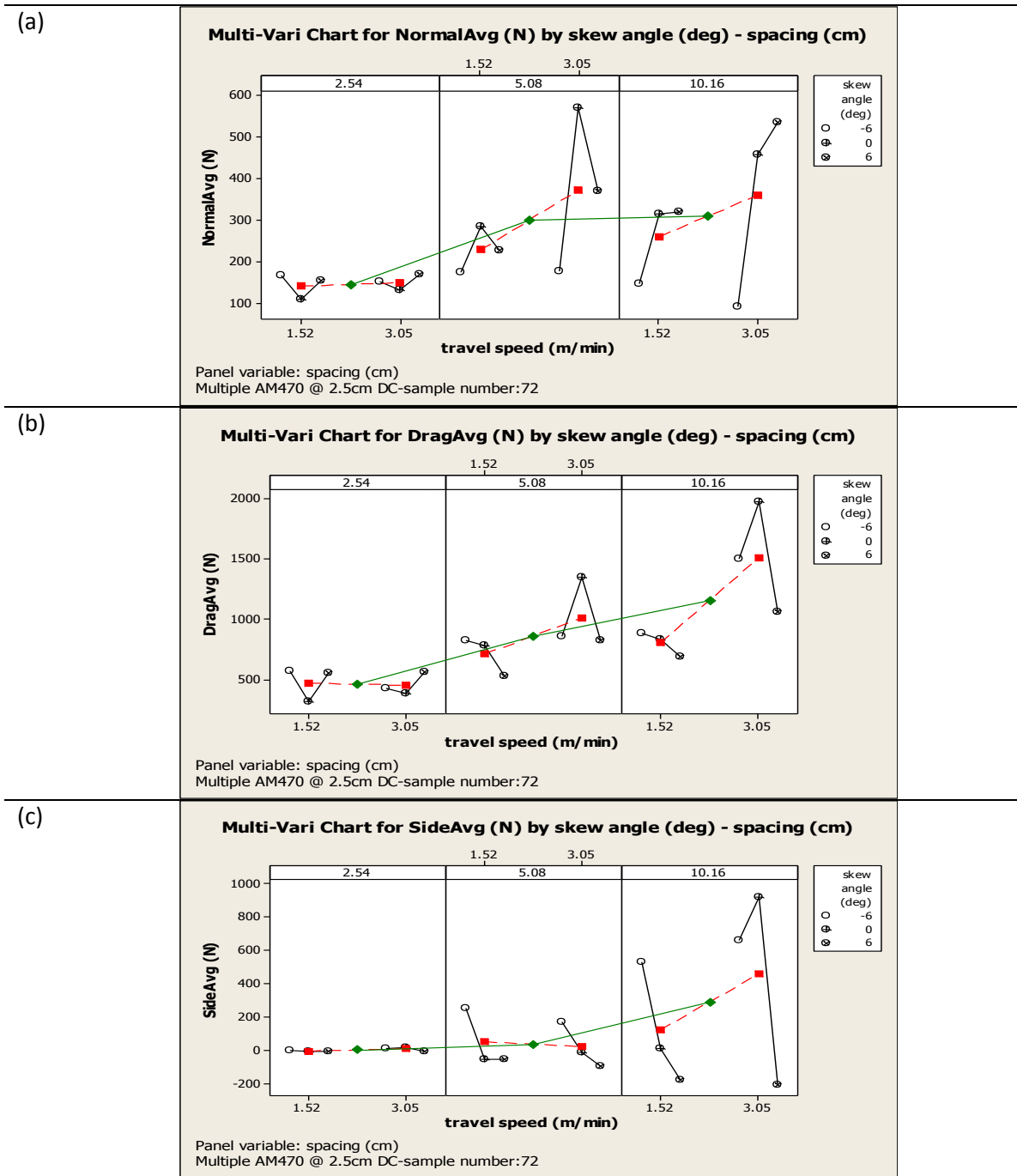


Figure 5-24 Multivariate plots of forces of multiple bit drum using AM470 bit at 2.5cm as a function of skew angle, spacing, and travel speed: (a) normal forces (b) drag forces (c) side forces

5.7.2 Results and analysis of rotary cutting tests with multiple bit drum using AM-470 bit at 2.5 cm (1") depth of cut

The data from full scale testing of AM-470 bit on the multi bit drum were analyzed to seek relationship between bit rotation, spacing, and skew angle. The results show that similar to the single bit rotary tests, increased spacing leads to reduced bit rotation. The data also shows that the direction of the skew angle (positive or negative) affects the direction of bit rotation (Figure 5-25). Although the highest bit rotation was observed at negative six and zero skew angles and at 10 cm (4") spacing this seem to be a bit of an exception to the norm and in general other tests resulted in smaller bit rotation at higher spacing.

Normal and drag forces increased while side forces and specific energy decreased with the spacing. The higher side forces coincided with higher bit rotation (Figure 5-25b-d). The result of testing confirms the intuitive notion that the maximum bit rotation occurs at conditions where high side force and low drag and normal forces are experienced.

To examine the relationship between travel speed, cut spacing, and bit rotation, and skew angle, statistical RSM analysis was used. In this analysis, spacing and skew angles significantly influenced bit rotation, but travel speed did not have meaningful impact on the bit rotation. RSM analysis shows that skew angle has the dominant effect (Figure 5-26ab). Interestingly in this series of testing negative six degree skew angle showed the largest bit rotation at 10cm (4") spacing. Figure 5-26 shows the lack of response between bit rotation and travel speed.

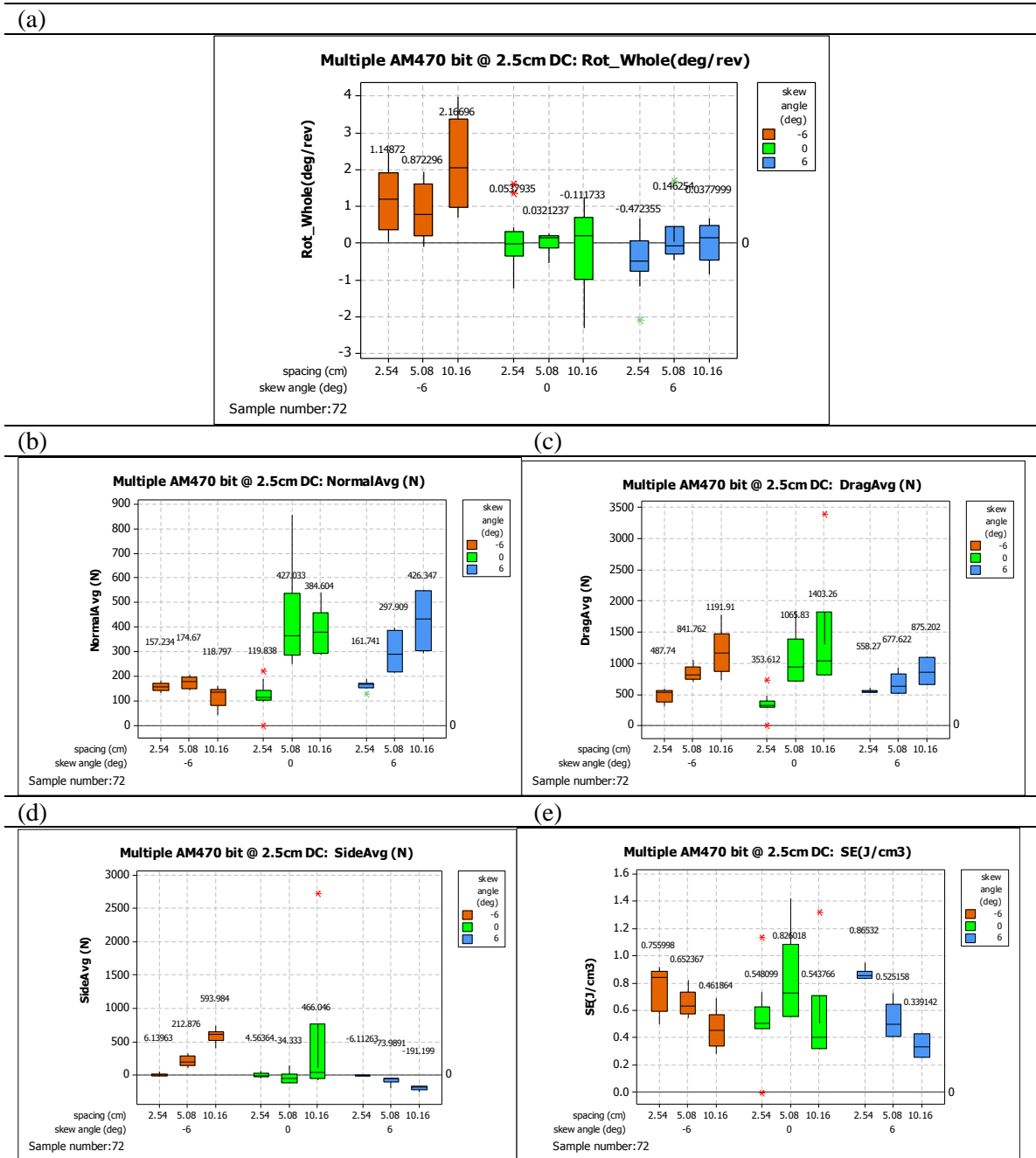


Figure 5-25 Box plot of data of multiple AM-470 bits at 2.5 cm (1”) depth of cut: (a) bit rotations (b) normal forces. (c) drag forces (d) side force (e) specific energy

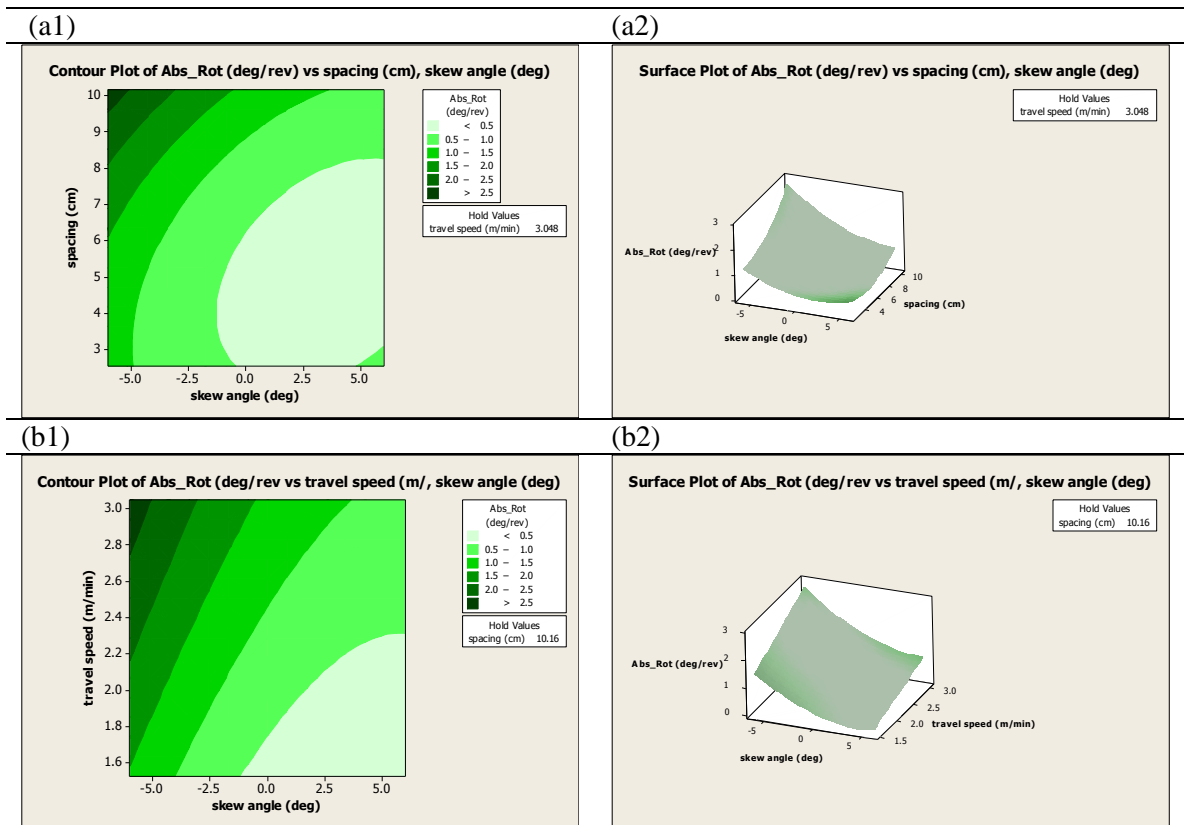


Figure 5-26 RSM analysis for bit rotation of multiple bit drum using AM470 bit at 2.5 cm (1") depth of cut against: **a**, skew angle and spacing at 2.3 m/min (7.5 ft/min) travel speed: (a1) contour plot (a2) surface plot ; **b**, skew angle and travel speed at 7.6cm (3") spacing: (b1)contour plot (b2) surface plot

5.7.3 Results and analysis of rotary cutting test with multiple bit drum using AM470 bit at 5cm (2") depth of cut

Preliminarily, collected data of multiple AM470 bits at 5cm (2") depth of cut were analyzed with multi-variate plots (Figure 5-27 and 5-28). The dominant factor on bit rotation is skew angle. Interestingly, bit rotation somehow shows little sensitivity to the travel speed and spacing. However, the numbers of data lines (36) are insufficient to confirm this phenomenon and these data needs future investigation. Forces were increased with increased with spacing and travel speed which were similar to the observation in the single bit cutting tests.

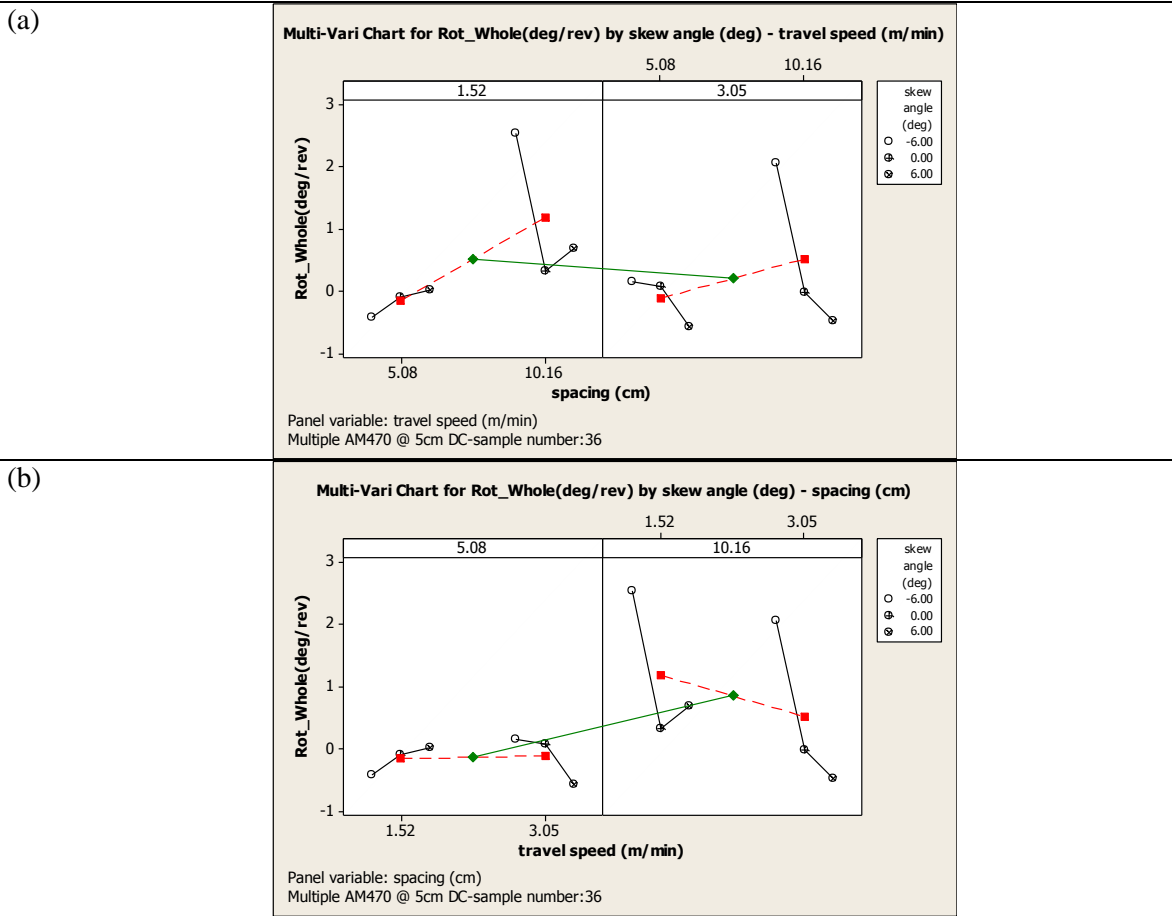


Figure 5-27 Multivariable plots of bit rotation of multiple bit drum using AM470 bit at 5cm (2") depth of cut as a function of skew angle, travel speed, and spacing regarding to: (a) travel speed (b) spacing

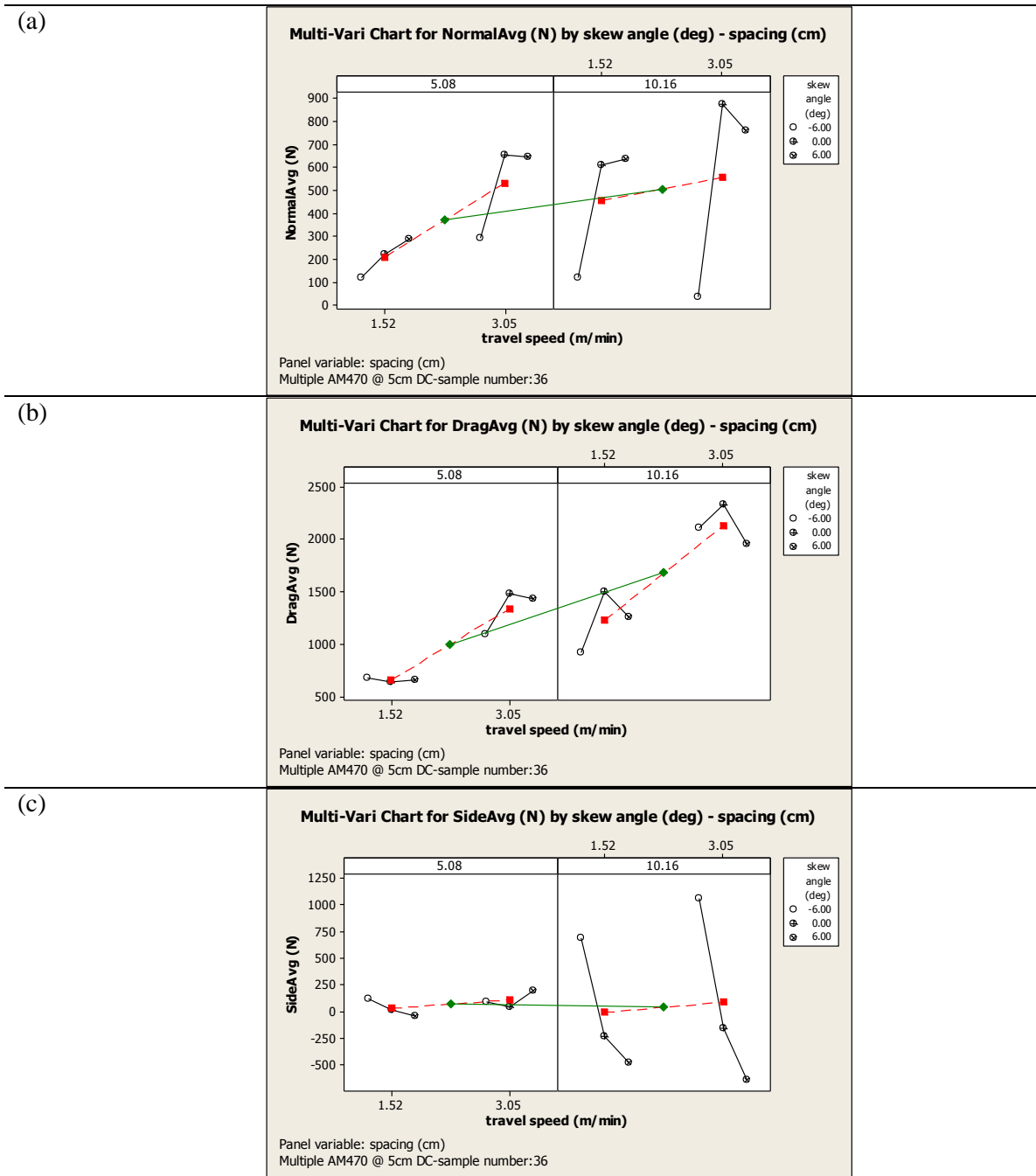


Figure 5-28 Multivariate plots of cutting forces of multiple bit drum using AM470 bit at 5cm regarding skew angle spacing and, travel speed: (a) normal forces (b) drag forces (c) side forces

More detailed statistical analyses were performed with box-plots. At 5cm (2") depth of cut, normal, drag, and side forces were increased and the specific energy was reduced with increased spacing. From these graphs, the highest bit rotation can occur at lower normal/drag

force and higher side force, similar to the tests at 2.5 cm (1") depth of cut (Figure 5-29). The box plots in Figure 5-29a does not show bit rotation as a function of skew angle and spacing (data from various travel speeds combined) as previous cases. The increasing spacing does not seem to affect the bit rotation in zero and positive skew angles, but increases bit rotation at the negative six degree skew angle. Overall, it seems like larger side forces coincide with bit rotation (Figure 5-29b-d).

To evaluate the relationship between travel speed, spacing, skew angle, and bit rotation, RSM statistical analysis was used (Figure 5-30ab). The result of rotary cutting tests at 5 cm (2") depth of cut shows that spacing and skew angles have significant impact on the bit rotation. But as before, travel speed does not have a notable impact on bit rotation. The analysis shows that the effect of skew angle is more influential comparing to other parameters. As in the rotary cutting tests of multiple bit drums at 5 cm (2") depth of cut, negative six skew angle showed large bit rotation at 10 cm (4") spacing. Figure 5-30b shows the insensitivity of bit rotation to the travel speed.

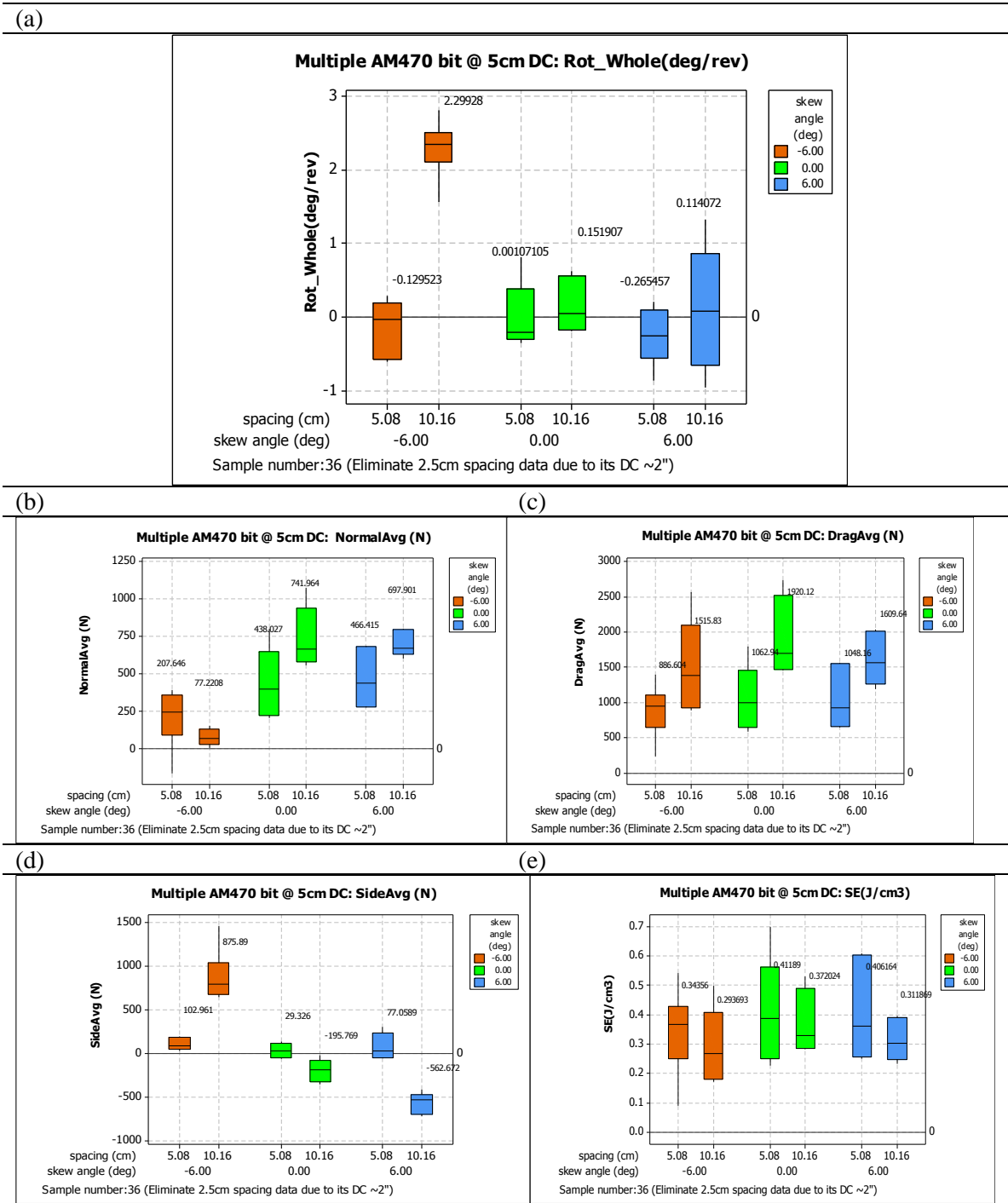


Figure 5-29 Box plots of rotary cutting tests with multiple bit cutting drum using AM-470 bit at 5 cm (2") depth of cut: (a) bit rotations (b) normal forces (c) drag forces (d) side forces (e) specific energy

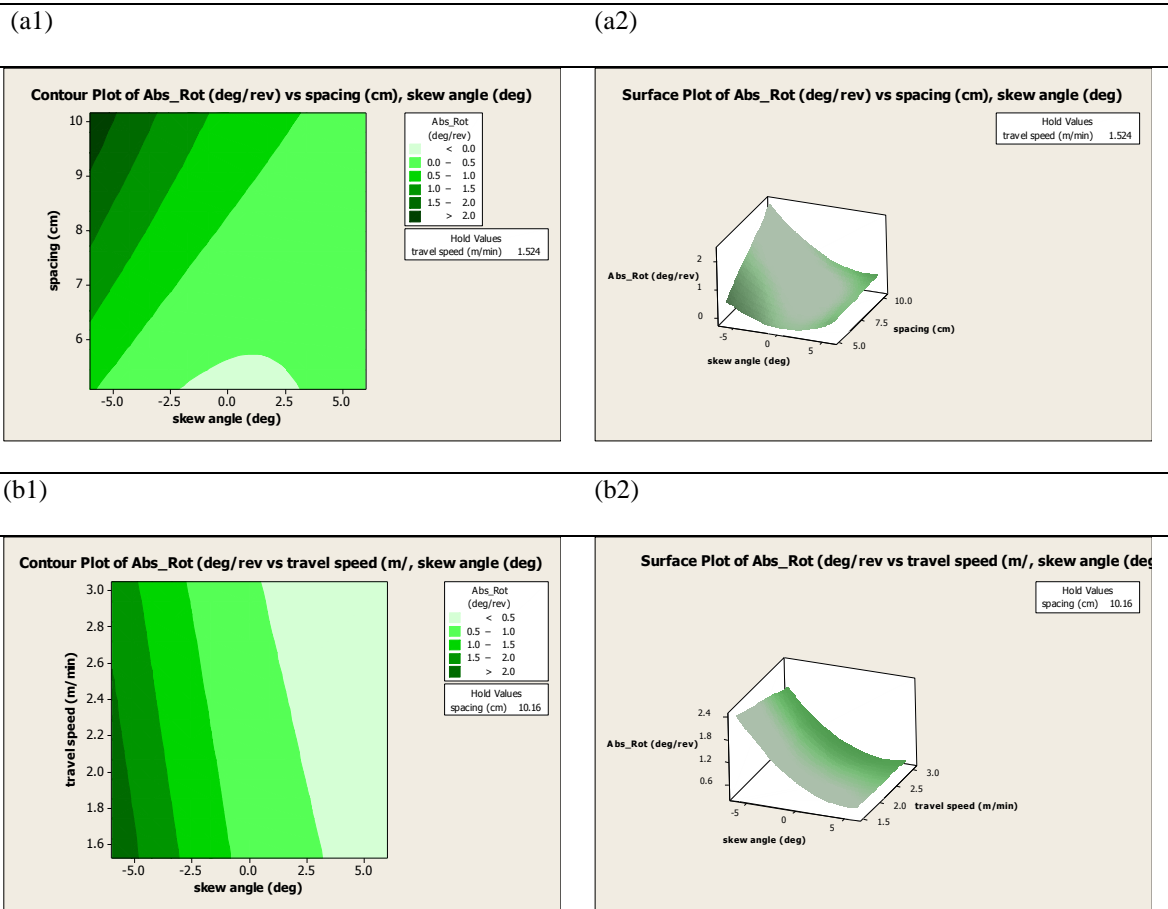


Figure 5-30 RSM plots for bit rotation of multiple bit drum using AM470 bit at 5 cm (2”) depth of cut against: a, skew angle and spacing at 1.5 m/min (5ft/min) (a1) contour plot (a2) surface plot; b, skew angle and travel speed at 10.18 cm (4”) spacing (b1) contour plot (b2) surface plot

5.7.4 Summary and conclusion on rotary cutting tests with multiple bit cutting drum using AM470 bit

This section discusses the overall results of rotary cutting tests with multiple bit drum using the AM-470 bit and cutting at two different depth of cuts of 2.5 and 5 cm (1” & 2”). The number of 72 comparison data of the 2.5 and 5 cm (1” & 2”) depth of cut shows no significant difference on the bit rotation (Figure 5-31).

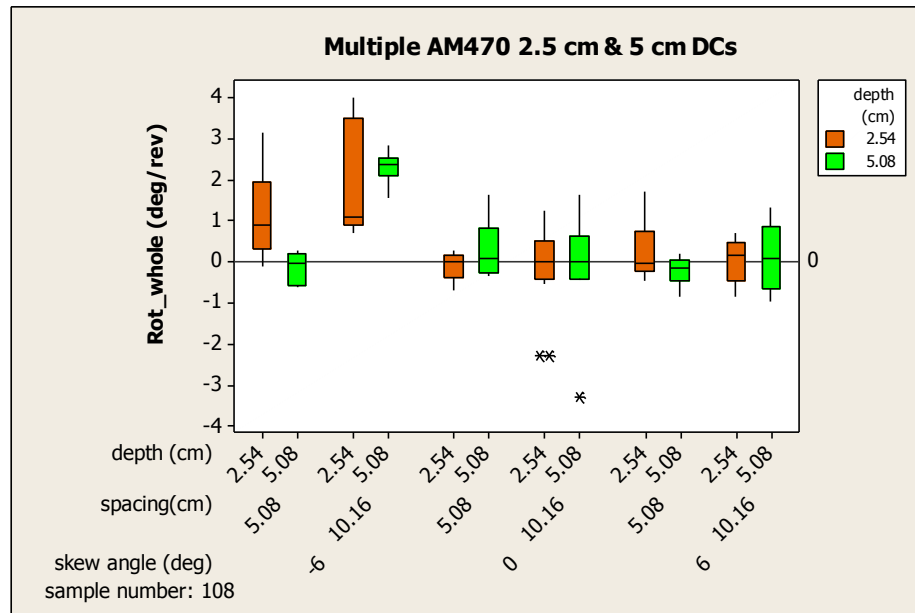


Figure 5-31 The comparison of bit rotations of the multi AM470 bit at 2.5 and 5 cm (1" & 2") depth of cut

The difference between the results of single bit and multiple bit drum tests was also performed using 34 tests at 2.5 cm (1") and 36 samples at 5cm (2") (Figures 5-32) depth of cut. The results of statistical analysis using the ANOVA method show that there is no difference between the bit rotations of multiple cutting and single cutting at each case. General Multivariate ANOVA (MANOVA) test was also considered using MINITATB 16®. This MANOVA test analyzes unbalanced data and covariates and nested or crossed data. Data were coded with 0 and 1 respectively to the single bit and multiple bit cases. Then, skew angle and travel speed were treated as covariates..

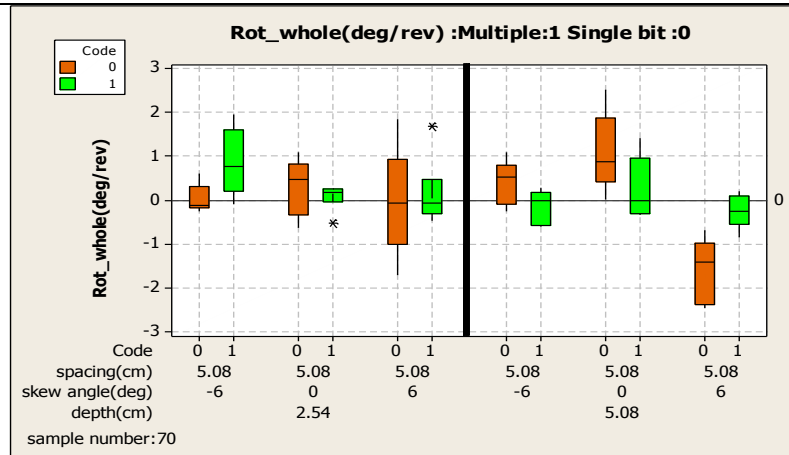


Figure 5-32 Box-plot of the results of MANOVA analysis for rotary cutting test with single and multi bit drum configuration with different skew angles: (left-side) 2.5 cm (1") depth of cut (right-side) 5 cm (2") depth of cut.

To compare the data sets, general best fit set using linear regression modeling was used. In this model, skew angle and code were included. As a result, there was no difference between single and multiple setting effects on the bit rotations relative to the testing parameters examined (p-value of Code: 0.922).

In this multiple cut, the direction of skew angle was defined based on the reference bit tip direction. Skew angle directions (positive and negative) were decided relative to the tip direction toward to the left or right hand side of the reference bit. The same logic was applied to the single bit skew angle direction. However, the situations that the reference bit was facing were different in single and multiple bit settings. In the case of single bit drum, positive skew angle referred to the bit tip facing to the breakage side and negative skew angle implied that the bit tip faced toward the intact rock or higher side on the cutting surface. In tests with the multiple bit drum, positive skew angle is towards the breakage side and negative skew angle was the bit facing the higher side of the block surface. The preset spacing apart from the reference bit, other bits were always cutting the sample. It means that the negative skew angle of the multiple bit cutting is same as positive skew angle in a single bit. Because when the reference bit cutting with negative

six skew angle, it was cutting with next cutting line and this neighboring cut line provoked the breakage of the side that bit tip was toward. It made the same breakage situation that positive skew angle setting in single cut. Thus, the bit tip direction was toward to the breakage side of the block which was conducted by the bit in next line. From this exercise, one could conclude that the positive and negative skew angle were similar cutting mechanisms.

The difference between the positive and negative skew angle in multiple bit drum testing was also in calculation of actual spacing between cuts. When positive skew angle was used, the spacing on the left side of the bit was larger than the negative skew angle. It means that the spacing between the reference bit and next cut line bits at positive 6 skew angle is larger than that of 0 skew angle. At negative skew angle, this spacing is smaller than the spacing at 0 skew angle. In other words, the actual spacing between the bits in the multiple bit drum testing were 9.3, 10, and 11 cm (3.67", 4", & 4.33") for negative six, zero, and positive six degree skew angles, respectively. The reason that highest bit rotation occurs at negative six degree skew angle might be the effect of actual spacing. Comparing the effects of spacing on bit rotation between the multi bit and single bit experience shows somewhat different results where for some reasons higher bit rotation was recorded at 10 cm (4") spacing in multi bit drum testing as compared to higher bit rotation observed at lower spacing in single bit tests. This could be caused by cut sequence at multiple bit drum testing, or it could be attributed to the surface conditions in multi bit drum testing where the cuts at lower spacing were conducted within the larger spacing cuts. To verify this effect one may reconfigure the multi bit drum and try to cut at 2.5cm (1") and 5cm (2") spacing and run the cutting tests in intact grout.

For future work, one of the ideas is to try to perform rotary cutting tests with the multi bit drum at different spacing between cuts and trial on the rock surface without the previous large spacing cuts to see the significance of the distance between cut lines. This can be done at various skew angles while monitoring the actual distance between the cuts.

When reviewing results of the entire rotary cutting tests, the following summary can be offered. The testing showed that normal and drag forces increase and side force and SE decrease with spacing as expected. The conclusion regarding the specific energy should be complemented by reviewing the surface condition of the sample to make sure that the fractures go across the cuts and high ridges are not built between the cuts. As for the bit rotation, skew angle and spacing are the more influential factors and travel speed did not affect the bit rotation as much.

5.8 Analytical and Numerical modeling of suggested solution using spring loading

As a part of the proposed solution to enhance bit rotation, various spring loading concepts were considered. This involves utilizing spring elasticity characteristics which moves the bit outward along the bit axis at initial loading. The delay of the gap between the back flange of the bit and bit shoulder closing time by spring's reaction leads to increases the time between the initial loading and the full contact of the back flange of bit and bit shoulder. A Longer time between the bit tip and the rock surface before full engagement of the bit cause less the resistive frictional forces between the back flange of bit and bit holder shoulder and can induce more rotation before the gap is getting closed. Thus, some modeling were performed to evaluate the amount of forces needed for inducing rotation of the bit under this condition and tested for the possibility of inducing rotation while the gap is getting closed.

To verify the effect of spring loading on the bit shank, three different scenarios were suggested. One is the use of a coiled spring at the end of the bit shank with full contact. The other possible configuration is the use of a coiled/spiral spring connected to the bit shank with the point contact at the center. Last scenario was no spring on the bit shank. Figure 5-33 illustrates configuration of spring loading and gaps between the bit shoulder and bit block. In cases a) and b), a bit will have the gap between the bit and the holder due to the spring before contact with the

rock. In case c), the gap is closed at beginning of the loading. Other possible spring loading configurations can be envisioned to achieve the same goal. Other possible scenarios includes using leaf spring or spring loaded washers but for the purpose of simplicity, in this dissertation, the modeling was limited to the coiled spring configurations.

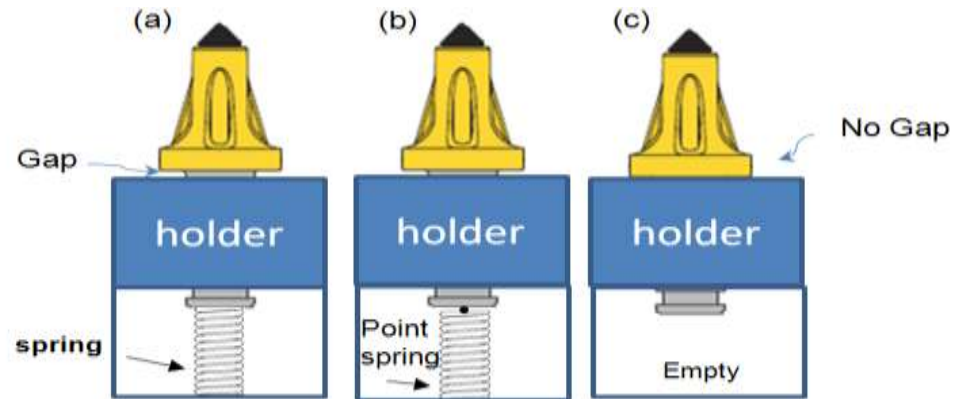


Figure 5-33 Three scenarios for calculating rotation forces (a) spring (b) point spring (c) no device.

5.8.1 Analytical solutions on the spring concept

For analytical modeling of the proposed modification of the bit to enhance rotation, an approach similar to that of the earlier modeling of interaction between the back flange of bit and bit block was used. In this case, an axial load was applied and the related distance between the back of bit flange and bit block, called gap, was estimated based on the spring reaction and spring factor. Simultaneously, the forces required for bit rotation was estimated relative to the configuration of the forces and bit geometry. The axial loading was gradually increased till the gap was closed and then the additional frictional torque developed between the bit shoulder and block. Figure 5-34 shows the estimated magnitude of the force needed to rotate the bit while it is under axial loading. The graph shows that each spring allows extension of time before the moment of very high forces needed for bit rotation. Especially, in the 2nd case of point spring case

demonstrates that at the initial stages of this case, it is not necessary to have large force to make a bit rotated than the 1st case (only spring case). However, the 3rd case (no spring, direct contact with bit block) requires very high forces for bit rotation immediately after the initial axial loading. In conclusion, the analytical calculations support the use of spring concepts and its potential benefits for bit rotation especially with point contact for spring loading scenario.

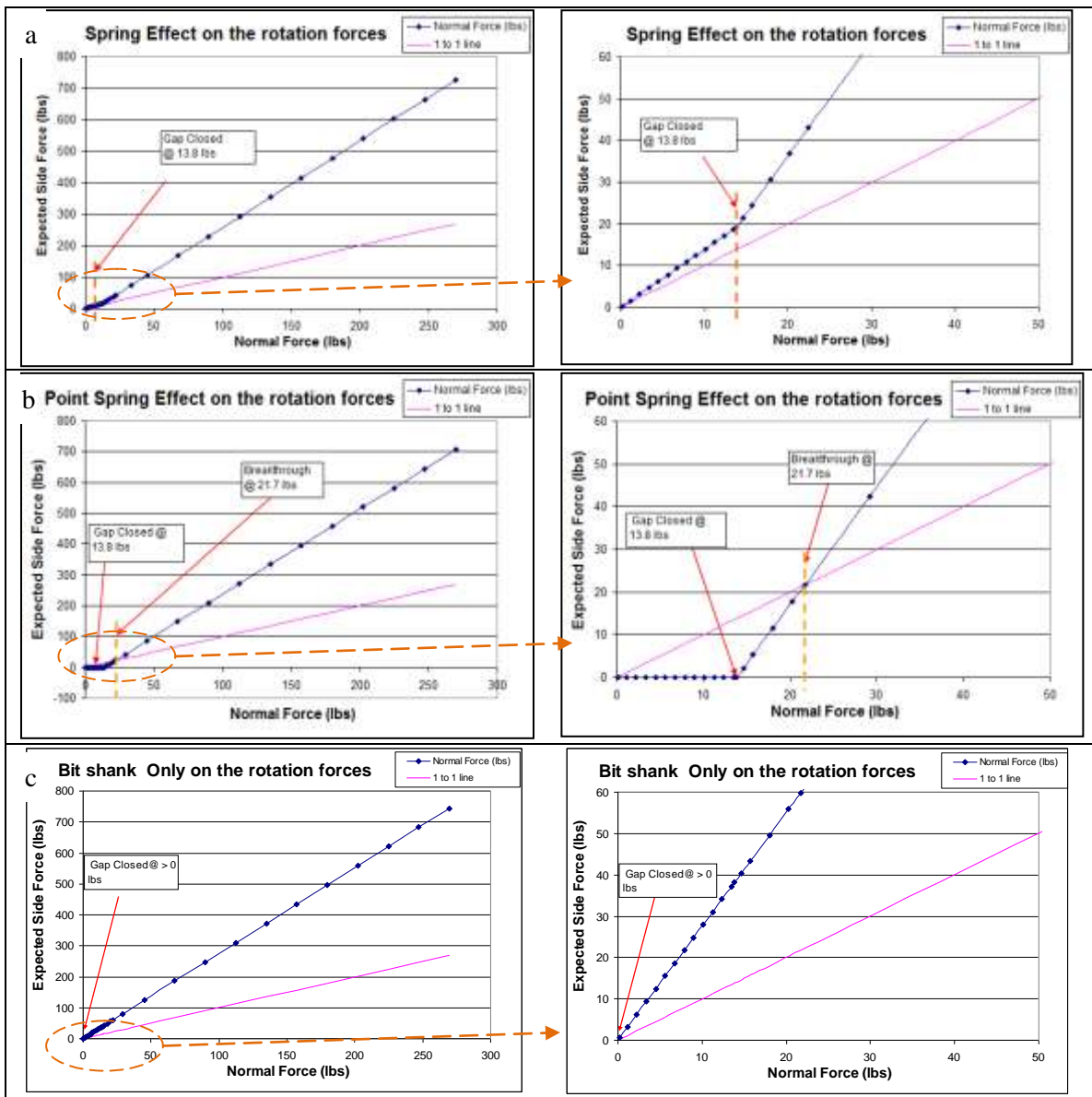
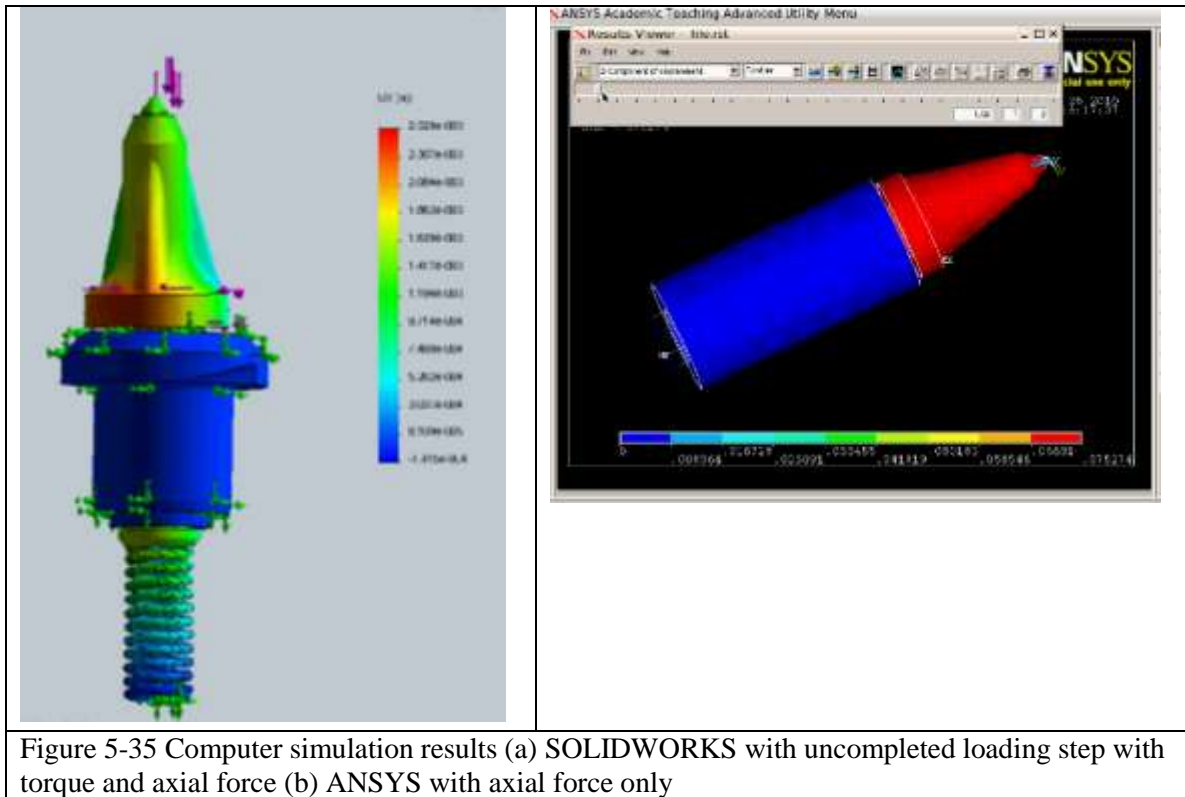


Figure 5-34 analytical calculation of forces for rotation :left (large scale),right(zoomed in case):
 (a) regular spring, (b) point spring, (c) no spring

5.8.2 Numerical modeling of the spring loading concept.

Numerical simulations have been utilized to show the effect of using a spring loading on the force needed for the bit rotation. Two different commercial finite element analysis software, SOLIDWORKS and ANSYS, was used for simulation of bit loading configuration while using various types of springs. In both case, a spring effect with axial force has been successfully modeled. But when implementing the torque for bit rotation, the solution cannot converge. When using SOLIDWORKS for simulation, the solution with axial force and torque converged with the 30% loading step and did not go further. It requires further consideration of the incomplete loading steps to yield any meaningful results. Alternatively when using ANSYS, application of torque along with the axial load and torque, the spring reaction caused the bit to be ejected from the block and as such the solution did not converge. For further study of this topic and possibly use of different element such as MPC184 and different boundary conditions may be required to derive an acceptable solution using the numerical modeling. Snapshot of the each simulation results are illustrated in Figure 5-35.



Chapter 6 Conclusions and Recommendations

The study of conical bit rotation is important for development of a system that could enhance rotation of the bits and thus improve bit life and its cutting efficiency. To study bit rotation an experimental program, including full scale cutting tests, was conducted on AM-470 and RZ-24 bits from mining and construction tools produced by Kennametal Inc to understand the phenomenon involved with bit rotations. Two series of tests were conducted, including linear cutting and rotary cutting tests. Following are the brief conclusions of testing results and subsequent analysis performed for this purpose.

6.1 Conclusions of bit rotation

Linear cutting tests were performed in blocks of Indiana limestone (with compressive strength of ~50 MPa or 7000 psi) and the engineered grout (~ 10.3 MPa (~1500 psi) and subsequently ~4.1 MPa (~600 psi) in strength). In the limestone sample, 582 lines were cut with the AM-470 bit and 326 lines were cut using the RZ-24 bit. The measured forces and bit rotations were analyzed for these cuts. Subsequently, 271 line cuts with the AM-470 and 239 line cuts using the RZ-24 bit were made in the grout sample and analyzed. Summary conclusions of linear cuttings test are as follows:

1. The linear cutting test setting represents the bit that is fully engaged with rock during the cutting. The overall conclusion of the testing of AM470 and RZ24 bits in various samples is that there was no bit rotation in linear cutting tests when bit was fully engaged to the rock.
2. Cutting forces measured in linear cutting tests had typical and anticipated trends with increased spacing and depth of cut.

3. A few incidents of full bit rotation were observed while testing the RZ-24 bit, but it was related to the bit body hitting the high ridges, a condition that should be prevented in actual field applications.
4. General lack of bit rotation of AM-470 and RZ-24 bits were examined by analyzing forces acting on the bit and using analytical and numerical solutions. The results of analysis matched experimental observations. Also, exceptional bit rotation cases in testing the RZ-24 bit were explained by analytical solutions.

The rotary cutting tests were conducted in ~4.1 MPa (~600 psi) grout with single and multiple bit laced drums. Rotary cutting tests in single bit laced drum included 267 lines of cut by AM-470 and 117 lines of cut using RZ-24 bits. Rotary cutting tests in multiple bit laced drum were performed with 108 lines of cut using the AM-470 bit. The summary of the conclusions from the rotary tests are as follows:

1. Rotary cutting tests showed that skew angle and spacing are important factors for bit rotation. In general lower skew angles of 0-6 degrees seem to be more favorable to bit rotation.
2. Higher skew angle will increase cutting forces and specific energy and thus makes the cutting less efficient.
3. Travel speed did not contribute much to the bit rotation at the given 60 RPM. However, there was a trend of observing higher rotation at certain combinations of cutting speed and RPM.
4. While testing the single bit cutting drum, higher bit rotations were observed at smaller spacing. The most favorable condition to bit rotation was observed in 0-6° skew angles at lower spacing.
5. The directions of the bit rotation (CW/CCW) showed a good correlation with the direction of skew angle (+/-).

6. The dominant factor in the determination of the direction of bit rotation is the face of the bit which hits the rock surface first.
7. In multiple bit laced drum, other bit actions did not play a major role of bit rotation. The most important moment for the bit rotation is the point of its entry and exit point of the cut.

6.2 Recommendations of bit rotation study

While a substantial number of tests and related analysis was performed on this topic, there is still much more to be done in way of understanding the process as well as developing a method to induce or enhance bit rotation. Thus the following recommendations are offered for follow up studies and testing.

1. Rotary cutting tests with a multiple bit laced drum are needed to continue to generate a more extensive set of data for subsequent analysis. The initial tests are interesting and somewhat promising. The available data are not sufficient to confirm the bit rotation pattern in this test setting.
2. Completion of FEA analysis of the proposed spring concept for bit rotation and further computer simulation regarding the other possible spring loading configuration can be continued.
3. As a follow up to the rotary cutting test using multiple bit laced drum, bit arrangement on the drum needs to be modified to verify the impact of cut spacing. The test setting should be arranged so that changing skew angles on the instrumented bit do not affect cut spacing.
4. Using an additional device or bit mounting system can be considered to improve bit rotation. Some of the proposed solutions have been discussed among the

project team and one will be selected to perform the actual full scale cutting tests. The solutions can utilize the momentary bit rotation when the bit enters/exits the cut.

5. Testing new concepts for enhancing and inducing bit rotation requires several trials on the design and the material property of related instruments and mechanisms, and their mounting configuration.
6. Subsequently, to improve the efficiency and precision of data analysis on experimental results, the enhanced MATLAB program can be used. If possible, current MATLAB code can be upgraded and some Graphic User Interface (GUI) components can be added into this program for user friendly operation as an object-oriented program. Also, conversion of the analysis program to an executable MATLAB program will make it easier for future users to use this program on computers which do not have MATLAB software packages. This allows for better utilization of the current data and future testing.
7. To increase the efficiency of the cutting machine at the Latrobe rock cutting facility one can consider increasing the capacity of the system to allow for a deeper cut and handle higher cutting forces than is currently available on the machine.
8. Performing additional numerical simulation with various material properties for the bit and bit body design to see the effect of this aspect on the results of the modeling, leading to the potential for improvement of bit rotation.

References

- Achanti, V.B., and Khair, A.W.** (1998). Laboratory assessment of the rock-fragmentation process by continuous miners. SME Transactions Volume 304, 1998 **Chapter Sec. 1 March - Papers published in Mining Engineering during 1998, Vol. 50**
- Anderson, J., and Rostami, J.** (1997). Criteria For Selection and Application of Rock Cutting Tools for Soft Rock Underground Mining. In SME/AIME 1998 Annual meeting & Exhibit, March 9-11, (Orlando, Florida).
- Appl, F.C., Wilson, C.C., and Lakshman, I.** (1993). Measurement of Forces, Temperatures and Wear of Pdc Cutters in Rock Cutting. *Wear* **169**, 9-24.
- Appleby-Thomas, G.J., Hazell, P.J., Stennett, C., Cooper, G., Helaar, K., and Diederer, A.M.** (2009). Shock propagation in a cemented tungsten carbide Journal of Applied Physics **105**, 109 (109 pages).
- Artsimovich, G.V., Poldko, E.N., and Sveshnikov, I.A.** (1978). Investigation and development of rock -breaking tool for drilling. In Nauka (Novossibirsk).
- Asbury, B., Ozdemir, L., and Rozgonyi, T.G.** (2001). Frustum bit technology for continuous miner and roadheader applications. In 6th International Symposium on Mine Mechanization and Automation, South African Institute of Mining and Metallurgy, 2001.
- Balci, C., and Bilgin, N.** (2007). Correlative study of linear small and full-scale rock cutting tests to select mechanized excavation machines. *International Journal of Rock Mechanics and Mining Sciences* **44**, 468-476.
- Bardetsky, A., Attia, H., and Elbestawi, M.** (2007). A fracture mechanics approach to the prediction of tool wear in dry high-speed machining of aluminum cast alloys - Part 1: Model development. *Journal of Tribology-Transactions of the Asme* **129**, 23-30.
- Barker, J.S.** (1964). a laboratory investigation of rock cutting using large picks. *International Journal of Rock Mechanics and Mining Science* **1**, 519-534.
- Bilgin, N., Dincer, T., and Copur, H.** (2002). The performance prediction of impact hammers from Schmidt hammer rebound values in Istanbul metro tunnel drivages. *Tunnelling and Underground Space Technology* **17**, 237-247.
- Bilgin, N., Demircin, M.A., Copur, H., Balci, C., Tuncdemir, H., and Akcin, N.** (2006). Dominant rock properties affecting the performance of conical picks and the comparison of some experimental and theoretical results. *International Journal of Rock Mechanics and Mining Sciences* **43**, 139-156.
- Brian Armstrong, H., louvry, Pierre, D., and Carlos Canudas de, W.** (1994). A survey of models, analysis tools and compensation methods for the control of machines with friction. *Automatica* **30**, 1083-1138.
- Brook, B.** (2002). Principles of diamond tool technology for sawing rock. *International Journal of Rock Mechanics and Mining Sciences* **39**, 41-58.
- Brooker, C.** (1983). Theoretical and practical aspects of cutting and loading by shearers drums. *Aust. J. Coal Min. Technol. Res* **osti.gov**.
- Cavender, B.** (1999). *Mineral Production Costs: Analysis and Mangement.* (Society for Mining Metallurgy & Exploration; 1st edition (January 15, 1998)).
- Chiang, L.E., and Elías, D.A.** (2008). A 3D FEM methodology for simulating the impact in rock-drilling hammers. *Int J Rock Mech Min* **45**, 701-711.

- Coetzee, C.J., and Els, D.N.J.** (2009a). The numerical modelling of excavator bucket filling using DEM. *Journal of Terramechanics* **46**, 217-227.
- Coetzee, C.J., and Els, D.N.J.** (2009b). Calibration of discrete element parameters and the modelling of silo discharge and bucket filling. *Computers and Electronics in Agriculture* **65**, 198-212.
- Cook, N.G.W., Hood, M., and Tsai, F.** (1984). Observations of crack growth in hard rock loaded by an indenter. *International Journal of Rock Mechanics and Mining Sciences & Geomechanics Abstracts* **21**, 97-107.
- Cundall, P.A., and Strack, O.D.L.** (1979). Discrete Numerical-Model for Granular Assemblies. *Geotechnique* **29**, 47-65.
- Cundall, P.A., and Hart, R.D.** (1993). Numerical modeling of discontinua. (Pregamon).
- Deketh, H.J.R.** (1995). Wear of rock cutting tools : Laboratory experiments on the abrasivity of rock. (A.A. BALKEMA/ROTTERDAM/BROOKFIELDS).
- Deliac, E.P.** (1992). Theoretical and Practical Rules for Mechanical Rock Excavation. In *Comprehensive Rock engineering*, Hudson, ed (Pregamon), pp. 177-227.
- Deliac, E.P.** (1994). Theoretical and practical rules for mechanical rock excavation : E.P. Deliac, *Comprehensive rock engineering*. Vol. 4, ed J.A. Hudson, (Pergamon), 1993, pp 177-227. *International Journal of Rock Mechanics and Mining Science & Geomechanics Abstracts* **31**, 203-203.
- Ersoy, A., and Waller, M.D.** (1995). Textural Characterization of Rocks. *Engineering Geology* **39**, 123-136.
- Evans, A.G., and Linzer, M.** (1976). High-Frequency Cyclic Crack-Propagation in Ceramic Materials. *International Journal of Fracture* **12**, 217-222.
- Evans, I.** (1961). A theory on the basic mechanics of coal ploughing. In *Journal:Proceedings of a symposium held at the University of Missouri (University of Missouri)*.
- Evans, I., and Pomeroy, C.D.** (1966). *Strength, Fracture, and Workability of Coal.* (New York: Pergamon Press).
- Gajewski, J., and Jonak, J.** (2006). Utilisation of neural networks to identify the status of the cutting tool point. *Tunn Undergr Sp Tech* **21**, 180-184.
- Gehring, K.H.** (1989). Roadheaders, a cutting comparison. *Tunnel and Tunnelling*, 27-30.
- Goffroy, H., and Minh, D.N.** (1997). Study on interaction between rocks and worn PDC'S cutter. *Int J Rock Mech Min* **34**, 95.
- Gertsch, L., Rostami, J., and Gustafson, R.** (2008). Review of Lunar Regolith Properties for Design of Low Power Lunar Excavators. In *Proceedings of 6th International Conference on Case Histories in Geotechnical engineering (Arlington, VA)*.
- Gertsch, R.E.** (2000). *Rock Touchness and Disc Cutting In Mining Engineering* (University of Missouri-Rolla).
- Goktan, R.M., and Gunes, N.** (2005). A semi-empirical approach to cutting force prediction for point-attack picks. *Journal of the South African Institute of Mining and Metallurgy* **105**, 257-263.
- Goktan, R.M., and Yilmaz, N.G.** (2005). A new methodology for the analysis of the relationship between rock brittleness index and drag pick cutting efficiency. *Journal of the South African Institute of Mining and Metallurgy* **105**, 727-733.
- Groover, M.P.** (2010). *Fundamentals of Modern Manufacturing : Materials, Processes, and Systems* (John Wiley & Sons, Inc).
- Hart, R.D.** (1993). *An introduction to Distinct element modeling for rock engineering.* (Pregamon).

- Hekimoglu, O.Z.** (1998). Investigations into performance of point-attack and radial-type rock- and coal-cutting picks. Transactions of the Institution of Mining and Metallurgy Section a-Mining Industry **107**, A55-A59.
- Hekimoglu, O.Z., and Ozdemir, L.** (2004). Effect of angle of wrap on cutting performance of drum shearers and continuous miners. Transactions of the Institution of Mining and Metallurgy Section a-Mining Technology **113**, A118-A122.
- Hentz, S., Donzé, F.V., and Daudeville, L.** (2004). Discrete element modelling of concrete submitted to dynamic loading at high strain rates. Computers & Structures **82**, 2509-2524.
- Holt, R.M., Kjolaas, J., Larsen, I., Li, L., Pillitteri, A.G., and Sonstebo, E.F.** (2005). Comparison between controlled laboratory experiments and discrete particle simulations of the mechanical behaviour of rock. International Journal of Rock Mechanics and Mining Sciences **42**, 985-995.
- Hoseinie, S.H., Aghababaei, H., and Pourrahimian, Y.** (2008). Development of a new classification system for assessment of rock mass drillability index(RDi). Int J Rock Mech Min **45**, 1-10.
- Hurt, K.G., and Evans, I.** (1981). Point attack tools : an evaluation of function and use for rock cutting. The Mining engineer **5**, 673-675.
- Hurt, K.G., and MacAndrew, K.M.** (1985). Cutting efficiency and life of rock-cutting picks Mining Science and Technology **2**.
- Ingraffea, A., and Saouma, V.** (1985). Numerical modeling of discrete crack propagation in reinforced and plain concrete. In Fracture mechanics of concrete : structural application and numerical calculation, pp. 171-225.
- Irfan, M.A., and Prakash, V.** (2000). Time resolved friction during dry sliding of metal on metal. International Journal of Solids and Structures **37**, 2859-2882.
- Jing, L., and Hudson, J.A.** (2002). Numerical methods in rock mechanics. International Journal of Rock Mechanics and Mining Sciences **39**, 409-427.
- Jun, H.J., N.V.Bangaru, and G.I.Block.** (2007). Advanced characterization and numerical simulation of indentation induced damage in hard stone. In Rock Mechanics: Meeting Society's Challenges and Demands (1st Canada-U.S. Rock Mechanics Symposium, Vancouver), pp. 647-653.
- Khair, A.W.** (2001). The effect of bit geometry and size on cutting parameters in linear cutting. In A Mining Odyssey - SME Annual Meeting February 26 - 28, (Denver, Colorado), pp. 12.
- Khair, A.W.** (2006). Analysis of Cutting Bits and Cutting Drum Affecting Ground Control in Coal Mines,. In 27th International Conference on Ground Control in Mining (ICGCM) pp. 10.
- Khair, A.W., Gehi, L.D., and Ahmad, M.** (1995). Effect of bit wear on productivity of continuous miners. In SME, Mining Transactions, pp. 1834-1838.
- Kim, E., Rostami, J., and Swope, C.** (2009). Measurement of Conical Bit Rotation In Proceedings of the 23nd symposium on U.S. rock mechanics, (Asheville, NC).
- Kim, E., Rostami, J., and Swope, C.** (2010). Full Linear Cutting Test with Conical Bit. In The 44th U.S. Rock Mechanics Symposium and 5th U.S.-Canada Symposium ,June 27-30, 2010 (Salt Lake City).
- Kou, S.Q., Liu, H.Y., Lindqvist, P.-A., and Tang, C.A.** (2004). Rock fragmentation mechanisms induced by a drill bit. International Journal of Rock Mechanics and Mining Sciences **41**, 2B11.
- Kuehl, R.O.** (2000). Design of Experiments: Statistical Principles of Research Design and Analysis. (BROOKS/COLE).

- Kumano, A., and Goldsmith, W.** (1982). Behavior of diorite under impact by variously-shaped projectiles. *Rock Mechanics and Rock Engineering* **15**, 25-40.
- Kutner, M., Nachtsheim, C., Neter, J., and Li, W.** (2004). *Applied Linear Statistical Models* (McGraw-Hill/Irwin).
- Ledgerwood 3, L.W.** (2007). PFC modeling of rock cutting under high pressure conditions. *Rock Mechanics: Meeting Society's Challenges and Demands* (1st Canada-U.S. Rock Mechanics Symposium, Vancouver, May 2007) **1**, 511-518.
- Lin, T.P., Hood, M., Cooper, G.A., and Li, X.H.** (1992). Wear and Failure Mechanisms of Polycrystalline Diamond Compact Bits. *Wear* **156**, 133-150.
- Linqvist, P.A.** (1982). Rock fragmentation by indentation and disc cutting. In *Univ. of Lulea*, pp. 194.
- Liu, Y., Mavroidis, C., Bar-Cohen, Y., and Chang, Z.** (2007). Analytical and Experimental Study of Determining the Optimal Number of Wedge Shape Cutting Teeth in Coring Bits Used in Percussive Drilling. *Journal of Manufacturing Science and Engineering* **129**, 760-769.
- Lundberg, B.** (1974). Penetration of Rock by Conical Indenters. *International Journal of Rock Mechanics and Mining Sciences and Geomechanics Abstracts* **11**, 209-214.
- Marrey, R.V., Burgermeister, R., Grishaber, R.B., and Ritchie, R.O.** (2006). Fatigue and life prediction for cobalt-chromium stents: A fracture mechanics analysis. *Biomaterials* **27**, 1988-2000.
- Mathworks, I.** (2010). *Matlab Manual 2010b*.
- Matsuda, Y., and Iwase, Y.** (2002). Numerical simulation of rock fracture using three-dimensional extended discrete element method. *Earth Planets Space* **54**, 367-378.
- MINITAB.** (2010). *Minitab16 Manual*.
- Mishnaevsky Jr, L.L.** (1994). Investigation of the cutting of brittle materials. *International Journal of Machine Tools and Manufacture* **34**, 499-505.
- Mishnaevsky, L.L.** (1995). Physical mechanisms of hard rock fragmentation under mechanical loading: A review. *International Journal of Rock Mechanics and Mining Sciences & Geomechanics Abstracts* **32**, 763-766.
- Muro, T., Tsuchiya, K., and Kohno, K.** (2002). Experimental considerations for steady state edge excavation under a constant cutting depth for a mortar specimen using a disk cutter bit. *Journal of Terramechanics* **10**, 143-159.
- Nishimatsu, Y.** (1972). The mechanics of rock cutting. *International Journal of Rock Mechanics and Mining Science & Geomechanics Abstracts* **9**, 261-270.
- Nobuyuki Mori, H.M., Akihiko Ikegaya, Sumitomo Electric Industries; Yutaka Shioya, Katsuhiko Ohbi, Japan National Oil Corporation.** (2003). Development of Highly Durable Materials for Drilling Hard and Abrasive Rocks. *SPE Asia Pacific Oil and Gas Conference and Exhibition*, 9-11 September 2003, Jakarta, Indonesia.
- Onate, E., Kargl, H., Labra, C., Akerman, J., Restner, U., Lammaer, E., and Zarate, F.** (2008). Prediction of Wear of Roadheader Picks using Numerical Simulations. *Geomechanik and Tunnelbau* **1**, 2008, Heft 1 **1**, 47-54.
- Ostermeyer, G.P.** (2003). On the dynamics of the friction coefficient. *Wear* **254**, 852-858.
- Ozturk, C.A., Nasuf, E., and Bilgin, N.** (2004). The assessment of rock cuttability, and physical and mechanical rock properties from a texture coefficient. *Journal of the South African Institute of Mining and Metallurgy* **104**, 397-402.
- Pang, S.S., and Goldsmith, W.** (1990). Investigation of crack formation during loading of brittle rock. *Rock Mechanics and Rock Engineering* **23**, 53-63.
- Pödra, P., and Andersson, S.** (1999). Simulating sliding wear with finite element method. *Tribology International* **32**, 71-81.

- Rånman, K.E.** (1985). A model describing rock cutting with conical picks. *Rock Mechanics and Rock Engineering* **18**, 131-140.
- Refahi, A., Mohandesi, J.A., and Rezai, B.** (2008). Numerical modeling of consumption energy and fracture behavior of spherical rocks in a jaw crusher. In 42nd US Rock Mechanics Symposium & 2nd US-Canada Rock MEchanics Symposium (Westin San Francisco Market Street), pp. ARMA 08 - 66.
- Rico Ramos, L.Y. Chin, and Enderlin, M.B.** (2008). Upscaling of Rock Mechanical and Petrophysical Properties from Grain-Scale to Log-Resolution Scale by Point-Load and Wedge Indentation Tests In 42nd US Rock Mechanics Symposium & 2nd US-Canada Rock MEchanics Symposium (Westin San Francisco Market Street), pp. ARMA -08 152.
- Rostami, J.** (1997). Developmnet of a force estimation model for rock fragmentation with disc cutters through theoretical modeling and physical measurement of crushed zone pressure In *Mining Engineering* (Golden, Colorado: Colorado School of Mines).
- Rostami, J.** (2008). Hard Rock TBM Cutterhead Modeling for Design and Performance Prediction *Geomechanik and Tunnelbau* 1, 2008, Heft 1 **1**, 18-28.
- Rostami, J., and Ozdemir, L.** (1993). A New Model For Performance Prediction Of Hard Rock TBMs. In *Proceedings of RETC* (Boston MA).
- Rostami, J., Ozdemir, L., and Neil, D.M.** (1994). Application Of Heavy Duty Roadheaders For Underground Development of the Yucca Mountain Exploratory Study Facility. In *Proceedings of International High Level Nuclear Waste Management Conference* (Las Vegas, NV).
- Rostami, J., Ozdemir, L., and Asbury, B.** (1995). Mini-Disc Equipped Roadheader Technology for Hard Rock Mining. *Proceedings of the 3rd International Symposium on Mine Mechanization and Automation*, June 12-14, 1995, Golden, Colorado.
- Rostami, J., Blair, B., and Eustes, W.** (1998). Review of the Issues Related to Extraterrestrial Drilling. In *Proceedings of Space 98 Conference* (Albuquerque, New Mexico).
- Rostami, J., Gertsch, L., Gustafson, R., and Swope, C.** (2009). Design and Preliminary Testing of Low-Energy planetary Excavator. In *SME Annual Meeting* (Denver, CO).
- Roxborough, F.F.** (1973). Cutting rock with picks. *The Mining Engineer*, 445–455.
- Roxborough, F.F., and Phillips, H.R.** (1975). Rock Excavation by Disk Cutter. *International Journal of Rock Mechanics and Mining Sciences* **12**, 361-366.
- Roxborough, F.F., and Pedroncelli, E.J.** (1982). A practical evaluation of some coal-cutting theories using a continuous miner. *The Mining Engineer*, 145–155.
- Roxborough, F.F., and Sen, G.C.** (1986). Breaking coal and rock. *Australasian Institute of Mining and Metallurgy*, 130-147.
- Saouma, V.E., and Kleinosky, M.-J.** (1984). Finite Element Simulation Of Rock Cutting: A Fracture Mechanics Approach. In *The 25th U.S. Symposium on Rock Mechanics (USRMS)*, June 25 - 27 (Evanston, IL).
- Schormair , N., and Thuro, k.** (2007). Fracture Pattern of anisotropic rock by drilling or cutting using the PFC. *Rock Mechanics: Meeting Society's Challenges and Demands* (1st Canada-U.S. Rock Mechanics Symposium, Vancouver, May 2007), 527-534.
- Shen, H.W., Hardy, J.R., and Khair, A.W.** (1997). Laboratory study of acoustic emission and particle size distribution during rotary cutting. *Int J Rock Mech Min* **34**, 121.e121-121.e116.
- Shenghua, Y.** (2004). Simulation of Rock Cutting by the Finite Element Method. In *2004 International ANSYS Conference Proceedings* (Shanghai Branch of China Coal Research Inc. Shanghai, China).

- Shmulevich, I., Asaf, Z., and Rubinstein, D.** (2007). Interaction between soil and a wide cutting blade using the discrete element method. *Soil & Tillage Research* **97**, 37-50.
- Smith, S.W.** (1997). *The Scientist and Engineer's Guide to Digital Signal Processing*. (California Technical Publishing).
- Speight, H.E.** (1997). Observations on Drag Tool Excavation and the Consequent Performance of Roadheaders in Strong Rock The AusIMM Proceedings **302**.
- Spencer, A.J.M.** (1992). *Continuum Mechanics*. (Dover Publications).
- Staroselsky, A.V., and Kim, K.** (1997). An analytical elucidation of the influence of surfactant on rock drilling by shear/drag bit. *Rock Mech Rock Eng* **30**, 145 - 159.
- Stavropoulou, M.** (2006). Modeling of small-diameter rotary drilling tests on marbles. *International Journal of Rock Mechanics and Mining Sciences* **43**, 1034-1051.
- Swain, M.V., and Lawn, B.R.** (1976). Indentation fracture in brittle rocks and glasses. *International Journal of Rock Mechanics and Mining Sciences & Geomechanics Abstracts* **13**, 311-319.
- T. Martín, Español, P., and Rubio, M.A.** (2005). Mechanisms for dynamic crack branching in brittle elastic solids: Strain field kinematics and reflected surface waves.
- Takacs, F., Koronka, F., and Andras, I.** (2003). The influence of rock properties on the wear of mining tools for rotating drilling. The annals of university "DUNĂREA DE JOS" of galati, Fascicle VIII, Tribology, 154-160.
- Tan, X.C., Lindqvist, P.A., and Kou, S.Q.** (1997). APPLICATION OF A SPLITTING FRACTURE MODEL TO THE SIMULATION OF ROCK INDENTATION SUBSURFACE FRACTURES. *International Journal for Numerical and Analytical Methods in Geomechanics* **21**, 1-13.
- Tan, X.C., Kou, S.Q., and Lindqvist, P.A.** (1998). Application of the DDM and fracture mechanics model on the simulation of rock breakage by mechanical tools. *Engineering Geology* **49**, 277-284.
- Tannant, D.D., and Wang, C.** (2002). Numerical and experimental study of wedge penetration into oil sands. *Cim Bulletin* **95**, 65-68.
- Teale, R.** (1965). The concept of specific energy in rock drilling. *International Journal of Rock Mechanics and Mining Science & Geomechanics Abstracts* **2**, 57-73.
- Thuro , K.** (2003). Prediction roadheader advance rates: Geological challenges and Geotechnical answers In ITU Maden Fakultesi 50.Yil Sempozyumu-50th Years symposium of The Faculty of Mines/Istanbul Technical University The Underground Resources of Turkey Today and Future 5-8 June 2003,Istanbul, Turkey-Invited Lecture
- Thuro, K., and Schormair, N.** (2008). Fracture Propagation in Anisotropic Rock During Drilling and Cutting *Geomechanik and Tunnelbau* **1**, 2008, Heft 1, **1**, 8-17.
- Tiryaki, B.** (2006). Evaluation of the indirect measures of rock brittleness and fracture toughness in rock cutting. *Journal of the South African Institute of Mining and Metallurgy* **106**, 409-423.
- Tiryaki, B.** (2008). Application of artificial neural networks for predicting the cuttability of rocks by drag tools. *Tunn Undergr Sp Tech* **23**, 273-280.
- Tiryaki, B., and Dikmen, A.C.** (2006). Effects of rock properties on specific cutting energy in linear cutting of sandstones by picks. *Rock Mechanics and Rock Engineering* **39**, 89-120.
- Tulu, I.B., Keith A. Heasley, H. Ilkin Bilgesu, and Sunal, O.** (2008). Modeling Rock and Drill Cutter Behavior. In 42nd US Rock Mechanics Symposium & 2nd US-Canada Rock MEchanics Symposium (Westin San Francisco Market Street), pp. ARMA 08- 342.
- Tuncdemir, H., Bilgin, N., Copur, H., and Balci, C.** (2008). Control of rock cutting efficiency by muck size. *International Journal of Rock Mechanics and Mining Sciences* **45**, 278-288.

- Verhoef, R.N.W., and Ockeloen, J.J.** (1996). The significance of rock ductility for mechanical rock cutting. In *Rock mechanics tools and techniques : proceedings of the 2nd North American Rock Mechanics Symposium: NARMS '96, a regional conference of ISRM* (Montreal, Qubec, Canada), pp. 19-21
- West, G.** (1989). Technical Note- Rock Abrasiveness Testing for Tunnelling. *International Journal of Rock Mechanics and Mining Sciences and Geomechanics Abstracts* **26**, 151-160.
- Whittaker, B.N., and Szwilski, A.B.** (1973). Rock cutting by impact action. *International Journal of Rock Mechanics and Mining Sciences & Geomechanics Abstracts* **10**, 659-671.
- Whittles, D.N., Kingman, S., Lowndes, I., and Jackson, K.** (2006). Laboratory and numerical investigation into the characteristics of rock fragmentation. *Minerals Engineering* **19**, 1418-1429.
- Yilmaz, N.G., Yurdakul, M., and Goktan, R.M.** (2007). Prediction of radial bit cutting force in high-strength rocks using multiple linear regression analysis. *International Journal of Rock Mechanics and Mining Sciences* **44**, 962-970.
- Yu, B., and Khair, A.W.** (2007). Numerical modeling of rock ridge breakage in rotary cutting *Rock Mechanics: Meeting Society's Challenges and Demands (1st Canada-U.S. Rock Mechanics Symposium, Vancouver, May 2007)*, 519-526.
- Zacny, K.A., and Cooper, G.A.** (2004). Investigation of diamond-impregnated drill bit wear while drilling under Earth and Mars conditions. *Journal of Geophysical Research-Planets* **109**, -.
- Zaman, M.T., Kumar, A.S., Rahman, M., and Sreeram, S.** (2006). A three-dimensional analytical cutting force model for micro end milling operation. *International Journal of Machine Tools and Manufacture* **46**, 353-366.
- Zhang, Y., and Ord, A.** (2008). Simulation of fracturing and mechanical damage in rocks In *42nd US Rock Mechanics Symposium & 2nd US-Canada Rock Mechanics Symposium (Westin San Francisco Market Street)*, pp. ARMA 08-111.

Appendix

Suppl. 1 Summary files of the Rotary cutting tests.

Table Suppl.A Summary table for the AM470 single bit in 2.5 cm (1”) depth of cut.

#of line	skew angle (deg)	depth(cm)	spacing(cm)	Trav.Speed (m/min)	Rot_who le(deg/rev)	Normal Avg (N)	SideAvg (N)	DragAvg (N)	Abs_Rot (deg/rev)	SE(J/cm ³)
3	-12	2.54	2.54	1.52	1.90	1317.42	-1557.23	3067.55	1.90	4.75
3	-6	2.54	2.54	1.52	0.68	238.15	-226.46	811.47	1.51	1.26
3	0	2.54	2.54	1.52	1.53	381.39	144.83	696.99	1.77	1.08
3	6	2.54	2.54	1.52	-1.33	785.02	587.35	2229.06	1.33	3.46
3	12	2.54	2.54	1.52	0.28	1587.49	1296.49	4335.06	0.84	6.72
3	-12	2.54	2.54	3.05	1.47	1757.30	-2220.33	4301.94	1.47	6.67
3	-6	2.54	2.54	3.05	2.31	408.49	-515.63	1282.19	2.31	1.99
3	0	2.54	2.54	3.05	1.89	471.67	256.81	857.73	2.63	1.33
3	6	2.54	2.54	3.05	-1.72	995.89	1244.05	3213.30	1.72	4.98
3	12	2.54	2.54	3.05	-1.24	1156.63	1541.29	3180.70	1.24	4.93
3	-12	2.54	2.54	4.57	1.39	1964.96	-2320.80	4919.56	1.39	7.63
3	-6	2.54	2.54	4.57	1.09	443.86	-652.00	1600.38	1.09	2.48
3	0	2.54	2.54	4.57	2.80	484.95	310.44	965.19	2.80	1.50
3	6	2.54	2.54	4.57	-1.58	1090.74	1297.93	3539.77	1.58	5.49
3	12	2.54	2.54	4.57	-1.89	1599.26	2321.45	4768.28	1.89	7.39
3	-12	2.54	3.81	1.52	-0.28	1478.21	-1051.05	3571.42	0.45	3.69
3	-6	2.54	3.81	1.52	1.22	369.75	-265.60	1055.19	1.22	1.09
3	0	2.54	3.81	1.52	1.89	402.67	112.11	708.14	1.89	0.73
3	6	2.54	3.81	1.52	-0.58	772.73	665.20	2471.55	1.14	2.55
3	12	2.54	3.81	1.52	0.25	1087.83	1060.52	3298.32	0.54	3.41
3	-12	2.54	3.81	3.05	0.03	1804.52	-1573.58	4426.53	0.38	4.57
3	-6	2.54	3.81	3.05	1.05	477.84	-439.51	1447.33	1.20	1.50
3	0	2.54	3.81	3.05	0.48	626.18	60.06	1355.45	0.95	1.40
3	6	2.54	3.81	3.05	-0.56	954.66	674.14	2906.01	0.56	3.00
3	12	2.54	3.81	3.05	-0.49	1432.64	1377.19	4640.43	1.23	4.80
3	-12	2.54	3.81	4.57	0.25	1966.86	-1716.30	5341.99	0.25	5.52
3	-6	2.54	3.81	4.57	0.27	616.40	-627.48	1897.97	0.57	1.96
3	0	2.54	3.81	4.57	2.13	530.87	241.54	1165.48	2.13	1.20
3	6	2.54	3.81	4.57	-0.01	1115.24	987.69	3808.09	0.35	3.94
3	12	2.54	3.81	4.57	-0.87	1815.50	1714.85	5963.98	0.87	6.16
3	-12	2.54	5.08	1.52	0.00	1769.32	-1339.85	4384.32	0.64	3.40
3	-6	2.54	5.08	1.52	-0.01	340.76	-143.12	995.44	0.17	0.77
2	0	2.54	5.08	1.52	0.51	623.09	58.48	1076.79	0.58	0.83
3	6	2.54	5.08	1.52	0.61	1058.37	64.02	2820.01	0.65	2.19
3	12	2.54	5.08	1.52	-0.08	1881.94	98.09	4849.69	0.61	3.76
3	-12	2.54	5.08	3.05	-0.13	2324.61	-1488.00	5679.38	0.54	4.40
3	-6	2.54	5.08	3.05	0.07	544.51	-313.34	1677.68	0.34	1.30

3	0	2.54	5.08	3.05	0.13	534.58	76.61	1121.41	0.55	0.87
2	6	2.54	5.08	3.05	-1.01	1734.58	383.28	4568.52	1.01	3.54
3	12	2.54	5.08	3.05	-0.90	1535.44	1096.50	4844.94	0.90	3.75
3	-12	2.54	5.08	4.57	-0.16	2924.94	-2404.89	7495.15	0.42	5.81
3	-6	2.54	5.08	4.57	-0.72	660.50	-352.23	2288.17	0.72	1.77
3	0	2.54	5.08	4.57	-0.11	968.28	263.11	2450.95	0.24	1.90
3	6	2.54	5.08	4.57	-0.40	1557.01	432.25	4931.49	0.42	3.82
3	12	2.54	5.08	4.57	0.07	1910.54	1365.05	6783.34	0.32	5.26

Table Suppl.B RZ24 bit single bit at 2.5 cm (1") depth of cut

# of lines	skew angle	depth (cm)	spacing (cm)	Trav. speed (m/min)	Rot. whole (deg/rev)	Normal Avg (N)	Side Avg (N)	Drag Avg (N)	Abs_rot (deg/rev)	SE(J/cm ³)
2	-12	2.54	5.08	1.524	-0.06	688.8	-241	1267	0.285	0.982
2	6	2.54	2.54	4.572	0.846	969.1	667.3	2095	0.846	3.247
2	12	2.54	2.54	1.524	2.504	502.9	562.9	1446	2.504	2.241
2	12	2.54	2.54	3.048	2.834	507.8	642.7	1141	2.834	1.768
2	12	2.54	5.08	3.048	-0.56	1607	608	2237	0.556	1.734
3	-12	2.54	2.54	1.524	-0.58	320.2	-202	752	0.577	1.166
3	-12	2.54	2.54	3.048	-0.24	806	-503	1515	0.237	2.348
3	-12	2.54	2.54	4.572	-0.4	871.1	-642	1846	0.487	2.862
3	-12	2.54	3.81	1.524	-0.26	458.6	-185	963.9	0.266	0.996
3	-12	2.54	3.81	3.048	-0.28	795.7	-424	1518	0.276	1.569
3	-12	2.54	3.81	4.572	-0.79	1042	-649	2079	0.793	2.148
3	-12	2.54	5.08	3.048	0.234	831.6	-206	1676	0.239	1.299
3	-12	2.54	5.08	4.572	-0.01	980.7	-319	1968	0.231	1.525
3	-6	2.54	2.54	1.524	0.177	788.3	-548	1457	1.338	2.259
3	-6	2.54	2.54	3.048	-0.9	927.5	-758	1861	0.901	2.884
3	-6	2.54	2.54	4.572	0.095	1205	-1039	2376	0.191	3.683
3	-6	2.54	3.81	1.524	0.121	762.7	-455	1411	0.121	1.458
3	-6	2.54	3.81	3.048	-0.11	1088	-691	2005	0.106	2.072
3	-6	2.54	3.81	4.572	-0.02	1413	-1187	2902	0.03	2.998
3	-6	2.54	5.08	1.524	0.144	834.3	-297	1454	0.144	1.127
3	-6	2.54	5.08	3.048	0.056	1183	-459	2271	0.066	1.76
3	-6	2.54	5.08	4.572	-0.28	1308	-288	2740	0.331	2.123
3	0	2.54	2.54	1.524	2.512	428.3	348.5	962.1	2.512	1.491
3	0	2.54	2.54	3.048	1.725	703.7	546.7	1455	1.725	2.255
3	0	2.54	2.54	4.572	0.04	1003	854	2151	0.179	3.334
3	0	2.54	3.81	1.524	0.039	669.8	453.3	1282	0.039	1.325
3	0	2.54	3.81	3.048	0.255	1077	735.9	2164	0.278	2.236
3	0	2.54	3.81	4.572	0.389	1418	1136	3000	0.389	3.1
3	0	2.54	5.08	1.524	-0.11	1034	308.2	1928	0.107	1.494
3	0	2.54	5.08	3.048	0.078	1173	550.2	2318	0.219	1.797
3	0	2.54	5.08	4.572	0.282	1402	617	2825	0.282	2.189
3	6	2.54	2.54	1.524	1.723	363.5	307.4	813.7	1.723	1.261
3	6	2.54	2.54	3.048	0.931	739.6	456.3	1448	0.931	2.244
3	6	2.54	3.81	1.524	0.259	514.5	230.1	1073	0.259	1.109

3	6	2.54	3.81	3.048	-0.16	683.4	316.9	1659	1.174	1.714
3	6	2.54	3.81	4.572	0.235	1074	698.9	2248	0.289	2.323
3	6	2.54	5.08	1.524	0.374	555.9	83.23	1101	0.374	0.853
3	6	2.54	5.08	3.048	0.008	799.3	180.8	1609	0.078	1.247
3	6	2.54	5.08	4.572	-0.76	1441	417.3	3077	0.756	2.384
3	12	2.54	2.54	4.572	3.706	1141	1274	2246	3.706	3.482
3	12	2.54	3.81	1.524	0.141	286.7	114.7	930.3	0.453	0.961
3	12	2.54	3.81	3.048	0.332	1263	791.4	423.3	0.686	0.437
3	12	2.54	3.81	4.572	0.306	880.3	586.4	817.1	0.306	0.844
3	12	2.54	5.08	1.524	-0.28	575.2	191.2	1124	0.284	0.871
3	12	2.54	5.08	4.572	-0.06	1154	486.7	1805	0.184	1.399

Table Suppl.C Summary table for the AM470 single bit in 5cm (2") depth of cut.

#of line	skew angle (deg)	depth(cm)	spacing(cm)	Trav.Speed (m/min)	Rot_whole(deg/rev)	Normal Avg (N)	SideAvg (N)	DragAvg (N)	Abs_Rot (deg/rev)	SE(J/cm ³)
3	-12	5.08	2.54	1.524	0.1559	901.25	-1592	2337.9	0.2853	1.8119
3	-6	5.08	2.54	1.524	0.0696	1179.9	-1930	2881.5	0.3837	2.2332
3	0	5.08	2.54	1.524	2.0132	701.79	393.97	1558.1	2.0132	1.2075
3	6	5.08	2.54	1.524	-0.71	326.18	670.52	1399.9	1.2799	1.0849
3	12	5.08	2.54	1.524	-0.912	795.2	2540.3	4008.2	0.9117	3.1064
3	-12	5.08	2.54	3.048	0.0485	1305	-2604	3431.3	0.1058	2.6592
3	-6	5.08	2.54	3.048	0.1307	1436.5	-2950	3760.6	0.2237	2.9145
3	0	5.08	2.54	3.048	3.016	841.25	942.16	1830.7	3.016	1.4188
3	6	5.08	2.54	3.048	-2.327	441.12	949.4	1898.7	2.3275	1.4715
3	12	5.08	2.54	3.048	-0.865	794.44	3246.1	5361.1	1.5487	4.1548
3	-12	5.08	2.54	4.572	0.526	1034.1	-1868	3256.1	0.526	2.5235
3	-6	5.08	2.54	4.572	0.2697	1564.1	-2925	4373	0.2697	3.3891
3	0	5.08	2.54	4.572	2.8393	845.48	1705.5	3096.9	2.8393	2.4001
3	6	5.08	2.54	4.572	-2.462	617.9	1281.5	2596.4	2.4618	2.0122
3	12	5.08	2.54	4.572	-1.218	1339.5	3590	7516.4	1.2179	5.8252
3	-12	5.08	3.81	1.524	1.3163	721.34	-1024	1973.2	1.3163	1.0195
3	-6	5.08	3.81	1.524	0.8446	885.96	-1256	2259.6	0.8446	1.1675
3	0	5.08	3.81	1.524	-0.101	809.27	578.62	1511.3	1.7926	0.7808
3	6	5.08	3.81	1.524	-3.052	440.54	572.77	1479.9	3.0524	0.7646
3	12	5.08	3.81	1.524	0.6014	1189	1959.5	4697.7	0.7379	2.4271
3	-12	5.08	3.81	3.048	1.3827	858.96	-1260	2457.4	1.3827	1.2697
3	-6	5.08	3.81	3.048	0.4907	988.79	-1826	3086.9	0.4907	1.5949
3	0	5.08	3.81	3.048	1.9849	1002.4	923.09	2393.2	1.9849	1.2365
3	6	5.08	3.81	3.048	-1.859	411.57	853.28	2132.4	1.8592	1.1018
3	12	5.08	3.81	3.048	0.2519	1457.5	3125.5	6769.6	0.7008	3.4976
3	-12	5.08	3.81	4.572	0.7479	1093	-1694	3558.6	0.7479	1.8386
3	-6	5.08	3.81	4.572	0.2196	1232.1	-2392	4111.5	0.7488	2.1243
3	0	5.08	3.81	4.572	2.8112	1069.6	1450.7	3274	2.8112	1.6916
3	6	5.08	3.81	4.572	-2.29	493.62	1090.5	2731.9	2.2897	1.4115
3	12	5.08	3.81	4.572	-0.875	1556.7	3638.4	8071	0.8754	4.17
3	-12	5.08	5.08	1.524	0.7111	844.43	-981.7	2218.8	0.7111	0.8598

3	-6	5.08	5.08	1.524	0.7062	1062.5	-1454	2734.4	0.7062	1.0596
3	0	5.08	5.08	1.524	0.585	825.53	572.72	1774.3	0.585	0.6876
3	6	5.08	5.08	1.524	-1.531	415.4	552.93	1807.9	1.5307	0.7006
3	12	5.08	5.08	1.524	0.6007	1688.2	1278.7	5462.6	0.6007	2.1167
3	-12	5.08	5.08	3.048	0.7701	1026.3	-1330	3038.8	0.7701	1.1775
3	-6	5.08	5.08	3.048	0.1388	1313.4	-2230	3816.1	0.3319	1.4787
3	0	5.08	5.08	3.048	1.5919	1132	1067.7	3108	1.5919	1.2044
3	6	5.08	5.08	3.048	-1.632	533.85	938.7	2861.4	1.6325	1.1088
3	12	5.08	5.08	3.048	0.1565	1662.7	2599	6874.9	0.4297	2.664
3	-12	5.08	5.08	4.572	0.7996	1553.5	-2442	4611.6	0.7996	1.787
3	-6	5.08	5.08	4.572	-0.26	1379.1	-2337	4555.1	0.3321	1.7651
3	0	5.08	5.08	4.572	-0.168	908.98	896.87	3257.1	0.6854	1.2621
3	6	5.08	5.08	4.572	-1.377	752.62	1254.6	3619.2	1.377	1.4024
3	12	5.08	5.08	4.572	0.0149	1618.4	3342.5	7252.7	0.3168	2.8104

Table Suppl.D Summary table for the multiple rotary cutting tests config. AM470 bits at 2.5 and 5 cm (1”& 2”) DCs.

# of line	depth (cm)	skew angle(deg)	travel speed (m/min)	spacing (cm)	Abs_Rot (deg/rev)	SideAvg (N)	Normal Avg (N)	DragAvg (N)	Rot_Whole(deg/rev)	SE(J/cm ³)
7	2.54	-6	3.05	2.54	0.85	10.62	150.55	427.27	0.85	0.66
6	2.54	-6	1.52	2.54	1.56	-0.13	166.60	572.40	1.56	0.89
8	2.54	0	3.05	2.54	0.72	19.63	151.99	450.87	0.26	0.70
3	2.54	0	1.52	2.54	0.29	-3.96	113.02	303.64	-0.13	0.47
3	2.54	0	1.52	2.54	0.23	-15.53	102.29	326.95	-0.23	0.51
6	2.54	6	3.05	2.54	0.78	-4.88	168.61	560.27	-0.72	0.87
5	2.54	6	1.52	2.54	0.47	-7.59	153.50	555.87	-0.18	0.86
6	5.08	-6	1.52	2.54	1.69	-3.71	167.07	566.00	1.34	0.44
6	5.08	-6	3.05	2.54	1.38	8.42	177.54	405.88	0.99	0.31
8	5.08	0	3.05	2.54	0.36	25.92	125.29	395.39	0.01	0.31
7	5.08	0	1.52	2.54	0.47	-14.40	103.33	359.43	-0.06	0.28
7	5.08	6	3.05	2.54	0.38	-4.95	173.79	548.46	-0.25	0.43
6	5.08	6	1.52	2.54	0.29	-11.25	160.14	579.08	-0.25	0.45
3	2.54	-6	1.52	5.08	0.43	254.95	173.27	823.39	0.37	0.64
3	2.54	-6	3.05	5.08	1.38	170.80	176.07	860.13	1.38	0.67
3	2.54	0	1.52	5.08	0.27	-55.06	283.39	781.40	-0.09	0.61
3	2.54	0	3.05	5.08	0.15	-13.60	570.68	1350.26	0.15	1.05
3	2.54	6	1.52	5.08	0.60	-52.55	227.67	531.01	0.57	0.41
3	2.54	6	3.05	5.08	0.27	-95.43	368.15	824.24	-0.27	0.64
3	5.08	-6	1.52	5.08	0.42	117.81	121.00	674.96	-0.42	0.26
3	5.08	-6	3.05	5.08	0.16	88.11	294.29	1098.25	0.16	0.43
3	5.08	0	1.52	5.08	0.25	13.77	222.88	638.87	-0.08	0.25
3	5.08	0	3.05	5.08	0.46	44.88	653.17	1487.01	0.08	0.58
3	5.08	6	1.52	5.08	0.14	-42.98	287.03	657.69	0.03	0.25
3	5.08	6	3.05	5.08	0.56	197.10	645.80	1438.63	-0.56	0.56
3	2.54	-6	1.52	10.16	0.95	529.35	147.45	884.54	0.95	0.34

3	2.54	-6	3.05	10.16	3.38	658.62	90.15	1499.27	3.38	0.58
3	2.54	0	1.52	10.16	0.35	10.70	313.35	836.92	0.30	0.32
3	2.54	0	3.05	10.16	1.36	921.40	455.86	1969.60	-0.53	0.76
3	2.54	6	1.52	10.16	0.48	-176.36	318.68	688.48	0.48	0.27
3	2.54	6	3.05	10.16	0.40	-206.04	534.02	1061.93	-0.40	0.41
3	5.08	-6	1.52	10.16	2.54	688.16	120.51	919.90	2.54	0.18
3	5.08	-6	3.05	10.16	2.06	1063.62	33.93	2111.76	2.06	0.41
3	5.08	0	1.52	10.16	0.45	-230.65	608.08	1505.60	0.32	0.29
3	5.08	0	3.05	10.16	0.16	-160.88	875.85	2334.64	-0.02	0.45
3	5.08	6	1.52	10.16	0.69	-482.34	635.34	1262.09	0.69	0.24
3	5.08	6	3.05	10.16	0.55	-643.00	760.46	1957.20	-0.46	0.38

VITA: Eunhye Kim

Education

PhD: Energy and Mineral Engineering (Option with Mining Engineering)	12/10
PhD Minor: Engineering Science and Mechanics, Pennsylvania State Univ., USA	
MS: Rock Mechanics, Seoul National Univ., S. Korea	02/06
BS: Civil Engineering & Computer Science, Ajou Univ., South Korea	08/03

Technical Publications

“ <i>Full scale linear cutting experiment to examine conical bit rotation</i> “ in International Journal of Rock Mechanics and Mining Science (submitted)	08/10
+Other three conference papers (ARMA, ARMS)	

Work Experiences in Academia

1) Teaching Assistant, Rock Mechanics Class (PSU & SNU)	SP05 & SP09 & SP10
*Design the class: developed syllabus, class & lab works, & homeworks with grading homeworks and lab reports	
*Design the course and teaching high school students	
* Managing and led student in laboratory sessions	
*Led student in participating in Lab session	
2) Teaching Assistant; Extra Teaching experiences (PSU&SNU)	SU08 & SP05
*Summer School of Dept. of Earth and Mineral Science; Introduction on rock mechanics and coolant system design (8weeks, PSU)	
*Helping design and publishing the text book “Development and Utilization of the Underground Space” for elementary school students with 2004 Future Korea (Korea Research Foundation & 3months, SNU), Teaching elementary school students based on that book (1week, SNU)	

Work Experiences in Industry Projects

1) Conical Bit rotation with Kennametal Inc, Latrobe, PA	03/08 - Present
*Developing measurement system	
*Retrofitting existing system	
*Performing the cutting test with Linear and Rotary Cutting Test	
*Data Analysis with developing VBA program and MATLAB	
*Finite Element Analysis (ANSYS, SOLIDWORKS)	
2) NASA project: Low –energy consumption machine with Orbitec. Inc	10/07- 06/08
* Data mining and analysis with developing VBA Program	
*Performing the Cutting Test of Low Energy Planetary Excavator design	
3) Rock Property Tests for several industry projects (PSU & SNU) 2yrs	
4) Pre-Blasting Report in Ul –san area Subcontractor with Korea Gas Cooperation & “Beepee” Exploration Company (4weeks)	
5) Experiment Assistant in Soil Laboratory at Ajou University (1semester)	

Certifications

FE/EIT Certification(in General; score: pass)(Pennsylvania State Board)	04/09
FE Certification (in Civil Eng.) (South Korea Engineering Board)	07/06
FE Certification (in Computer Eng.)(South Korea Engineering Board)	12/03

Scholarship/Awards

Reg Hardy Memorial Award for Excellence in Mining, PSU	03/10
Outstanding participant Award in the 08 Summer Experience in EMS, PSU	07/08
Scholarship from University Office of Global Programs, PSU	09/07
Scholarship for graduate, Seoul National University, South Korea	09/04
Scholarship for undergraduate, Ajou University, South Korea	09/1999

Professional Affiliations

ARMA, ASCE, SME, UCA of SME, ISEE